TRANSCRIPTIONALLY DEFINED SUBPOPULATIONS OF CUTANEOUS NEURONS: EFFECTS OF NERVE INJURY AND REGENERATION

by

Peter C. Adelman

B.S. Biochemistry, B.A. Neuroscience, University of Delaware, 2009

Submitted to the Graduate Faculty of

the School of Medicine in partial fulfillment

of the requirements for the degree

PhD in Neuroscience

University of Pittsburgh

2016

UNIVERSITY OF PITTSBURGH

SCHOOL OF MEDICINE

This dissertation was presented

by

Peter C. Adelman

It was defended on

June 24, 2016

and approved by

Brian M. Davis, PhD, Professor

Kathryn M. Albers, PhD, Professor

Sarah E. Ross, PhD, Assistant Professor

Anne-Marie Oswald, PhD, Assistant Professor

Lorne M. Mendell, PhD, Professor

Dissertation Advisor: H. Richard Koerber, PhD, Professor

TRANSCRIPTIONALLY DEFINED SUBPOPULATIONS OF CUTANEOUS NEURONS: EFFECTS OF NERVE INJURY AND REGENERATION

Peter C. Adelman, PhD

University of Pittsburgh, 2016

Primary sensory neurons are responsible for cutaneous somatosensory transduction. These neurons can transduce mechanical force, temperature, and chemical sensitivity, which we perceive as pressure, position, heat, cold, itch, and pain. It has long been recognized that different afferents are specific for distinct modalities, but it has not been clear if afferent sensitivities represent a continuum or unique populations of afferents with common properties. I found that mouse dorsal root ganglion afferents can be clearly divided into groups by their transcriptional expression and that these groups share common modality sensitivities and functional properties. Further investigation revealed that the levels of some individual transduction channels may be an even more accurate way to track modality sensitivity, giving a potential molecular signature for function in murine afferents. These findings imply that recognized histological projection bands in the spinal cord (Substance P, CGRP, IB4, etc.) reflect subpopulations of afferents with unique properties that are projecting to unique areas of the spinal cord. This is relevant to sensory coding models, but may also be very important for the development of neuropathic pain after nerve injury. Nerve injury and regeneration alters mRNA and protein expression, and causes parallel changes in afferent properties. These functional changes in afferents could cause unusual activity in corresponding spinal cord circuits (e.g. a spinal cord circuit that is normally mechanically insensitive would receive mechanical input). I investigated this possibility and discovered population-specific regulation of transcripts. This included a mechanotransducer, *Piezo2*, which is upregulated in the small peptidergic subpopulation. Subsequent knockdown using *Piezo2* siRNA reduced the number of mechanically sensitive afferents. These findings suggest that *Piezo2* is necessary for mechanotransduction in injured afferents and could be responsible for induced neuropathic pain.

TABLE OF CONTENTS

LIST OF FIGURES

PREFACE

This document contains work from my last two and a half years at the University of Pittsburgh, but is the culmination of seven years of scientific growth. My journey would have been much less enjoyable if not for the support of my friends and mentors. In specific, I thank Dr. Koerber for all of the disagreements (and subsequent agreements) we have had in the last few years. Civil disagreements are the productive form of discussion, and I would not have it any other way. Robert Friedman also deserves substantial credit for the impressive molecular biology experience he brought to these experiments. Without Rob, very few of the experiments outlined in this document would have been possible. I would also like to thank Dr. Kuan Lee, Dr. Margaret Wright, and Dr. Charles Anderson for their roles as sounding boards for thesis ideas and as proofreaders of the completed document. I would further like to thank the members of the Center for Pain Research and auditory research triumvirate. These two amalgamations of labs helped shape me as a scientist and provided an enjoyable work environment. Finally, I would like to thank my feisty wife, Melissa Day, and the rest of my family for their support over these seven long years. It is highly unlikely that I would have jumped all the hurdles and made it to this defense without your encouragement.

LIST OF ABBREVIATIONS

ANOVA	analysis of variance
ARTN	artemin
ASIC1	acid sensing ion channel 1
ASIC2	acid sensing ion channel 2
ASIC3	acid sensing ion channel 3
Ax488	Alexa Fluor® 488 dye
Ax555	Alexa Fluor® 555 dye
BDNF	brain-derived neurotrophic factor
CALCα	calcitonin related polypeptide alpha
CC	cold sensitive C-fiber
Cck	cholecystokinin
CGRP	calcitonin gene-related peptide
CH	heat sensitive C-fiber
CoV	coefficient of variation
CM	mechanical sensitive C-fiber
CMC	mechanical and cold sensitive C-fiber
CMH	mechanical and heat sensitive C-fiber
CMHC	mechanical, heat, and cold sensitive C-fiber
CTβ	cholera toxin subunit beta
DNA	deoxyribonucleic acid
DRG	dorsal root ganglia
FRAP	fluoride-resistant acid phosphatase
Gal	galanin
GDNF	glial cell line-derived neurotrophic factor
GFRα1	growth factor receptor alpha 1
GFRα2	growth factor receptor alpha 2
GFRα3	growth factor receptor alpha 3
HTMR	high threshold mechanoreceptor

IB4	isolectin binding protein 4
L	lumbar
LTMR	low threshold mechanoreceptor
min	minute
mL	milliliter
mm	millimeter
mN	millinewton
ms	millisecond
MRGPRA3	MAS-related G-protein coupled receptor, member A3
MRGPRD	MAS-related G-protein coupled receptor, member D
Nppb	natruiretic peptide b
NEFH	neurofilament heavy chain
NGF	nerve growth factor
NK1R	neurokinin-1 receptor
NRTN	neurturin
NT3	neurotrophin-3
Nts	neurotensin
P	post-natal day; *refers to an age*
P2RX3	P2X receptor, subunit 3
P2RY1	P2Y receptor, subunit 1
P2RY2	P2Y receptor, subunit 2
PCR	polymerase chain reaction
PEN1	Penetratin-1
PIEZO1	piezo-type mechanosensitive ion channel component 1
PIEZO2	piezo-type mechanosensitive ion channel component 2
PVALB	Parvalbumin
RA	rapidly adapting
RET	receptor tyrosine kinase
RNA	ribonucleic acid
SA1	slowly adapting type 1
SCN9A	voltage-gated sodium channel subunit alpha Nav1.7

SCN10A	voltage-gated sodium channel subunit alpha Nav1.8
SCN11A	voltage-gated sodium channel subunit alpha Nav1.9
sec	second
SEM	standard error of the mean
siRNA	small interfering RNA
SP	substance P
Sst	somatostatin
Tac1	tachykinin, precursor 1
Th	tyrosine hydroxylase
TrkA	tyrosine receptor kinase A
TrkB	tyrosine receptor kinase B
TrkC	tyrosine receptor kinase C
TRPA1	transient receptor protein cation channel, subfamily A, member 1
TRPM3	transient receptor protein cation channel, subfamily M, member 3
TRPM8	transient receptor protein cation channel, subfamily M, member 8
TRPV1	transient receptor protein cation channel, subfamily V, member 1
TRPV2	transient receptor protein cation channel, subfamily V, member 2
TRPV3	transient receptor protein cation channel, subfamily V, member 3
TRPV4	transient receptor protein cation channel, subfamily V, member 4
VGLUT2	vesicular glutamate transporter-2
WGA	wheat germ agglutinin
µL	microliters
µm	micrometers

1.0 INTRODUCTION

1.1 PERIPHERAL NERVE INJURY AND REGENERATION

Though there may be an antecedent in antiquity, the concept of peripheral nerve regeneration following injury was introduced to modern biological sciences by William Cruikshank's 1776 account of regeneration in dog vagus nerve (Ochs 1977; Cruikshank 1795). His observations and the subsequent experimentation of his colleagues firmly established the phenomenon of peripheral nerve regeneration. Over the next century and a half, a great deal of work was done studying peripheral nerve regeneration, establishing time courses for regeneration and eventually culminating with Ramón y Cajal demonstrating that growth occurred from the dorsal root ganglion back out to the periphery (Ramón y Cajal 1928).

The increasing technical viability of electrophysiology inspired another set of questions about the regenerative process following primary sensory neuron injury. Work in the 1960s began to dissect how exactly the different populations of electrophysiologically defined afferents recover function (Brown 1963; Burgess et al. 1974; Terzis & Dykes 1980; Burgess & Horch 1973). These studies showed that afferent degeneration can cause changes in target tissue end organs, like Merkel cell complexes, and implied that nerve injuries change the distribution of primary afferent subtypes (Burgess & Horch 1973).

The development of molecular biology techniques and their application to dorsal root ganglia underscored the heterogeneity of primary afferents in the late 20th century (Price 1985; Gerhard Skofitsch & Jacobowitz 1985; Gibbins et al. 1987). Although the molecular techniques did generate hypotheses, interpretations of the data were limited by their inability to integrate the extant body of electrophysiological research on regenerated axons, as the two types of studies use different classification schemes and there was no clear mapping between them.

Electrophysiological studies rely on functional classifications, while molecular studies rely on molecular markers.

The early 21st century saw some studies begin to link molecular markers to functional properties by combining electrophysiology with genetics or recording followed by histology (Rau et al. 2009; Li et al. 2011; Luo et al. 2009; Ling Bai et al. 2015; Lawson et al. 2008; Koerber & Woodbury 2002; Jankowski et al. 2009), but these studies were limited by the noise inherent in single-factor molecular classification schemes. Further refinement of molecular biology techniques has since enabled the quantification of multiple transcript levels in single cells. Thus, we now have the opportunity to map function to molecular profile and use the resulting rubric to interpret changes after nerve injury and look for potential therapeutic targets.

1.2 FUNCTIONAL AND ANATOMICAL CLASSIFICATION OF PRIMARY AFFERENTS INNERVATING HAIRY SKIN

Numerous functional classification schemes have been proposed with the purpose of dividing the dorsal root ganglion (DRG) into groups of cells with similar responses to mechanical and thermal stimuli. These schemes typically recognize conduction velocity distinctions and involve a modality component (Horch et al. 1977). Additionally, distinctions are recognized between similar fiber types on the basis of their responses to equivalent stimuli or thresholds of activation. The distinction between conduction velocities (CVs) is based on the trimodal distribution of CVs observed in the sensory nerves of mammals (Burgess et al. 1968; Brown & Iggo 1967; Harper & Lawson 1985). In mice, the three modes can be split into Aβ (CV>10m/s), Aδ (10m/s>CV>1.2m/s), and C (CV<1.2m/s) fibers (Kress et al. 1992; Koltzenburg et al. 1997; Lawson et al. 2008).

In mouse hairy skin, Aβ and Aδ mechanoreceptors can be classified into three groups on the basis of their firing properties in response to square wave force stimuli (Li et al. 2011; Abraira & Ginty 2013). The first fiber type associates with hairs using multiple vertical projections parallel to the hair, termed a longitudinal lanceolate ending. These cells fire in response to dynamic mechanical stimuli, but the firing rate quickly adapts to static pressure and they typically only fire one spike to the onset and offset of a rapidly applied mechanical

stimulus. Thus, they are termed rapidly adapting (RA) fibers. They typically have low mechanical thresholds, can have Aβ or Aδ conduction velocities, and are thought to potentially encode indentation velocity (Horch et al. 1977; Brown & Iggo 1967). Recent work has split the Aβ and Aδ subpopulations, using genetic tools to show that Aβ-RA fibers tend to innervate guard and awl hairs while some Aδ-RA fibers innervate awl and zigzag hairs in the mouse and are directionally selective in back skin (Li et al. 2011).

The remaining A-fibers adapt more slowly in response to static pressure. These are subdivided into slowly adapting type I (SA1) afferents, which are Aβ fibers that associate with Merkel cells and have an irregular discharge rate in response to static pressure (Horch et al. 1974). The other slowly adapting or non-adapting fibers in mice are believed to form circumferential endings around all types of hair or free nerve endings unassociated with hairs. These two types of afferents are commonly distinguished using the coefficient of variation (CoV) of the distribution of interspike intervals during the static phase of a stimulus (McIlwrath et al. 2007; Wellnitz et al. 2010). SA1 fibers have a high CoV (>0.5) while the other slowly adapting fibers have a low CoV (<0.5).

A strong consensus has not been reached regarding the terminology for the remaining, low CoV fibers, but it has been noted that these fibers can be split into two groups on the basis of mechanical threshold. While both groups encode pressure, some will only respond to intensities of pressure that could damage the skin. These may be referred to as high threshold mechanoreceptors (HTMRs) or A-fiber nociceptors, they tend towards the Aδ conduction velocity range, and they are suspected to form free nerve endings in the skin (Burgess & Perl 1967). Low threshold, regular fibers can be either Aβ or Aδ and respond over a wide dynamic ranges (WDR) of pressures. At least some of these are likely to form circumferential endings around hairs or free nerve endings (Ling Bai et al. 2015). The term “field receptor” has recently been repurposed as a name for these WDR A-fibers (Ling Bai et al. 2015; Koerber et al. 1991). The final class of low threshold mechanoreceptors is the slowly adapting type II cells, which terminate in Ruffini endings, spontaneously discharge, and encode skin tension or stretch (Chambers et al. 1972; Chambers & Iggo 1967). These will not be discussed further due to the absence of reports of both stretch sensitive cells and Ruffini endings in mouse skin. In summary, there are three types of slowly adapting afferents in the mouse: 1) SA1 fibers, which discharge

irregularly, 2) HTMR fibers, which have high mechanical thresholds, and 3) WDR fibers, which encode force over a wide range.

Though they are reliably reported in larger mammals, thermally sensitive A-fibers are less common in the mouse and represent 25% of myelinated nociceptors or fewer in adult Swiss Webster mice (Ye & Woodbury 2010). Thermal responses are also occasionally reported in LTMRs, but opinions are divided about the validity of those reports. Most thermal stimuli possess an unavoidable mechanical component, and even truly isolated thermal stimulation causes mechanical stimulation via thermal contraction/expansion of the skin. These minor movements may explain why cooling sensitivity is occasionally reported in the most sensitive mechanical receptors (Adriaensen et al. 1983; Brown & Iggo 1967; Li et al. 2011). As such, further attention will not be given to this class of fibers in this document.

Mouse C-fibers are thought to be free nerve endings in the skin and are classified by the modalities they are sensitive to, with a single exception: C-fiber low threshold mechanoreceptors (C-LTMRs). C-LTMRs form longitudinal lanceolate endings comparable to RA fibers around zigzag and awl hairs and have very low mechanical thresholds (Li et al. 2011; Li & Ginty 2014). All other C-fibers are simply named for their modalities (e.g. a fiber responsive to pressure, warming, and cooling is a C-mechano-heat-cold). Histology can be combined with anatomy to distinguish these fibers from RA fibers. All of the fibers form longitudinal lanceolate endings, but Aβ fibers are heavily myelinated up to a point very near the hair, Aδ fibers are more lightly myelinated and demyelinate some distance from the hair, and C fibers are entirely unmyelinated (Luo et al. 2009; Li et al. 2011). This particular example represents the fusion of anatomy, function, and genetics, but attempts have also been made to determine correlated afferent function directly with histological labeling.

1.3 HISTOLOGICAL CLASSIFICATION OF PRIMARY AFFERENT TYPES

The rise of molecular biology and transgenic models has brought about a competing, non-functionally based set of classification schemes that are easiest to understand if examined in the order in which they were developed. The first lasting histological distinction was between “peptidergic” and “nonpeptidergic” afferents (Coimbra et al. 1974; Barber et al. 1979; Gibson et

al. 1981; Hunt & Rossi 1985), which mirrored the pre-existing “small dark” versus “large light” anatomical distinctions to some extent (Lawson et al. 1974). Two major markers for nonpeptidergic, unmyelinated afferents have been used: fluoride-resistant acid phosphatase (FRAP) and isolectin binding protein 4 (IB4). These two nonpeptidergic markers largely overlap, and exclude the neuropeptide substance P (SP)-expressing population in mice and rats (Taylor-Blake & Zylka 2010).

Other than SP, neuropeptides expressed in the uninjured mouse dorsal root ganglia include calcitonin gene releasing peptide α (CGRP), neurotensin (NTS), somatostatin (SST), natriuretic peptide b (NPPB), and galanin (GAL) (G Skofitsch & Jacobowitz 1985; Skofitsch et al. 1985; Gerhard Skofitsch & Jacobowitz 1985; Zhang et al. 2010). The initial definition of the “peptidergic” class focused on substance P, but was readily expanded to include CGRP as it was discovered. In rodents, CGRP labels a superset of afferents including the SP population, a myelinated population, and some unmyelinated fibers that are SP negative (Gibson et al. 1984; Lee et al. 1985). Depending on the author and publication, sometimes other neuropeptides may also be included in the peptidergic category, though for the most part “peptidergic” in modern literature is used to mean “expresses CGRP or SP.” It is worth noting that the overlap of histologically defined populations (via neuropeptide expression, the binding of IB4, etc.) varies widely between mammalian animal models (Noguchi et al. 1990; Garc a-Caballero et al. 1989; Gibbins et al. 1987; Taylor-Blake & Zylka 2010). As such, the remainder of this thesis will focus on mouse histology when at all possible.

Histology also provides the opportunity to create arbitrary classification schemes based on the staining of any given probe or combination of probes. Specific probes have been used to infer function, notably myelination and transducer expression. Markers of myelination have included Schwann cell associated proteins, like S100B (Fujiwara et al. 2014) and Necl-1 (Ho & O’Leary 2011), as well as structural elements related to larger axon diameter, like NF200 (Trojanowski et al. 1986). The explosion of known transduction channels in the last two decades (i.e. TRP family, ASIC family) has led people to use antibody staining for these channels as a surrogate for receptor function. There is unfortunately no way to know that positive antibody staining indicates functional protein expression, as the protein could be localized incorrectly or post-translationally modified to inactivity, but it is not uncommon to infer that immunoreactivity equates to channel function (Kobayashi et al. 2005; Abe et al. 2005).

A handful of studies have analyzed the correlation of function and immunoreactivity. It is difficult to generalize histological results across species, but the original work attempting to build a link between histology and function was done in guinea pig *in vivo* (Lawson et al. 2002; Lawson et al. 1997). These studies showed a link between neuropeptide expression and nociceptive character, but some low threshold mechanoreceptors were also indicated to express each neuropeptide. More recent studies done in mice have assayed for TRPV1, IB4, and CGRP immunoreactivity in characterized cutaneous afferents (Woodbury et al. 2004; Lawson et al. 2008). These studies support the idea that TRPV1 is expressed by a subset of afferents that can respond to heat but not mechanical or cold stimuli and are negative for IB4 in uninjured animals. The majority of cells labeled with IB4 were found to be C-polymodal (mechanoheat or mechanoheatcold) fibers. Antibodies for CGRP labeled several functionally characterized C-polymodal DRG cells, as well as some slowly- or non-adapting A-fiber nociceptors. A-LTMRs were not labeled by these markers, but SA1s and a subpopulation of A-fiber nociceptors have been found to be immunoreactive for TRKC and ASIC3 (McIlwrath et al. 2007). These studies do not establish decisive mappings between immunohistochemistry and cell function, but the observed correlations between immunoreactivity and function are encouraging and provide hope that such a mapping may exist.

1.4 DORSAL ROOT GANGLIA CELL TRANSCRIPTIONAL PROFILING

Several recent studies have used transcriptomic techniques to quantify differences between mouse DRG populations. Some have chosen to characterize the differences between genetically defined subpopulations of afferents (Goswami et al. 2014; Thakur et al. 2014), but the most interesting and informative have used next generation sequencing to look at RNA expression profiles of single DRG cells and sort them into groups accordingly (Chiu et al. 2014; Usoskin et al. 2014; Li et al. 2015). Each of these three studies used a slightly different method and reached different specific conclusions about the make-up of the DRG, but they do share some features. Given that this thesis is interested in the different populations of cutaneous somatosensory neurons, these studies and the methodologies employed in these studies warrant examination in

depth. This section will emphasize the strengths and weaknesses of respective studies, compare them, and offer some potential explanations for their differences.

The first of these papers came from the Woolf lab (Chiu et al. 2014). This paper used Cre-lox recombinase and RNA-seq to characterize the differences between three genetically and histochemically defined, non-overlapping populations of sensory neurons. Specifically, the authors used a Parvalbumin (*Pvalb*) Cre driver and a Voltage Gated Sodium Channel 1.8 (Nav1.8, *Scn9a*, SNS) Cre driver to cause recombination and expression of a fluorescent reporter (tdTomato) in different subpopulations of DRG cells. They further subdivided *SNS-Cre* using fluorescently tagged IB4 labeling, and then sorted the DRG cells on the basis of fluorescence. Having obtained a purified sample, the authors used RNA-seq to survey the total transcript expression in each fluorescently defined population. RNA-seq, also known as whole transcriptome shotgun sequencing, is a process wherein sample mRNA is split, reverse transcribed into short cDNA, and then sequenced. Some of the resulting sequences of cDNA can be mapped unambiguously to specific transcripts, scaled by the probability of obtaining a transcript from that gene and other assumed biases of the process, and interpreted relative to the total number of sequences obtained. Ultimately, this technique can be used to assess the abundance of all known transcripts in the sample and results are comparable within samples using exactly the same technique.

Chiu et al. (2014) compared three subpopulations of afferents, intending primarily to include all cells in the DRG within one of the three, non-overlapping populations:

- *Pvalb-Cre:tdTomato*$^{+}$ cells, a mix of (95%) myelinated and (5%) unmyelinated nonpeptidergic afferents that was used with the intention of labeling proprioceptors.
- IB4^{+}/*SNS-Cre:tdTomato*$^{+}$ cells, an unmyelinated nonpeptidergic population that is nearly identical to the nonpeptidergic nociceptor population normally labeled by IB4 alone (98%) in mouse due to the ubiquity of SNS-Cre recombination in unmyelinated afferents.
- IB4^{-}/*SNS-Cre:tdTomato*$^{+}$ cells, a mix of myelinated (30%) and unmyelinated (70%) afferents. Though it is heterogeneous, this population includes all CGRP^{+} cells that do not label with IB4, which is the majority of peptidergic afferents (Liu et al. 2009).

It is likely that this combination of Cre-drivers excludes a population of myelinated nonpeptidergic fibers that do not label with parvalbumin, but otherwise they have largely met their stated goal. The authors observed transcriptional differences between these populations

using RNA-seq and were thus motivated to look for further subpopulations using an 80 gene Taqman assay. This technique was used to analyze the expression of 334 single neurons obtained from their different, labeled populations using flow cytometry ($Pvalb^+$=92, $IB4^+$=132, and $IB4^-$/$Sns:tdT^+$=110, respectively) at unspecified spinal segments.

The authors found the 80 genes could be used to sort cells into seven distinct subpopulations. The raw data for this analysis is unavailable, but the authors suggest that the populations are approximately: I) MAS-related G-protein coupled receptor, member D positive (*MrgprD*$^+$) nonpeptidergic cells, II) Transient receptor protein cation channel, member V1 positive (*TrpV1*$^+$) peptidergic cells, III/IV) cells that did not express identifying transcripts, V) Tyrosine hydroxylase positive (*Th*$^+$) cells, VI) *Nppb*$^+$ cells, and VII) *Pvalb*$^+$ cells.

One major limitation of this work is that the 80 genes for their single cell assay were chosen from the set of genes enriched in single populations of their previous RNA-seq data. This likely decreased the informative content of their assay due to redundancy and potentially eliminated informative genes that were expressed in multiple populations due to their nonspecific population criteria. For instance, their $IB4^-$/Sns-Cre:$tdTomato^+$ population was a mix of myelinated and unmyelinated afferents. Thus, their 80 genes do not include markers of myelination and their assay fails to create a group for peptidergic myelinated fibers. Given the heterogeneous and functionally meaningless populations labeled by these Cre lines, selecting the genes for their chip using the literature would likely have been more informative.

The second paper came from the Ernfors lab (Usoskin et al. 2014). This paper used a unique form of single cell RNA-seq on 864 cells from mouse L4-6 DRGs, 242 of which were discarded for being low quality or suspected non-neuronal cells. They then used iterative principle component analysis (PCA) and cluster cutting to split off different groups of afferents. Three iterations of PCA created 8 groups, and a fourth iteration was applied at the authors' discretion.

The authors made their full data set available, so reanalysis was possible. Given that iterations of PCA involve an arbitrary cluster-cutting step, exactly recreating all their groups from this sorting scheme cannot be expected, but their data clearly supports the existence of seven of their eight third-level groups of cells. Named by their groups in the paper, these would be NF1/2/3) *Pvalb*$^-$ myelinated cells, NF4/5) *Pvalb*$^+$ myelinated cells, TH) *Th*$^+$ unmyelinated cells, NP1) *MrgprD*$^+$ unmyelinated cells, NP2/3) MAS-related G-protein coupled receptor,

member A3 positive (*MrgprA3*$^+$) unmyelinated cells, PEP1) Tachykinin-1 positive (*Tac1*$^+$) unmyelinated cells, and PEP2) *Calcα*$^+$ myelinated cells. Further subdivision of these groups may be possible but does not seem warranted by the data.

This study has several methodological advantages over Chiu et al. (2014), including a massive increase in the number of transcripts being assayed (>8,000 detectable transcripts vs. 80) and no gene selection bias. It has two issues, however, that limit the conclusions that can be drawn from the data. First, this study shows a very strange preference for specific subpopulations of cells. The *Th* population makes up 37% of their cells (TH$^+$ DRG estimations – rat: 1% (Price & Mudge 1983), mouse: 10-15% (Brumovsky et al. 2006)), while myelinated peptidergic fibers (PEP2) account for only 3% of their cells (NF200$^+$/CGRP$^+$ colocalization estimation – mouse: 11% (Li et al. 2015), 24% (Kestell et al. 2015)). After reviewing the data, the bias towards the TH population appears to potentially be caused by cluster cutting decisions, but the bias away from the PEP2 population is difficult to explain. The apparent presence of cell selection bias indicates that the final distributions may not be representative and could be missing populations.

The second issue with this study is their inability to detect the expression of certain transcripts, which is likely due to the chosen cDNA library creation method before amplification and RNA-seq. Unlike standard RNA-seq, which uses probability to account for the 5'-bias of reverse transcription, the author's reverse transcription method requires the creation of a full-length cDNA transcript (Islam et al. 2012). Unfortunately, mRNA transcripts have secondary structure that may make them difficult to reverse transcribe. Some particularly long and complicated transcripts may be unlikely to ever create a full length cDNA, which will subsequently make them nearly impossible to detect using this technique. As such, many transcripts in this study are not detected at the prevalence one would expect and the relative level of any individual gene needs to be interpreted with caution. There is no reason to believe that these gene biases are unevenly distributed throughout the different populations, so they likely have no impact on the clustering.

The final paper came from the Zhang lab (Li et al. 2015). This paper did single cell RNA-seq on 197 cells from L5 mouse DRGs (64 IB4$^+$ small, 69 IB4$^-$ small, and 64 large). These cells were subsequently clustered based on the 1,745 differentially expressed genes, which created 8 populations. Despite initially identifying 8 populations, the authors go on to discuss ten populations for the rest of the paper, some of which have very few members (C7: 3, C10: 2).

Based on a heat map of selected genes, the ten populations are: C1) small *Gal*$^+$ cells, C2) *Nppb*$^+$, C3) *Th*$^+$, C4) *MrgprA3*$^+$, C5) *MrgprD*$^+$, C6) *MrgprD*$^+$/S100b$^+$, C7) *Pvalb*$^+$/S100b$^+$, C8) *S100b*$^+$, C9) *Htr1d*$^+$/*S100b*$^+$, C10) large *Gal*$^+$ cells.

Unlike Chiu et al. (2014) and Usoskin et al. (2014), this paper also attempted some *in vivo* L5 cutaneous physiology to identify afferent properties, which they followed with aspiration and single cell PCR for 14 transcripts. Cells were assigned to a group based on the prevalence of these 14 population-marking transcripts as measured. The exact assignment method is unclear and the data are unavailable, although the authors do note that cells which failed to fit into any other group were put in class C6. It is also not clear how they identified cutaneous cells, as some cells appear to be insensitive to all stimuli. Regardless, they classified 69 afferents and generated some unexpected results. Every *Th*$^+$ cell responded to brush, but not necessarily to more intense pressure or pinch. The *MrgprA3*$^+$ population was 1/3 of their recorded afferents. They only recorded five *MrgprD*$^+$ afferents, and only two of those were mechanically sensitive. These results disagree substantially with the literature and have some internal consistency issues that render them questionable (i.e. some groups have characterized fibers that are insensitive to all stimuli).

In a similar vein, the Li et al. (2015) RNA-seq survey data is available for reanalysis but does not include a mapping between cell and the assigned cell group. It has a total of 204 samples, with 7 outliers that were discarded. Despite the presence of outliers, the cell indexing is nonsequential and the *Actb* and *Gapdh* expression average/standard deviation values differ from the values presented in the paper. It is not possible to replicate their analysis or figures without substantially more information than is presented in the paper.

Although each of these three studies assessed single cell expression differently, they were all assessing the distribution of transcriptional profiles of mouse DRG cells. As such, it is possible to make an approximate composite of the different studies (Figure 1). It is difficult to decisively place the data from Li et al. (2015) into the classification scheme, but the data from Chiu et al. (2014) and Usoskin et al. (2014) tell stories that largely agree with each other and previous histology literature. Though it has always been clear that the DRG is functionally and histologically heterogeneous, these studies make it clear that the heterogeneity is finite and not a continuous spectrum of cell properties and expression. Now that we grasp the root of this

heterogeneity, it is possible to investigate how the populations may be differentially affected following injury.

	Myelinated				Unmyelinated					
Woolf	#N/A	#N/A	#N/A	VII	II*	VI	II*	I	V	#N/A
Ernfors	PEP2	NF3	NF1/NF2	NF4/NF5	PEP1	NP3	NP2	NP1	TH	#N/A
Zhang	C8-2	C8-1(/C7?)	C9-1/C9-2	C7	C1(/C10?)	C2	C4	C5(/C6?)	C3	C8?
Markers	Nefh TrkA Calcα	Nefh Asic1 TrkC	Nefh Gfrα2 TrkB?	Nefh Pvalb	Tac1 Gfrα3 TrpV1 Calcα Gal	Sst Nppb TrpV1	MrgA3 Gfrα1 Calcα	MrgD Gfrα2 P2rX3	Th Gfrα2 P2rY1	Tac1 TrpM8 Asic1

Figure 1. Summary of single cell transcriptome studies. Markers were used to identify a given population in at least one study and largely agree with mouse immunohistochemistry results. The color code for populations will be kept consistent throughout this thesis.

1.5 NERVE INJURY AND REGENERATION IN HUMANS

Peripheral nerve injury primarily occurs in humans during violent accidents or surgeries. These injuries can be split into two different categories on the basis of whether or not the endoneurium remains intact (Seddon 1943). Nerve injuries that do not disrupt the endoneurium are named axonotmesis, a separation of the axons. Axonotmesis is frequently caused by nerve stretching or crush and is a common outcome of high speed impacts. Regenerative prognosis is promising in these cases. Nerve injuries that do disrupt the endoneurium are termed neurotmesis, a separation of the nerve. These injuries are caused by trauma, and specifically transection of the nerve. Neurotmesis regenerative progress in these cases can be stymied by the formation of a neuroma. Fortunately, axonotmesis is more common than neurotmesis by a factor of 9:1 (Razaq et al. 2015).

Following either type of injury, axons in the proximal stump of the injured nerve undergo Wallerian degeneration and retreat back to their cell bodies in the dorsal root ganglia. The orphaned distal axons degrade themselves while injured cells form an axonal growth cone and send their axons back out along the remaining endoneurium pathways in an attempt to return to their original target tissue. In the event of neurotmesis, Schwann cells form an axonal bridge

connecting the severed endoneurium segments and the axons must cross the bridge. If successful, after reaching a target tissue the axons will reinnervate their target sensory structure (muscle spindle, Merkel cell complex, hair follicle, Pacinian corpuscle, etc.). Problems with pathfinding are not uncommon; motor neurons have been observed projecting to sensory organs and vice versa (English 2005; Brushart 1988; Langley & Hashimoto 1917; Koerber et al. 1989). Cells that fail to reinnervate properly can die, presumably for want of neurotrophic factors (McKay Hart et al. 2002).

Even in the case of axonotmesis, full functional recovery of long sensory nerves in humans, as quantified with psychophysical tests, is rare and the regeneration process can last for almost a year (Razaq et al. 2015; BULUT 2015; Deng et al. 2016; Lu Bai et al. 2015; Jaworucka-Kaczorowska et al. 2015). This injury and regenerative process can result in hyposensitivity, paresthesia, and neuropathic pain, any of which can become chronic. Hyposensitivity is the most direct consequence of sensory denervation (De Alvarenga Yoshida et al. 2012; Bagheri et al. 2009; Bagheri et al. 2010). Paresthesia, abnormal sensations that typically manifest as a pins and needles sensation, can be induced by pressure on a regenerating peripheral nerve and is used diagnostically as a way to identify regenerating nerves (e.g. Tinel's sign). Patients find these sensory aberrations aversive, and they represent the chief complaint in the majority of patients (Susarla et al. 2007).

The final symptom of a regenerating peripheral nerve is neuropathic pain, which is thought to be present in 6 to 10% of the population (Van Hecke et al. 2014). Neuropathic pain can be spontaneous or evoked through somatosensory stimulation (Jensen & Finnerup 2014). Both types of pain dramatically affect quality of life for suffers, and both types are thought to rely to on primary somatosensory afferent input (Haroutounian et al. 2014). Evoked neuropathic pain, which is pain in response to stimulus, necessarily involves somatosensory transduction (Truini et al. 2013). It can be classified as either hyperalgesia, an exaggerated pain response to a painful stimulus, or allodynia, a painful response to a nonpainful stimulus.

Studies currently treat all regenerating axons as equals, only occasionally differentiating between motor and sensory regeneration, and do not consider the massive variability in afferent type when doing regeneration research. It could be that allodynia and hyperalgesia are a byproduct of aberrant expression of transduction channels in afferent subpopulations that do not normally express them.

1.6 TRANSCRIPTIONAL CHANGES DURING NERVE INJURY AND REGENERATION

Injured primary sensory neurons undergo a two stage process during regeneration. Immediately following injury injured neurites fire rapidly and their activity triggers a Jun-kinase cascade (Berdan et al. 1993; Leah et al. 1991). Those changes combine with the loss of normal internal axonal signaling as well as target-tissue-supplied neurotrophic factor and account for the first influence on the afferents' transcriptional profiles (Makwana & Raivich 2005). These now-altered cells form an axonal growth cone that migrates down the uninterrupted epineurial sheaths. When the growth cone reaches a target tissue, it receives a new complement of neurotrophic factors that triggers a second transcriptional shift. This second transcriptional shift attempts to restore the neuron back to its original state (Jankowski et al. 2009).

The expression of various growth factors, transduction channels, and structural elements are changed after nerve injury in these regenerated axons (Jankowski et al. 2006; Jankowski et al. 2008; Reinhold et al. 2015). Previous literature has typically not examined the potential subpopulation-specific nature of these changes, but it seems likely that there would be subtype dependence, given the massive transcriptional heterogeneity that exists within the uninjured dorsal root ganglia (Usoskin et al. 2014; Chiu et al. 2014). It is also uncommon to see transcriptional analysis of reinnervated afferents. Work from our lab has examined changes in expression following saphenous axotomy at the whole DRG level and found that some transcripts, including *TrpV1* and *Asic3*, were still elevated ten weeks after nerve injury (Jankowski et al. 2009).

There exists a substantial body of literature that assess DRG transcriptional changes in Sprague-Dawley or Wistar rats following sciatic nerve injuries (crush, axotomy with resection and/or ligation) or L5 spinal nerve root injuries (spinal nerve ligation, spinal nerve injury). Rat subpopulations may not be identical to mice. IB4 labels a larger population of fibers that overlaps with the peptidergic subpopulation, and some types of fibers are myelinated in rats that are not myelinated in mice. Regardless, agreement between rat studies and the two mouse studies on transcriptional changes after nerve regeneration does increase confidence in the latter's results (Jankowski et al. 2009; Staaf et al. 2009).

Changes in expression are commonly quantified either through histology as the change in percent of cells positive for a given marker or through molecular biology as a change in mRNA or protein levels. These two approaches seem different, but every relative labeling method uses a threshold to determine which cells are positive for the relevant marker. As such, an increase in the percent of cells labeled by a given marker does not necessarily reflect *de novo* expression, and could just be an increase in level in sub-threshold expressing cells. Likewise, an increase in mRNA or protein level does not necessarily reflect an increase in expression within the normal population for a given protein and could reflect *de novo* expression. Papers assessing nerve injury changes have tended to use histological methods to assess expression changes after injury, and the results agree with whole DRG mRNA level changes and protein level changes when examined.

Neuropeptides levels change after injury. The proportion of cells expressing substance P, CGRP, and SST all decrease after injury, while neurotensin (NT), galanin (Gal), and vasoactive intestinal peptide (VIP) increase (Jessell et al. 1979; Nielsch et al. n.d.; Doughty et al. 1991; Zhang et al. 1995; Zhang et al. 1996; Rydh-Rinder et al. 1996; Bennett et al. 1998; Bennett et al. 2006; Brumovsky et al. 2006; Staaf et al. 2009; Wang et al. 2014; Medici & Shortland 2015). These changes are typically reported to be transient and revert to near normal levels three weeks after injury. There are no obvious differences reported between the different types of injury (L5 spinal nerve axotomy or sciatic axotomy mid-thigh) or species (rat, guinea pig, or mouse).

Voltage-gated ion channels are also regulated after injury. Voltage-gated potassium, calcium, and sodium channels have all been examined extensively (Ishikawa et al. 1999; Fukuoka et al. 2015; H.-S. et al. 2002; Dib-Hajj, Black, et al. 1998; Dib-Hajj et al. 1996; Kim et al. 2001; Kim et al. 2002). Changes in voltage-gated sodium channels (Nav) are particularly interesting, as this class of channels is responsible for the upswing of the action potential and subthreshold gain. Upregulation of Nav 1.3 and downregulation of Nav1.8 and Nav1.9 have been consistently reported (Dib-Hajj et al. 1996; Kim et al. 2001; Dib-Hajj, Tyrrell, et al. 1998). Nav1.3 and 1.8 each are responsible for moving the majority of current during an action potential, so this pair of changes can be seen as a substitution of the slowly activating and inactivating Nav1.8 for the rapidly activating and inactivating Nav1.3 (Rogers et al. 2006). The downregulation of Nav1.9 likely decreases cellular excitability, as Nav1.9 largely constitutes a

leak current in naïve DRG cells that is thought to keep cells slightly closer to the activation threshold (Baker & Bostock 1997).

Finally, neurotrophic factor receptors are differentially regulated after nerve injury, which is important because the effects of their agonists are diverse and well documented (Godinho et al. 2013). Growth factor receptors (Gfr) 1 and 3 are upregulated, while *Gfr2* is downregulated (D. L. Bennett et al. 2000; Kashiba et al. 1998; Bennett et al. 1998; Jankowski et al. 2009). Regulation of the Tropomysin receptor kinase (Trk) family, which also responds to growth factors, is more nuanced. TrkA is reported to decrease following nerve injury (Krekoski et al. 1996; Kashiba et al. 1998; Webber et al. 2008), but is elevated in the regenerating proximal nerve stump (Webber et al. 2008). This could reflect axonal localization of TrkA mRNA and subsequent axonal protein synthesis, which is known to occur in regenerating axons (Zheng et al. 2001). TrkB is upregulated one day after nerve injury, but returns to baseline by three days post-injury (Funakoshi et al. 1993). TrkC levels do not seem to change following injury (Funakoshi et al. 1993).

Agonists for these channels tend to be neuroprotective in dissociated cultures of DRG cells (Bennett et al. 2006; Bennett et al. 1998; Omura et al. 2005). *In vivo*, however, the complicated chemical environment of the regenerating axon makes it very difficult to predict exactly what role each individual neurotrophic factor receptor plays at physiological concentrations. siRNA mediated knockdown reveals potential receptor-expression dynamics, with each receptor affecting the expression of a constellation of different proteins and ultimately affecting physiological phenotype. Artemin/GFRα3 signaling, for instance, causes increased TRPV1 expression, which in turn causes increased heat sensitivity (Jankowski et al. 2012; Jankowski et al. 2010; Ikeda-Miyagawa et al. 2015).

1.7 PHYSIOLOGICAL CHANGES FOLLOWING NERVE REINNERVATION

Transcriptional changes are accompanied by alterations in the functional properties of neurons. Previous work from our lab has shown that certain populations of regenerated axons are very different from axons that have never been axotomized, and that some of those changes can persist for at least 12 weeks (Jankowski et al. 2009). Regenerated A-fiber nociceptors, as well as

C-mechanoheat and C-mechanoheatcold cells, all showed a decrease in heat thresholds that lasted at least 12 weeks. The polymodal C-fibers also showed an increased maximal firing frequency during heat ramps (Jankowski et al. 2010). Additionally, it appears that the proportion of mechanically insensitive, heat sensitive C-fibers significantly increases (Koerber et al. 2010; Jankowski et al. 2009). These populations of regenerated afferents appear to be sensitized to thermal stimuli, which could manifest perceptually as thermal hyperalgesia.

Mechanical transduction changes were also found following injury in both LTMR populations and nociceptors. SA1 afferents showed decreased firing rates following axotomy and regeneration, possibly reflecting the atrophied associated Merkel cell complex essential for their normal function (Jankowski et al. 2009; Nurse et al. 1984a; Nurse et al. 1984b; Maricich et al. 2009; Baumbauer et al. 2015). A-fiber nociceptors showed substantially decreased thresholds 4-6 weeks after injury that recovered by 10-12 weeks (Jankowski et al. 2009). C-fibers show a more long-lasting, but also more subtle change. Under normal conditions, TRPV1 expression is restricted to mechanically insensitive heat sensitive fibers (C-heat; CH), but a population of mechanically sensitive $TRPV1^+$ DRG cells emerges following nerve injury and regeneration. This could reflect a gain in mechanical sensitivity in the heat sensitive, peptidergic population that normally projects into Lamina I-IIo and contacts the projection neurons thought to be involved in the perception of pain. Thus, the gain of mechanical sensitivity in these fibers could be involved in mechanical hyperalgesia or allodynia.

A number of these changes were shown to be blocked by the manipulation of transcript expression levels. Immediate post-injury *Gfrα3* or sustained *TrpV1* knockdown reverses the expansion of the C-heat population (Jankowski et al. 2010; Jankowski et al. 2012). *Gfrα3*, but not *TrpV1*, knockdown also eliminates gain of mechanical sensitivity in the CH population. Notably, however, axotomy-induced mechanical threshold changes in myelinated nociceptors were consistently unaffected, and no mechanical transducer has been conclusively tied to either of the injury-induced mechanical phenotypes.

In summary, there are changes to the functional properties of specific nociceptor subpopulations that potentiate both mechanical and thermal transduction in specific subpopulations. These changes could be reflected perceptually as hyperalgesia. Some of the thermal changes can be blocked by knockdown of specific transcripts, but the transducers necessary for the mechanical transduction changes are currently unknown.

1.8 THE ROLE OF PIEZO2 IN CUTANEOUS MECHANOSENSATION

PIEZO2 is one possible candidate for these mechanical transduction changes. The PIEZO proteins are a family of two recently discovered transduction channels that respond transiently and proportionally to mechanical force (Coste et al. 2010). When overexpressed in heterologous expression systems, both family members cause rapidly inactivating currents in response to cell membrane deformation. Both family members are expressed at similar levels in mechanosensitive organs including the lungs, colon, and bladder. However, the two proteins are differentially expressed in the skin and the DRGs. PIEZO1 levels are high in the skin, while PIEZO2 levels are high in the DRGs. While either could be involved in cutaneous transduction of mechanical force, this discussion will focus on PIEZO2 as it is expressed in sensory neurons and has been shown to be important for mechanosensation (Ranade et al. 2014).

The primary evidence for the involvement of PIEZO2 in mechanical transduction comes from dissociated DRG cells that were cultured for 2-3 days before recording (Coste et al. 2010). In this experiment, DRG cells were whole-cell patched and recorded while being probed using a glass rod held by a micromanipulator in 1μm increments. The resulting currents were fit to an exponential decay formula and their decay constant was recorded. The authors choose to split their results into four groups, mechanically sensitive cells, cells $\tau<10$ms, 10ms$<\tau<$30ms, and $\tau>30$ms based on a weakly bimodal distribution of τ values (at 10ms) with a long tail (>30ms). In order to analyze the effect of PIEZO2 on these cells, the distribution of mechanical currents observed in each of these three categories was compared between cells transfected with *Piezo2* siRNA and scrambled siRNA. The authors observed a decrease in the number of cells with mechanical current τ below 10ms and an increase in the number of mechanically insensitive cells, implying that PIEZO2 expression is essential for mechanical transduction in a subpopulation of DRG cells.

Good evidence that these cells are essential for hind limb motor coordination came from studies of a transgenic mouse that has *Piezo2* knocked out of certain sensory neurons, including the proprioceptive afferents (*Piezo2*^{CKO}*/Pvalb-Cre* animals) (Woo et al. 2015; Florez-Paz et al. 2016). These animals were observed to be uncoordinated, almost as if they have limited joint position feedback. The two qualifications that accompany these papers are that Pvalb-Cre has never been validated as an exclusive marker of proprioceptors in mice (Hippenmeyer et al. 2005)

and the behavioral assays used (balance beam, two limb hanging, and rotarod) (Florez-Paz et al. 2016) measure proprioception only to the extent that proprioception manifests as coordination. However, the behavioral phenotype is striking in video form and it is clear there is some kind of deficit because the animals are visibly less coordinated than their wildtype counterparts. The phenotype becomes even more striking when *Piezo2* is knocked out of most neural tissues caudal to C4 using the HoxB8-Cre driver (Witschi et al. 2010; Woo et al. 2015). This driver unfortunately also knocks *Piezo2* out of a variety of nonneuronal tissue, including striated muscle, and it is possible that these effects are developmental to some degree, but a convergence of evidence does seem to indicate that PIEZO2 expression is essential for limb position information.

The importance of PIEZO2 to cutaneous mechanosensation has also been investigated, but the evidence for it is less compelling (Ranade et al. 2014). In this paper, *Piezo2* is conditionally removed from most sensory neurons in adulthood using *Piezo2*^{CKO}*/Advillin-CreER2* mice. This transgenic inducible knockout animal was assessed using an *ex vivo* skin-nerve preparation, leading to three main findings. First, there was a reduced number of mechanically sensitive Aβ fibers, as assessed by comparing electrical responsiveness to mechanical responsiveness. Next, the authors found a reduced firing rate during ramp stimuli for slowly and rapidly adapting fibers (>1mm/s and 16mm/s, respectively). Finally, the authors found an increase in mechanical threshold (75mN to 150mN) for Aδ slowly adapting fibers. They did not detect changes in down hair (D-hair) fiber ramp responses or C-fibers and A-nociceptors firing rates in response to constant mechanical force. The distribution of fiber types recorded was not significantly different between *Piezo2* knockout animals and wildtypes. There are some issues with the data set, namely that they do not use a consistent threshold for distinguishing Aβ and Aδ fibers, as can be seen in their Extended Figure 5, and the distribution of A-fiber conduction velocities appears to be continuous. As published, however, the paper shows that PIEZO2 expression is important for velocity encoding in uninjured Aβ fibers and that PIEZO2 levels control the threshold of Aδ mechanoreceptors.

Behavioral observations revealed a deficit in von Frey response rates at mechanical forces below 3 grams, as well as decreased responses to swiping the animal's feet with a cotton swab and decreased number of attempts to remove a piece of sticky tape stuck to their back (Ranade et al. 2014). Animals also no longer found the movement of a shaking platform

aversive. There are two ways to interpret these results. Given the proprioceptive phenotype revealed in (Woo et al. 2015), the ability of animals to detect a shaking table can potentially be explained as an inability to detect joint movement and failures to respond to innocuous stimuli could reflect a change in response ease rather than changes in stimulus detection. Alternatively, it could be that PIEZO2 expression is important for low threshold mechanosensation.

The lack of a reported proprioceptive phenotype in (Ranade et al. 2014) is somewhat confusing given the larger manipulation (~20% of cells for *Pvalb-Cre* vs. ~90% of cells for induced Advillin-CreER2). One explanation is developmental; proprioceptive phenotypes were generated by knockouts of *Piezo2* early in development, while the Advillin-CreER2 knockout was in adults. Another possibility is that the proprioceptive phenotype was observed but not reported. Finally, it could be that the Pvalb-Cre and HoxB8-Cre both label a complete, essential population, while adult Advillin-CreER2 induction spares enough of the population that the remaining expression is sufficient for normal limb coordination.

Regardless, current literature suggests that PIEZO2 is important for normal proprioception and likely is also important for innocuous cutaneous mechanosensation. The mechanical changes observed following nerve injury do not involve these specific subpopulations of afferents, but they do likely involve a channel capable of transducing low threshold mechanical inputs. It could be that *Piezo2* is upregulated in a population of regenerated afferents where it does not normally appear, thus giving rise to mechanical hyperalgesia. In order to address this possibility, we have utilized single cell qPCR, a technique that will allow us to assess mRNA levels in individual cells and assign them to subpopulations based on their transcription profiles.

2.0 TRANSCRIPTOME PREDICTS FUNCTION IN PRIMARY AFFERENTS

The experiments described in this section are part of a manuscript prepared by myself.

My contributions:

-Discussing experimental design and data analysis with Dr. Koerber.

-Writing the manuscript, with edits from Dr. Koerber.

-Collecting data for all figures.

-Analyzing data for all figures.

Contributions from other authors:

-Rob Friedman did all single cell PCR and primer design contained herein.

-Figure 4 - Dr. Shah assisted with the calcium imaging and provided insight into proper calcium imaging data analysis procedures.

-Dr. Jankowski pioneered cell recovery following saphenous *ex vivo* recording.

-Dr. Baumbauer substantially refined the technique and transferred it to me.

2.1 INTRODUCTION

Primary afferent function is often implied using non-functional properties. Somal diameter has been used to infer nociceptive character (Holzer 1991). Tyrosine hydroxylase expression has been used to infer low mechanical threshold (Kupari & Airaksinen 2014). Menthol responsiveness has been used to infer cells are cold sensitive (Abe et al. 2005). Some of these rules are accurate, but many are at least partially inaccurate simplifications. For instance, it has been recognized for years that both myelinated and unmyelinated cells can be nociceptors (Burgess & Perl 1967) and tyrosine hydroxylase expression in murine sensory neurons is primarily restricted to small cells (Brumovsky et al. 2006). Given the extreme heterogeneity of

DRG afferents, it is unsurprising that these single-factor rules often fail. However, the application of next generation sequencing techniques to single cells has opened the door for multi-factor analyses that could potentially provide a molecular signature for function.

The function of any given afferent is determined by its area of innervation and protein expression, which determine the stimuli it is exposed to and its ability to transduce and transmit them. The action potentials of two cells with identical protein expression may cause very different sensations if one projects to skin while the other projects to the colon, not only because they will be exposed to very different stimuli, but also because the spinal cord circuits they project to may be different (Koerber et al. 1991). Similarly, fibers projecting to a single target tissue can show heterogeneous protein expression, which allows them to respond to different modalities and in different ways to the same modality. In this study, we have chosen to focus on understanding how the molecular profile of cutaneous fibers contributes to their functional properties when transducing physiologically relevant stimuli. This system is very well functionally characterized, with groups of afferents that are clearly distinguishable by their functional properties.

Unfortunately, single cell proteomic techniques still have a few hurdles to overcome before they become viable, but techniques to assess single cell mRNA levels, a proxy for protein expression, have been in use for over a decade. The data generated by surveying primary afferents using single cell PCR techniques can be used to create transcriptional afferent classification schemes (Usoskin, 2015; Chiu, 2015) that represent the coordinated regulation of many different mRNA, and thus may predict function. However, there also exists the possibility that single cell mRNA levels themselves are indicative of function. Previous work by Schulz et al. (2006) successfully correlated mRNA amount with ion channel conductance in the *C. borealis* stomatogastric ganglion. If this were the case, a more accurate predictor of function might be transducer mRNA levels. Later, I will investigate the merits of both possibilities.

Herein, we have 1) shown we can identify these transcriptionally distinct groups via single cell qPCR with a limited set of genes; 2) determined the correlation between mRNA and functional protein expression using calcium imaging; 3) examined how well transcriptional group or specific transducer expression predicts function.

2.1.1 Animals

Experiments were conducted on adult (4-8 week) Swiss-Webster mice (Hilltop Farms or Jackson Labs). Animals were group-housed with a 12-hour light-dark cycle and *ad libitum* access to food and water. The initial survey used four animals for each dye, and care was taken to ensure the animals were sampled evenly. All procedures were approved by the Institutional Animal Care and Use Committee at the University of Pittsburgh and were in accordance with AAALAC-approved practices. No differences were observed between animal providers.

2.1.2 Backlabeling

Mice were anesthetized with isoflurane (2%) and an incision was made on the medial surface of the right thigh, near the knee. The saphenous nerve was isolated with the minimum amount of soft tissue damage and insulated from the surrounding tissues using parafilm. The chosen dye (1% Alexa 488-Isolectin binding protein 4 [IB4], 1% Alexa 488-wheat germ agglutinin [WGA], or 0.5% Alexa 488-cholera toxin subunit β [CTB]) was injected into the nerve via a quartz pipette using a picospritzer (World Valve Corporation, Picospritzer II). The area was rinsed with saline, the parafilm was removed, and the wound was closed using silk sutures.

2.1.3 Cell dissociation and pickup

Twenty four hours after backlabeling, L2 and L3 DRGs were removed and dissociated as described previously (Malin et al. 2007). Briefly, DRGs were treated with Papain (30 U) followed by Collagenase type II (10 U) and Dispase type II (7 U), centrifuged (1 minute at 1000RPM), triturated in MEM, and plated onto laminin-coated coverslips in 30mm diameter dishes. Cells were cultured in an incubator at 37^{o}C for 45 minutes. Dishes were removed and flooded with collection buffer (140mM NaCl, 10mM Glucose, 10mM HEPES, 5mM KCl, 2mM $CaCl_2$, 1mM $MgCl_2$). Twelve labeled cells were picked up from each animal's cultures using glass capillaries (World Precision Instruments) held by a 3-axis micromanipulator, transferred to tubes containing 3uL of lysis buffer (Epicentre, MessageBOOSTER kit), and stored at -80^{o}C.

Qualitative cell size measurement was noted, and effort was taken to sample both large and small cells from WGA and CTB backlabeled animals. Cells were found and captured within 1 hour of removal from the incubator and within 4 hours of removal from the animal.

2.1.4 Calcium imaging

Cells were dissociated from L2 and L3 DRGs as described above and incubated with 2µM Fura2AM calcium indicator dissolved in HBSS (imaging media) for thirty to sixty minutes before recording. The coverslips were moved to the inverted microscope (Olympus), where they were continuously superfused with HBSS using a tribarrel drug application device (Exfo Burleigh PCS-6000). A suitable field of view was located and ROIs were marked over cells identified with the white light transmittance. Experimentation and shutter control was automated (Lambda DG-4/Lambda 10-B, Sutter Instruments) and two application protocols were used: 1 second 50µM αβmeATP, 1 second 50mM K^+, and 1 second 1µM capsaicin, or 5 seconds 100µM 2-methylthioADP, 1 second 50mM K^+, and 1 second 1µM capsaicin. Following imaging, a 3-axis micromanipulator with borosilicate glass electrodes was used to pick up cells into 3µL of lysis buffer (Epicentre, MessageBOOSTER), their ROI identifier was recorded, and the cells were stored at -80ºC until they could be amplified.

2.1.5 Single cell amplification and qPCR

The RNA collected from each cell was reverse transcribed and amplified using T7 linear amplification (Epicentre, MessageBOOSTER kit for cell lysate), cleaned with RNA Cleaner & Concentrator-5 columns (Zymo Research), and assessed using qPCR as described previously (Jankowski et al. 2009) with optimized primers and SsoAdvanced SYBR Green Master Mix (BIO-RAD). Cycle time (Ct) values were determined via regression. Quantification threshold for PCR was defined as the point at which there was a 95% replication rate (35 Ct) (Reiter et al. 2011). GAPDH threshold was thus defined as 25 Ct to ensure we were capable of detecting transcripts at least a thousand-fold less common than GAPDH in all cells. The amount of effort spent validating this technique and choosing these thresholds for quantitation cannot be

understated, and further validation details and proofs are available in Appendix A.

2.1.6 Primer creation and validation

Unique forward and reverse primer sequences (Figure 17) were chosen for each gene within 500 bases of the 3' end. Stock solutions of cDNA were generated by extracting RNA from the whole DRG as described in Jankowski et al. (2009) and both 10 and 160pg aliquots of the RNA were amplified using the same procedure described above for single cells. Serial dilutions of these aliquots were used to calculate primer efficiencies (Figure 17) over the range of RNA concentrations observed in single cells as described in Pfaffl (2001). Expression is determined relative to GAPDH and corrected for these primer efficiencies (Pfaffl 2001), which was found to gives more consistent results than our transcriptional spike.

2.1.7 *Ex vivo* saphenous preparation (functionally defined sensory neurons)

The saphenous *ex vivo* preparation has been described previously (McIlwrath et al. 2007; Lawson et al. 2008). Briefly, mice were anesthetized with a Ketamine (90mg/kg)/Xylazine (10mg/kg) mixture and perfused using 10-12^{o}C oxygenated (95% O_2/5% CO_2) ACSF (127mM NaCl, 26mM $NaHCO_3$, 10mM D-glucose, 2.4mM $CaCl_2$, 1.9mM KCl, 1.3mM $MgSO_4$, 1.2mM KH_2PO_4). The spinal column and right hindlimb were removed and placed in a circulating bath of the same oxygenated ACSF. The hairy skin was isolated with the connected saphenous nerve, L1-L5 DRGs, and associated spinal cord, and was transferred to a second recording chamber with circulating oxygenated ACSF, where they were slowly heated to 31^{o}C.

DRG cells were impaled using quartz microelectrodes (>200MOhm) containing 0.05% Alexa dye (555 or 488 nm) in 1M potassium acetate. Electrical search stimuli were delivered using a suction electrode on the saphenous nerve. Mechanical receptive fields were discovered using a brush and further localized using Von Frey filaments or a small glass rod. If no mechanical receptive field was found, thermal fields were detected by applying hot (52^{o}C) or cold (0^{o}C) saline (0.9%) to the skin. Cells without receptive fields were not characterized further.

Once the receptive field was located, peripheral conduction velocity was calculated using spike latency and the distance between stimulation and recording electrodes. Controlled

mechanical stimuli (square waves) were presented using a force-modulating mechanical stimulator (Aurora Scientific) with a 1mm diameter plastic foot. Thermal stimuli (rapid cooling to 4^{o}C or a 12s heat ramp from 31 to 52^{o}C) were presented using a 3mm by 3mm Peltier element (Yale University Machine Shop). Cells were given 30 seconds to recover between stimuli. After characterization, cells were iontophoretically filled with Alexa dye. Following the experiment, DRGs were removed, dissociated, and the labeled cells were collected and amplified as described above. Stained cells were recovered after dissociation 30% of the time and successfully amplified 75% of the time (23% final rate, 39/173 stained cells.) Responses were analyzed offline (Spike2 software, Cambridge Electronic Design).

2.1.8 Automated hierarchical clustering

All backlabeled and functionally characterized cells were clustered using the unweighted pair group method with averaging (UPGMA) on the expression information obtained from single cell PCR. Our preprocessing for this data analysis consists of taking the ΔCt values, replacing the samples that failed to generate a value for a given gene with the detection limit for that gene. We then use MATLAB's UPGMA implementation, which clusters agglomeratively using Euclidean distance. For display purposes, characterized cells were removed from Figure 2 and presented later.

2.2 RESULTS

2.2.1 Clustering cutaneous afferent types by single cell qPCR

Eighty-one cutaneous cells for single cell qPCR were obtained by backlabeling the saphenous nerve with commonly used tracers (IB4 n=14, WGA n=56, and CTβ n=11), with another thirty nine obtained through *ex vivo* recording and subsequent cell pickup. The specific tracers used were chosen due to their prevalence in the literature and preference for different subpopulations of afferents. The tracer IB4 is thought to label unmyelinated nonpeptidergic fibers, while WGA

allegedly has a peptidergic bias and CTB is known to label nonpeptidergic myelinated fibers. When combined with blindly recorded cells, this approach allowed the generation of a comprehensive distribution of cutaneous afferents, which were then clustered autonomously and interpreted. The emergent groups were most similar to the classification scheme put forth by the Ernfors lab (Usoskin et al. 2014), so we will be drawing analogy to their groups when appropriate.

The last node in the cell dendrogram (Figure 2D) splits the cells into two groups that can be distinguished by their expression of Neurofilament heavy chain (*Nefh*) transcript levels, a part of the NF200 complex that is commonly used as a myelination marker. The low-*Nefh* cluster can be further subdivided into six populations of putative unmyelinated fibers, each with an identifying gene marker. The green *MrgprD*-containing cluster (MrgprD, Ernfors group: NP1) is nonpeptidergic and contains some of the highest levels of *P2rX3*, *Asic2*, and *Gfrα2*, as would be expected from the extensive literature on this population (Dong et al. 2001; Rau et al. 2009; Zylka et al. 2005). It is labeled the most prevalently with IB4, and is likely our closest analog for the IB4+ population.

The pink *Sst*-containing cluster (Sst, Ernfors group: NP3) is mostly identified and distinguished from the yellow cluster that has high levels of *MrgprA3* (MrgprA3, Ernfors group: NP2) by its *Sst* expression and lower levels of *TrkA*. Both clusters contain some level of *MrgprA3* and *TrpV1* with low to undetectable levels of *Gfrα2*. The *Sst* population has been previously identified as being separate from the SP population (Hökfelt et al. 1976), but the uniqueness of these cells was not fully appreciated until recently (Usoskin et al. 2014; Stantcheva et al. 2016). Similarly, *MrgprA3* was identified as a population unique from the *MrgprD* population that is positive for TRPV1, P2X3, CGRP, and c-RET protein expression, but not NF200 complex or SP (Liu et al. 2009; Han et al. 2013). Although on average there is 11 times more *MrgprA3* in the MrgprA3 subpopulation than the *Sst*-containing group (t-test: $p=0.011$), there have been reports in the literature that *MrgprA3* colocalizes with another marker for the NP3 population, *Nppb* (Mishra & Hoon 2013), indicating that there may be functional MRGPRA3 expression in both populations.

The red *Tac1*-containing cluster (Tac1, Ernfors group: PEP1) is likely a large component of the SP-positive peptidergic unmyelinated cluster, with high levels of *Calcα*, *TrkA*, *Gfrα3*, and *TrpV1* (Gerhard Skofitsch & Jacobowitz 1985; Hokfelt et al. 1975; Tominaga et al. 1998;

Bennett et al. 2006). Histological methods of identifying peptidergic afferents tend to rely on the products of these five transcripts, so it seems safe to say that this population would be consistently identified as a part of any peptidergic population.

The only group missing from Usoskin et al. (2014) is the orange transient receptor potential cation channel, member M8-containing cluster (*TrpM8*). In addition to *TrpM8*, these cells express *Asic1*, *Gfrα3*, and *Tac1*. Notably, these fibers express a complement of sodium channels that is unique among small cells. They lack detectable levels of *Scn11a* (Nav1.9) and have low to undetectable levels of *Scn10a* (Nav1.8), both of which are typically associated with small afferents and are expressed at high levels in the rest of our low-*Nefh* fibers.

The final low-*Nefh* cluster, the grey *Th*-containing cluster (Th, Ernfors: TH), expresses the other known markers of the population like *Gfrα2*, *Ret*, and *Piezo2* (Li et al. 2011; Usoskin et al. 2014), but it also expresses high levels of *TrkC*, *P2rY1*, and *Asic1*. The relatively low prevalence of this population is not surprising given that it is thought to be only 10-15% of the mouse DRG and is poorly labeled by IB4 and WGA (Brumovsky et al. 2006).

The high-*Nefh* clusters are also clearly split into peptidergic and nonpeptidergic groups. The purple Calcitonin-related polypeptide alpha (*Calcα*)-expressing group (Calcα, Ernfors: PEP2) has high levels of *Calcα*, *TrkA*, and *Asic3*, while the blue Growth factor receptor 1 nonpeptidergic cluster (*Gfrα1*, Ernfors: NF1-5) has high levels *Gfrα1*. The blue nonpeptidergic cluster can be further split between a group with higher levels of *Scn9a* (Scn9a, dark blue) expression and one with high *Asic1* (Asic1, light blue). These differences in expression are mirrored by the split between NF1-3 (*Pvalb*$^{-}$) and NF4-5 (*Pvalb*$^{+}$) from Usoskin et al. (2014), which was unexpected as parvalbumin is a marker of proprioceptors in other mammals (Ernfors et al. 1994). Assessing these nonpeptidergic, large afferents for *Pvalb*, however, supported the NF4-5 group assignment (Figure 3). Thus, transcriptional *Pvalb* groups are not exclusively proprioceptors, which is a finding that could be reasonably expected to generalize to the Pvalb-Cre transgenic mouse line.

Gene-clusters (Figure 2D, Y-axis dendrogram) has several groups of genes that are correlated, with lowest nodes on the tree showing the highest correlation. Splitting the dendrogram at the first node into a top and bottom half isolates genes that are expressed in both large and small cells (top) from those that are expressed primarily in a single small cell subpopulation (bottom), with *Asic3* and *Nefh* being the two gene expressed almost predominately

in large cells. The TTX-resistant voltage-gated sodium channels *Scn10a* and *Scn11a* are part of a larger group containing *Calcα* and *TrkA*, all of which are expressed in peptidergic large and small cells. *Gfrα1*, its co-factor *Ret*, and the rest of that cluster are primarily expressed in nonpeptidergic large and small cells. The bottom cluster has subclusters of genes that label individual subpopulations in the order of Tac1, MrgprD, TrpM8, Sst and MrgprA3, and Th.

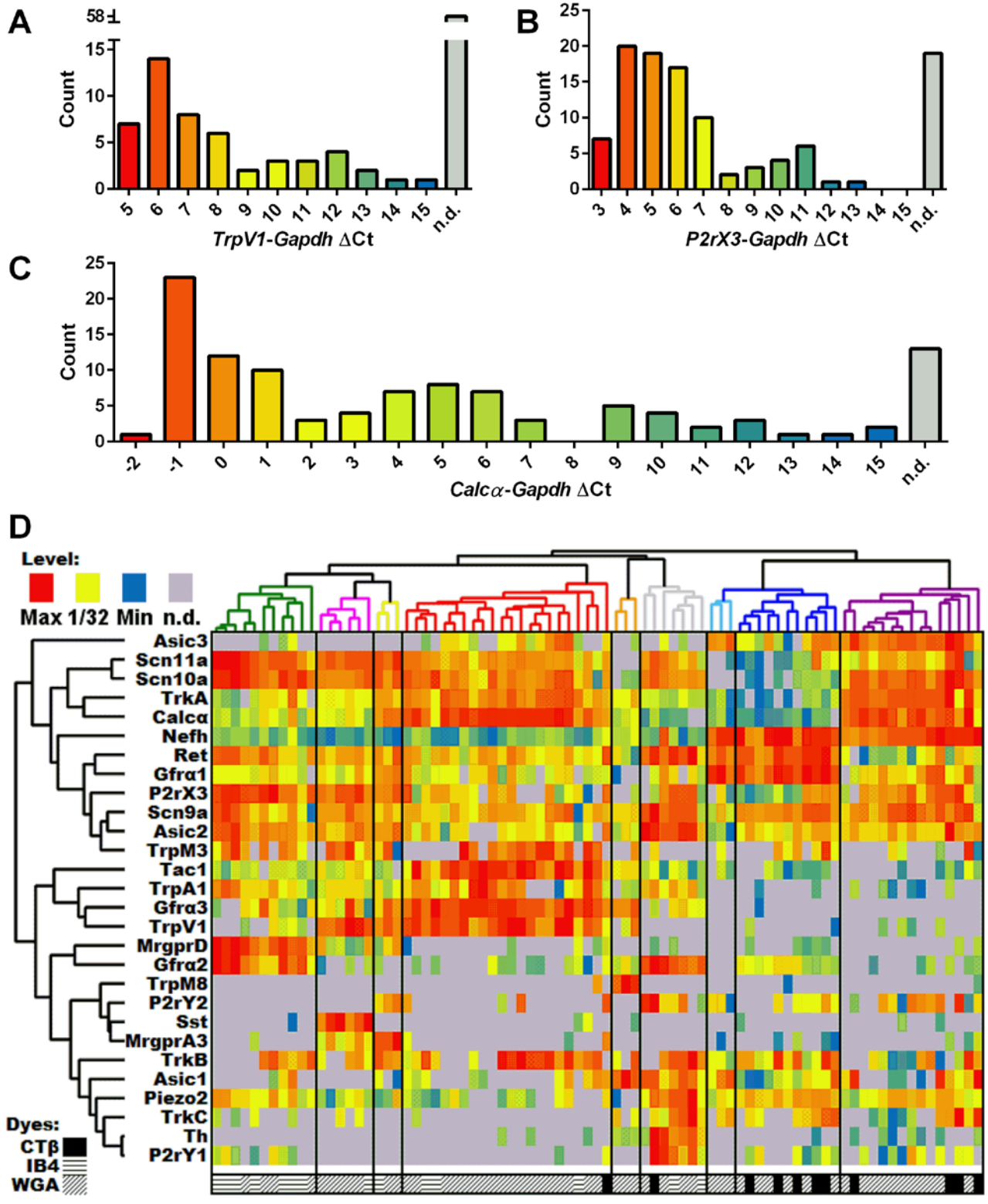

Figure 2. DRG profiling of backlabeled afferents using single cell PCR. A-C) Frequency distribution of *TrpV1*, *P2rX3*, and *Calcα* ΔCt values. D) Single cell qPCR results from

backlabeled afferents, with each column being a unique cell and rows representing genes. Heatmap temperatures for the histogram are scaled to expression, with red representing the maximum level, yellow representing 1/32 of the maximum level, blue representing the minimum level, and grey representing an undetectable level of transcript. Distributions were typically left-skewed, so scaling the heatmap in this way ensures the upper mode of the distribution will be colored red, orange, or yellow, while the lower tail is green or blue. Both cells and genes have been clustered using the same UPGMA algorithm. The texture below each column indicates the dye used for backlabeling

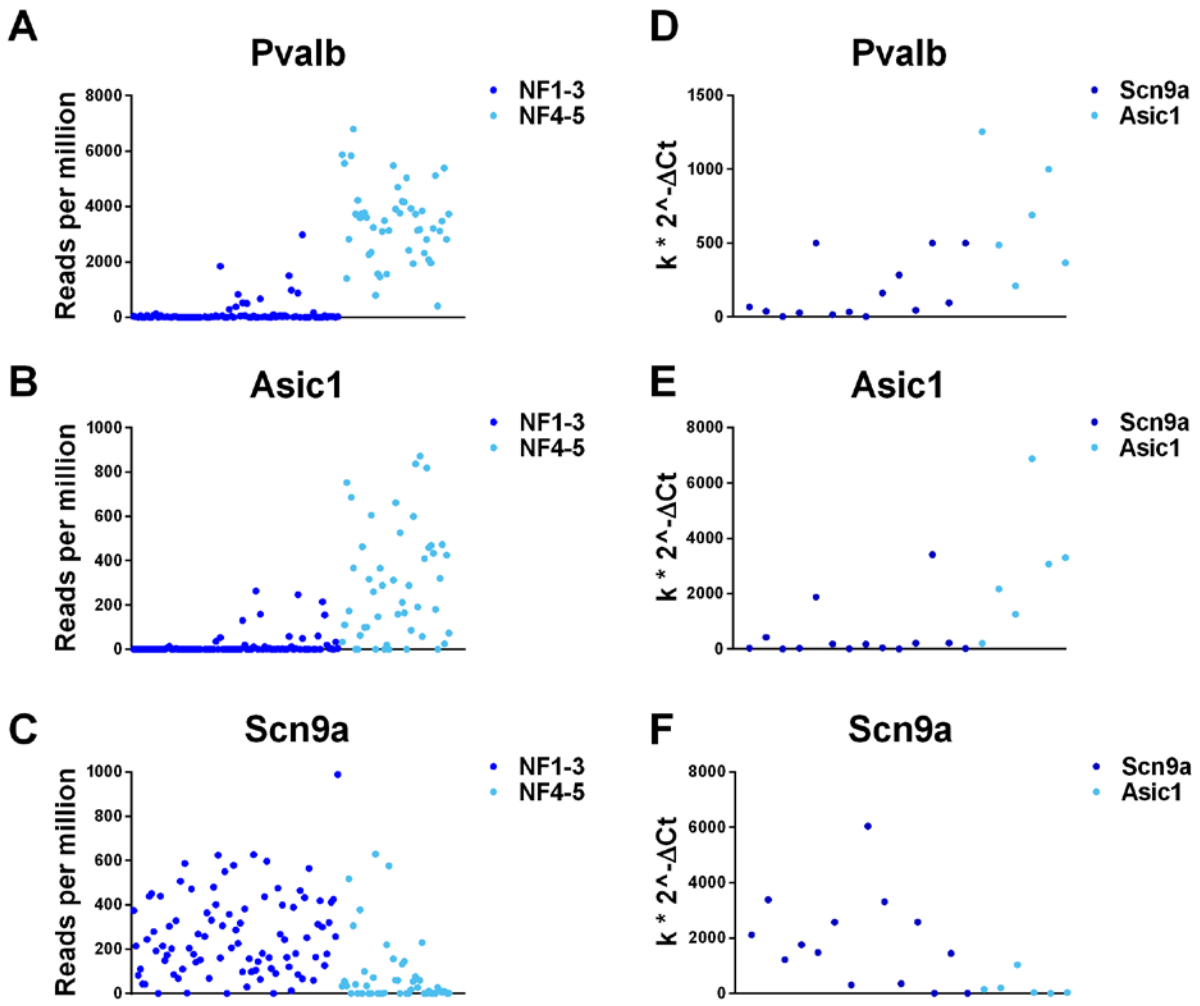

Figure 3. Expression of nonpeptidergic myelinated cells. (A-C) Data replotted from Usoskin et al. (2014) shows the expression of Pvalb, Asic1, and Scn9a in the NF1-3 and NF4-5 myelinated nonpeptidergic clusters for individual cells (x-axis). Expression level (y-axis) is the number of RNA-seq reads per million RNA-seq reads for each cell. (D-F) Data from this thesis shows the expression of Pvalb, Asic1, and Scn9a in individual cells from our two subpopulations of myelinated nonpeptidergic fibers. Relative expression level (y-axis) that was originally ΔCt has been converted to linear units and multiplied by a scalar (k=100,000) for the sake of comparison with RNA-seq data.

2.2.2 Correlating channel function and relative transcript levels

Backlabeling reveals wide ranges of transcript levels between cutaneous afferents, with thousand-fold differences between maximum and minimum expression levels (Figure 2A-C). Additionally, measurable transcript levels are occasionally expressed in cell types not thought to contain the associated protein (e.g. *Calcα* in the nonpeptidergic population). These observations imply that our technique may be detecting transcript levels that do not translate to protein. In order to address these issues and examine the relationship between function and transcript levels, we compared agonist responses with relative single cell transcript levels using single cell PCR following calcium imaging of cultured DRG neurons. *TrpV1*, *P2rX3*/*P2rX2*, and *P2rY1* were chosen as target transcripts because their respective receptors possess specific agonists and are thought to be differentially expressed across the DRG cell subpopulations. P2X3 and P2X2 are reported to be expressed in nonpeptidergic C-fibers (Guo et al. 1999; Petruska et al. 2000); TRPV1 should be expressed largely in the peptidergic population (Michael & Priestley 1999); P2Y1 should be expressed in large cells (Nakamura & Strittmatter 1996).

Capsaicin responders and nonresponders were clearly divided by their relative *TrpV1* transcript level (Figure 4B). Cells responsive to capsaicin always expressed detectable *TrpV1* transcript (16/16), while nonresponders did not (7/24). Notably, transcript levels predicted whether a cell would respond to capsaicin. No capsaicin responses were observed in cells with a *TrpV1* ΔCt over 9, while every cell below 9 ΔCt responded to capsaicin (Fig.2C). Applying the threshold to our single cell survey results predicts that our Tac1 (ΔCt 4.57-10.39, $\overline{\Delta Ct}$. 6.54; 21/22 predicted functional), MrgprA3 (ΔCt 6.03-7.54, $\overline{\Delta Ct}$ 7.01; 3/3 predicted functional), Sst (ΔCt 4.58-7.05, $\overline{\Delta Ct}$ 5.98; 6/6 predicted functional), and TrpM8 (ΔCt 6.72, 11.15; 1/3 predicted functional) cells would contain functional TRPV1. These results agrees with previously published histology, which primarily show TRPV1 expression in $CGRP^{+}/NF200^{-}$ cells (Christianson et al. 2006; Guo et al. 1999; Michael & Priestley 1999). Among responders, there is no correlation between ΔCt and absolute or relative response amplitude.

Similarly, *P2rX3* levels predict whether imaged cells respond to α,β-meATP (Figure 4C). Only one significant α,β-meATP response was observed with a ΔCt over 6, while every cell below that point was responsive to α,β-meATP (Fig.2D). The responsive cell without *P2rX3* transcript had the highest recorded expression level of *P2rX2* (ΔCt=6.70), another ATP receptor.

P2rX2 was only observed in 3 cells (ΔCt=6.70, 10.82, 12.35) and the other two were not responsive to α,β-meATP. Applying a 6 ΔCt threshold to our backlabeled cutaneous afferents indicates that 10/11 MrgprD and 5/9 MrgprA3 and Sst cells likely express functional levels of P2rX3, while only 2/22 cells from the Tac1 group do. Interestingly, 8/22 of myelinated cells expressed levels of P2rX3 that would be predicted to be functional. This is not entirely unexpected, given that large or myelinated cells have been observed expressing *P2rX3* via *in situ* (Chen et al. 1995), immunohistochemistry (Bradbury et al. 1998), and function (Dowd et al. 1998; Hamilton et al. 2001). Among responding cells, there is no correlation between ΔCt and relative or absolute response amplitude (slope=0.16, r=0.46).

Unlike the previous two ionotropic channels, relative expression levels of the metabotropic receptor *P2rY1* correlate poorly with 2-methylthioADP responsiveness (Figure 4D). Only 11 out of 18 ADP responders expressed detectable levels of *P2rY1* (Average ΔCt 10.54), while 5 of 13 ADP nonresponders also expressed *P2rY1* (Average ΔCt 10.00). Neither the percent of cells with detectable expression (Fisher's exact test: p=0.29), nor the expression levels (t-test: p=0.70) were significantly different between the samples. The 8 cells that respond to ADP but do not express *P2rY1* may indicate that *P2rY1* mRNA is not maintained at a constant level, but may be transcribed on demand or post-transcriptionally regulated. The 7 cells that did not respond to 2-methylthioADP but did express *P2rY1* may indicate that the other required components of the Gq coupled receptor pathway are not omnipresent, limiting P2Y1's ability to generate a calcium transient. Alternatively, there may be another ADP receptor.

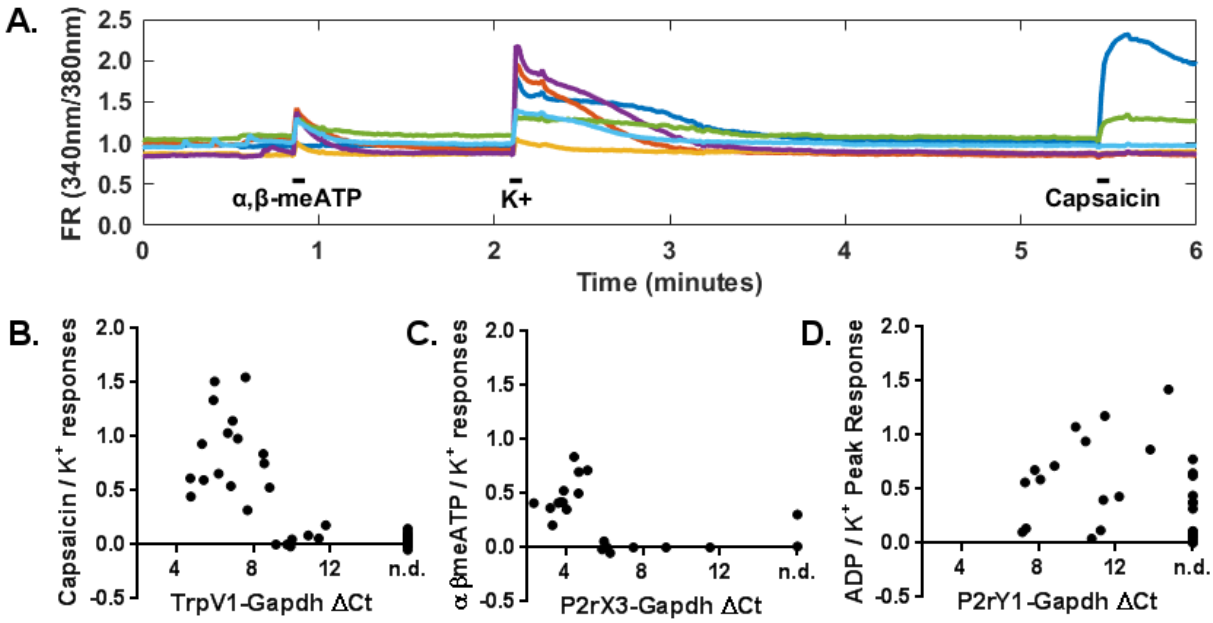

Figure 4. Calcium imaging reveals apparent thresholds of function for two ionotropic channels. (A) Example Fluorescence Ratio (FR) traces in response to 50µM α,β-meATP, 1M KCl, and 1µM Capsaicin (100mM ADP not shown). (B-D) Ratio of agonist to KCl responses versus relative receptor transcript expression for (B) *TrpV1*, (C) *P2rX3*, and (D) *P2rY1*.

2.2.3 Correlating function and transcriptional class

The apparent thresholds for functional ionotropic channel expression raise the possibility that individual transduction channels correlate with physiological properties in characterized afferents. Thus, we assessed functionally characterized afferents using single cell PCR and looked for correlations between transducer transcription levels and their related functions.

Results from characterized cells largely confirm the earlier supposition regarding Nefh levels and myelination (Figure 5). Characterized cells in the high-Nefh clusters had an average conduction velocity of 9.5m/s, while the other clusters had an average conduction velocity of 0.55m/s. The peptidergic myelinated cluster tended to have a lower conduction velocity than the nonpeptidergic myelinated cluster, but the effects on average CV (8.9m/s vs. 10.4m/s, t-test p=0.18) and distribution of Aβ and Aδ (Fisher's exact test p=0.37) were not significant.

As can be observed in Figure 5, though all characterized myelinated fibers were mechanically sensitive, average mechanical thresholds differed significantly between cells in the

purple peptidergic and blue nonpeptidergic clusters (35mN vs. 8mN, respectively; t-test p=0.025). Common divisions between firing patterns were also apparent in our clusters. The peptidergic cluster contained regular spiking fibers, with an average interspike interval coefficient of variation (ISI CoV) of 0.42. The nonpeptidergic cluster contained both SA1 fibers with irregular discharge (light blue cluster, high Asic1, average ISI CoV of 0.80) and rapidly adapting fibers (dark blue cluster, low Asic1, average of 1.14 spikes per square wave force stimulus). As would be expected from the literature, the SA1 cluster had significantly higher ISI CoVs than cells in the regular spiking purple cluster (t-test, p=0.017).

Cells in the green MrgprD cluster were all mechanically sensitive, with an average threshold of 17mN. The thermal properties were more varied, with heat thresholds spanning almost the entire dynamic range of our Peltier heater, going from 37.6 to 49.7°C, with an average of 42.2°C. Despite the similar average threshold to the red clusters, none of these cells expressed TRPV1 at levels we would predict to be functional from the calcium imaging data. Those that were cold sensitive had thresholds between 7.6 and 16.0°C, with an average of 11.7°C. Except that they tended more towards cold-insensitivity, cells in the pink Sst and yellow MrgprA3 groups had response properties that were not distinguishable from the MrgprD cluster. Although this population is noted for its multi-modality, it is worth noting that the firing rates of these neurons is very low (<15 Hz peak instantaneous rate) to thermal stimuli over the tested range. Also, though referred to as nonpeptidergic nociceptors (Molliver et al. 1995; Stucky & Lewin 1999), this subpopulation has many members with sub-noxious mechanical thresholds (<10mN).

The red Tac1 unmyelinated cluster contains heat sensitive cells, with thresholds from 42-43°C. These heat thresholds are near the 42°C threshold for heterologously expressed TRPV1 channel opening at neutral pH (Tominaga et al. 1998; Caterina 2000). *TrpV1* is expressed in these cells at a level that would be expected to produce functional channels from the calcium imaging data, so it appears likely that TRPV1 expression is conferring heat sensitivity to this population. Additionally, these cells had higher peak instantaneous firing rates (50.8-56.42Hz) than the other heat sensitive fibers (1.65-14.43Hz) in response to heat stimulation, as has been reported previously when comparing the CH population to CPM population (Lawson et al. 2008).

The cells recorded in the orange TrpM8 group were all cold sensitive, with much higher peak instantaneous firing rates in response to cold (29.4, 158Hz) than the other cold sensitive

fibers (0.65-5.14Hz). Previously recorded primary afferents that stain positively for TRPM8 have shown similarly high instantaneous frequencies (Koerber lab, unpublished data), which may be due to the cluster's fairly unique complement of voltage gated channels, including a noted lack of the tetrodotoxin (TTX) insensitive *Scn10a* and *Scn11a* (Nav1.8 and 1.9, respectively). Despite the notable cold resistance of Nav1.8, TTX insensitive sodium channels are relatively slow and thus it would make sense if this subpopulation did not rely on them for action potential generation (Djouhri et al. 2003; Sarria et al. 2012). In support of this, TTX sensitive cold and menthol responses have been previously reported in dissociated culture (Reid et al. 2002; Xing et al. 2006).

Finally, the single cell in the Th group was highly mechanically sensitive, but not an outlier compared to the MrgprD fiber's sensitivities. This is consistent with previously published work identifying members of the Th^{+} population as C-LTMRs (Li et al. 2011).

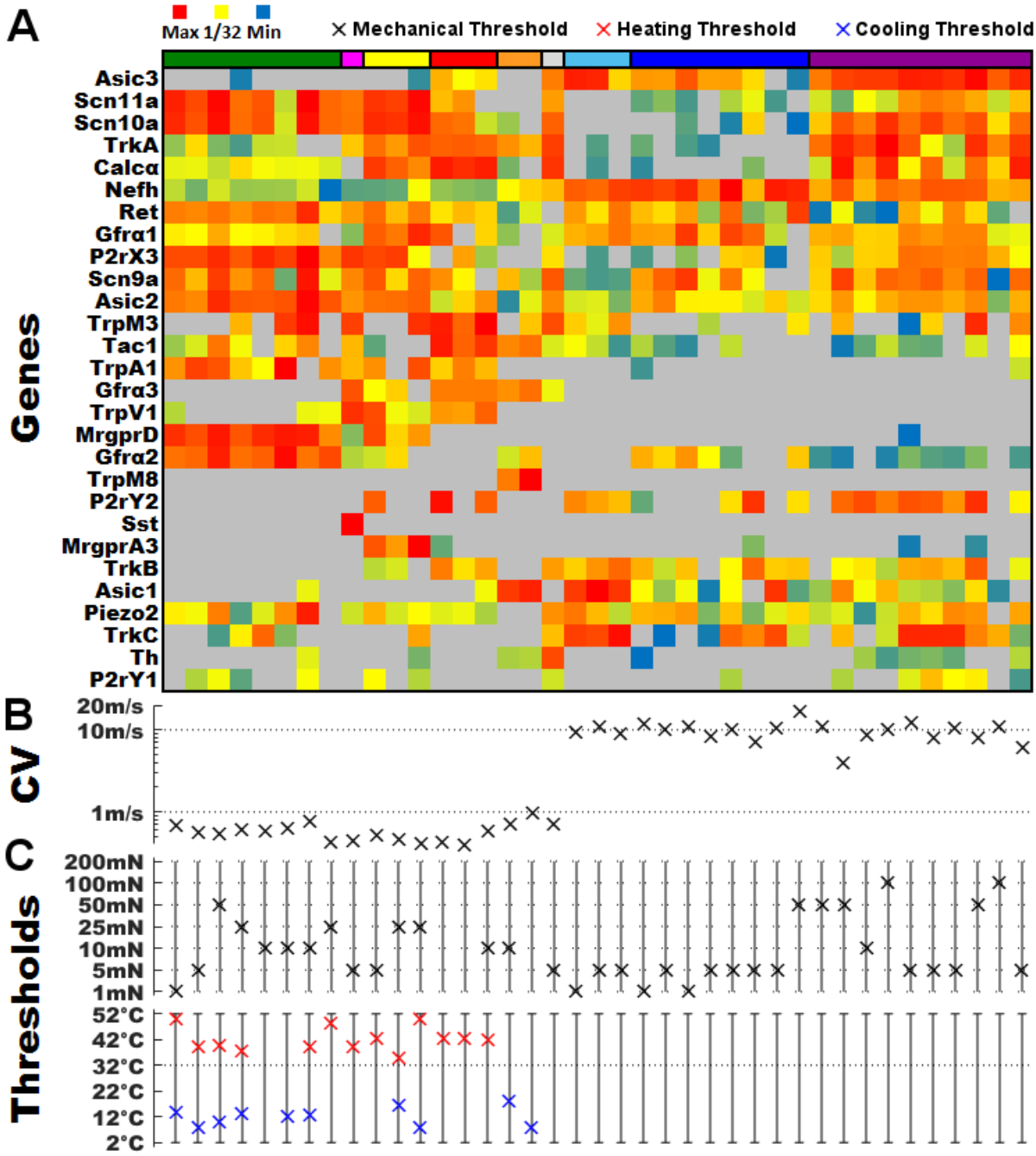

Figure 5. Transducer levels and the associated thresholds in characterized cells. (A) *top*: transcriptionally defined group color code *bottom*: Expression levels of transducer mRNA relative to GAPDH for individual characterized cells (B) conduction velocity for each cell (C) mechanical and thermal thresholds for each cell.

2.2.4 Correlating afferent properties and relative transcript levels

Thus far, we have demonstrated that primary afferents can be separated into groups that differentially express transcripts (Figure 2D) and that these transcriptional groups correlate with function (Figure 5). Furthermore, we showed that the two analyzed ionotropic channels have a fairly direct relationship between relative transcript level and functional channel expression (Figure 4B-D).

Transducers tend to be differentially expressed between transcriptional groups (Figure 2), so individual transducers have many covariate transcripts and it is difficult to conclusively assign function to a single transcript without manipulation. However, there exist some transduction channels (e.g. TRPV1, PIEZO2, TRPM8) that confer modality sensitivity when overexpressed in heterologous recombination systems, so it is possible that treating them in such an isolated way is not unreasonable (Coste et al. 2010; McKemy et al. 2002; Tominaga et al. 1998).

As can be seen in Figure 6, there were correlations between function and measured expression regardless of class. Cells with proposed functional levels of *TrpV1* had thermal thresholds of 43°C or less (Figure 6A), which is consistent with TRPV1's 43°C thermal threshold (Caterina et al., 2000). Heat sensitive nonpeptidergic cells are known to transduce through a TRPV1/2 independent mechanism (Woodbury et al. 2004) and correspondingly the few that express detectable *TrpV1* have non-functional levels ($\Delta Ct>9$). The transcript for a putative cold sensor, *TrpA1*, appears to be roughly correlated with noxious cold sensitivity (Figure 6B) and all cells with less than $5\Delta Ct$ have cold thresholds at or below the 17°C threshold seen with heterologous *TrpA1* expression (Story et al. 2003; Munns et al. 2007; Brignell et al. 2008). *Piezo2* levels above a certain point were also predictive of low mechanical threshold for A-fibers (Figure 6C), which is consistent with previous work indicating that Piezo2 expression is important for LTMR transduction (Ranade et al. 2014). Finally, Nefh levels could be used to distinguish A- and C-fibers, with *Nefh* $\Delta Ct<1$ indicating the cell was an A-fiber and $\Delta Ct>3$ indicating the cell was a C-fiber (Figure 6D).

There were no obvious functional implications of having P2X3 levels high enough to respond to α,β-meATP in culture, but functional *P2rX3* expression was strongly correlated with transcriptional group. The groups identified by predicted-functional levels of *P2rX3* were all mechanically sensitive, and P2X3 has been previously implicated in the development of

mechanical hyperalgesia (Barclay et al. 2002), but without more thorough investigation it is difficult to convincingly assign function.

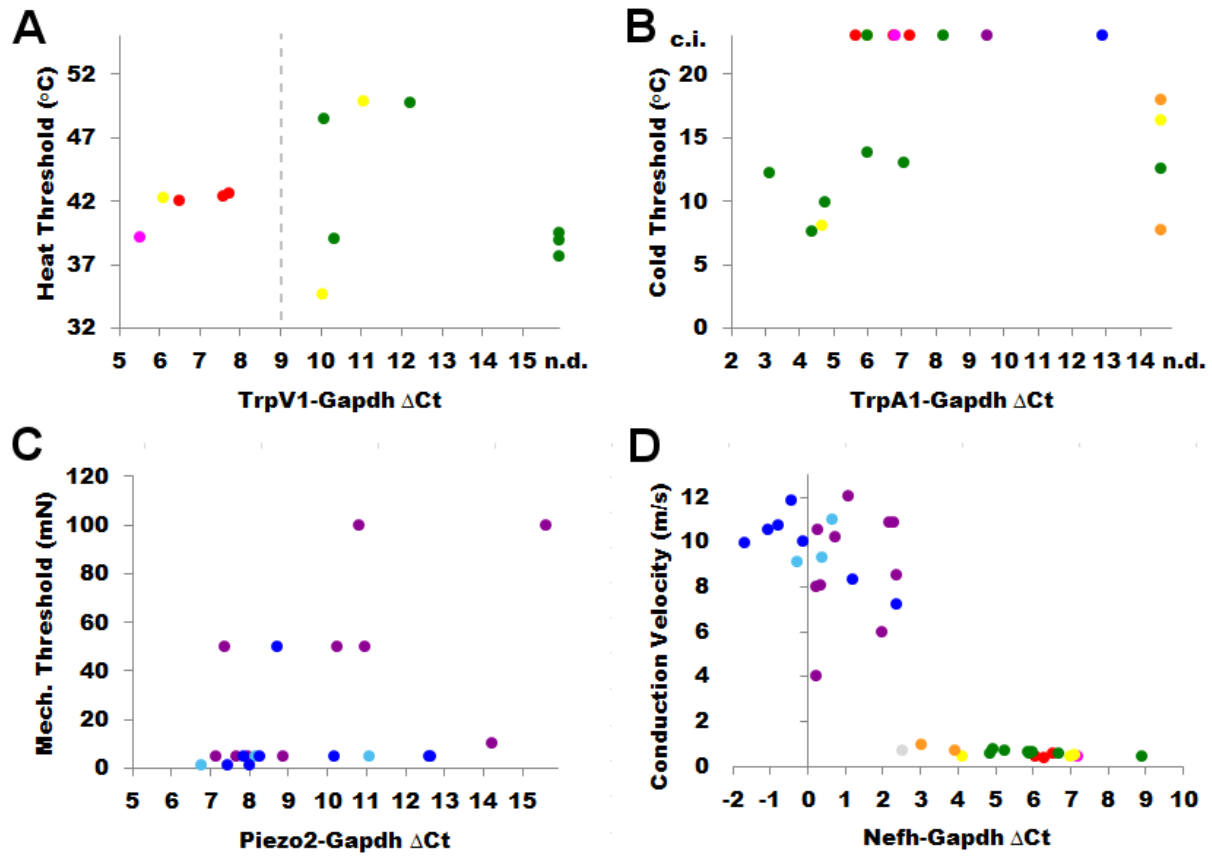

Figure 6. Physiological correlates of expression in cutaneous afferents. (A) Heat threshold versus relative *TrpV1* expression. Dashed line indicates the expression threshold for capsaicin sensitivity obtained from the calcium imaging experiments. No heat insensitive neurons that expressed *TrpV1* were observed. (B) Cold threshold versus relative *TrpA1* expression. The "c.i." neurons were insensitive to cold but expressed *TrpA1*. (C) Mechanical threshold versus relative *Piezo2* expression in characterized A-fibers. No mechanically insensitive A-fibers that expressed *Piezo2* were observed. (D) Conduction velocity versus relative *Nefh* expression. Cells that both failed to express detectable transcript and failed to be sensitive in a given modality were not plotted. "n.d." indicates a transcript was not detected.

2.3 DISCUSSION

This chapter showed it is possible to assign cells to functionally meaningful transcriptional groups using the relative expression of 28 selected genes, which were analogous to those seen in Usoskin et al. (2014). Our automated clustering algorithm extracted an additional *TrpM8+* cluster with unique expression of ion channels and functional properties. In general, functional properties were consistent within transcriptional groups, although specific properties may be better predicted by individual relative transcript levels than transcriptional group.

All extant RNA-seq studies of single DRG cells have used afferents with unspecified target tissues (Chiu et al. 2014; Usoskin et al. 2014; Li et al. 2015). Despite this, eight of our transcriptionally defined classes of cutaneous afferents closely resemble groups from Usoskin et al. (2014) (MrgprD-NP1, MrgprA3-NP2, Sst-NP3, Tac1-PEP1, Calcα/Nefh-PEP2, Th-TH, Scn9a/Nefh-NF1-3, Asic1/Nefh-NF4-5). However, our automated clustering algorithm also created one group that was not previously distinguished in these studies. This group notably expressed *TrpM8* and had little to no *Scn10a* and *Scn11a* (Nav1.8 and 1.9). Consistent with previous histological reports using TRPM8 antibodies and GFP inserted into the *TrpM8* locus, the group did not label with IB4 and expressed very little CGRP (Wang et al. 2013; Dhaka et al. 2008). Interestingly, the members of this population also expressed substantial levels of *Tac1*, which matches the previous observation that TRPM8 expression in the spinal cord is tightly restricted to the most superficial extent of the SP band (Dhaka et al. 2008; Takashima et al. 2010). SP release from these afferents may explain the flare observed following the application of high concentrations of menthol (Wasner et al. 2004).

The recorded and recovered cells from the TrpM8 group showed exquisite cooling sensitivity, adaptation to cool temperatures, and high peak instantaneous frequencies, all of which are consistent with the previously described menthol-sensitive C-cold and C-mechanocold receptors (Zimmermann et al. 2009; Campero et al. 2009; Hensel et al. 1960). Anecdotally, I have caused a burst of action potentials in one of these cells by sighing while attempting to localize a receptive field and having my breath travel over the damp skin in an otherwise warm bath. Given their adaptation properties, it could be that these cells encode rate of temperature decrease rather than an absolute temperature. It is counterintuitive that such seemingly innocuous information directly projects to Lamina I of the spinal cord, whose projections are thought to

transmit pain signals out of the spinal cord, but it could be that mild cooling is actually more aversive than is typically recognized. Swimming in a cool pool on a hot day can be relaxing, but why is the initial plunge met with such trepidation? Who enjoys having damp hands after cleaning dishes? Neither menthol activation nor innocuous cooling is typically considered painful, but high concentrations of menthol can be painful (Wasner et al. 2004) and lower concentrations can potentiate other stimuli. Solutions of menthol with camphor, cinnamaldehyde, or capsaicin decreased thermal pain thresholds more than those without menthol (Averbeck et al. 2013). Perhaps most convincingly, alternating cool and warm bars applied to the skin ("thermal grill") give the sensation of burning cold pain despite not including temperatures capable of activating "noxious cold" receptors (Iggo 1969; Pierau F-K et al. 1975; Leung et al. 2005; Craig & Bushnell 1994). This experiment implies that menthol sensitive cooling fibers drive the sensation of cold pain. Indeed, mice lacking the menthol receptor, TRPM8, show no preference for room temperature over 5ºC (Colburn et al. 2007).

In this chapter, we correlated autonomously assigned transcriptional group with the functional properties of cutaneous sensory afferents. MrgprD, MrgprA3, and Sst cells were found to be consistently mechanically sensitive and could give tepid thermal responses with a wide range of thresholds. Tac1 cells are consistently thermally sensitive and give vigorous heating responses with thresholds near 43ºC. The single, recovered Th cell was exclusively mechanically sensitive and had a low threshold. Peptidergic A-fibers were slowly or nonadapting with high threshold or wide dynamic ranges. Nonpeptidergic A-fibers were neatly split out SA1 afferents from RA and WDR fibers. Given the consistency of our identified groups largely recapitulate an earlier study (Usoskin et al. 2014), this finding indicates that others will be able to replicate these findings and begin to recognize potential afferent properties based on expression. Among other outcomes, this will aid in the creation of intersectional genetic strategies to label specific functional fiber types.

Previous histological work with these populations indicates that the identified subpopulations of afferents have distinct projection bands in the dorsal horn. Combining the physiological results from this chapter with the previous histological results, one can understand the functional topography of dorsal horn projections. From the outer extents of Lamina I, these different immunolabeled populations of afferents synapse in overlapping bands with the order: TrpM8, Tac1, Sst, MrgprA3, MrgprD, Th, and then myelinated LTMRs (Dhaka et al. 2008; Liu

et al. 2009; Zylka et al. 2005; Li et al. 2011). High firing rate thermoceptors project to Lamina I, but thermal sensitivity decreases and mechanical responses become more prominent deeper in the dorsal horn. Myelinated peptidergic fibers are the exception to this progression, as they have been reported to arborize extensively throughout the spinal cord, from Lamina I to Lamina V (Woodbury & Koerber 2003).

Our study implies a fairly strong correlation between the expression of some mRNAs and proteins in DRG cells. The degree to which mRNA levels predict protein levels has been assessed many times in many different systems with a wide variety of answers (Spearman rank correlations 0.2-0.8) (Greenbaum et al. 2003; de Godoy et al. 2008). There are numerous sources of potential variance on these comparisons, ranging from cell cycle-related regulation of transcription and translation to simple instrumental error in mRNA and protein quantification. These factors are largely minimized by our use of a type of quiescent mammalian cell, neurons, and assay comparing channel function with the expression levels of the single, directly related transcripts. Although it will always need physiological confirmation, sufficiently precise measurement of single cell mRNA levels can be used to generate specific hypotheses about functional of individual afferents and afferent populations. This tool could be further used to examine differences between conditions. Expression changes in afferent populations following injury would predict corresponding changes in afferent function, and thus this technique could be used to assay for the cause of sensory abnormalities after injury, like mechanical allodynia.

3.0 SUBPOPULATION-SPECIFIC REGULATION AFTER NERVE INJURY: PIEZO2 CONTRIBUTES TO MECHANICAL HYPERSENSITIVITY

The experiments described in this section are part of a manuscript currently in preparation by myself.

My contributions:

-Discussing experimental design and data analysis with Dr. Koerber.

-Writing the manuscript, with edits from Dr. Koerber.

-Collecting data for all figures.

-Analyzing data for all figures.

Contributions from other authors:

-Rob Friedman did all single cell PCR and primer design contained herein

3.1 INTRODUCTION

Injured cutaneous primary afferents change during the regeneration process. This process can be separated into approximately three regimes: initial insult and degeneration, regeneration, and reinnervation. The initial damage causes a burst of activity and incites transcriptional changes prior to the formation of an axonal growth cone (Leah et al. 1991; Berdan et al. 1993). This growth cone migrates down the intact epineurium, seeking neurotrophic factors that can sustain the sensory neuron (Kelamangalath et al. 2015). Upon reaching a target tissue, the neuron is exposed to a new complement of neurotrophic factors and resumes normal gene expression, which triggers a transcriptional shift back towards the original functional phenotype (Jankowski et al. 2009).

While it is possible that there some afferents might convert from one functional subtype to another during the injury and regeneration process, there are reasons to believe it is unlikely. Physiological properties seem stable even in situations where muscle afferents regenerate to the skin (Johnson et al. 1995) and spinal cord circuits appear to receive the same types of afferent inputs before and after injury (Koerber et al. 1995). Thus, there is no compelling evidence to suggest that primary afferents of one class (e.g. C-mechanoheat) are a different functional class (e.g. Aδ-RA) after nerve injury.

Although afferents may return to approximately the same functional phenotype after nerve injury, they do not quite return to their naïve state (Koerber et al. 1995). Previous work has shown that regenerated afferents are molecularly and physiologically different from uninjured afferents (Bradbury et al. 1998; Ishikawa et al. 1999; Jankowski et al. 2009). Regenerated afferents show increases in thermal sensitivity, both by decreasing the heat thresholds of polymodal C-fibers and increasing the proportion of cells responsive exclusively to heat (Jankowski et al. 2009). Some of these changes have been shown to be driven by alterations in expression that depend on growth factor receptor signaling. Knockdown of either *Gfrα3* or *TrpV1* levels returned the proportion of C-fibers responding exclusively to heat to naïve levels, but did not affect the decreased thermal thresholds for C-fibers that respond to multiple modalities (Jankowski et al. 2010; Jankowski et al. 2012). Additionally, regenerated myelinated nociceptors seem to have lower mechanical thresholds than unmyelinated afferents and this change is not mediated by GFRα3 or TRPV1.

Expression analysis of homogenized, injured DRGs has failed to identify a potential transducer responsible for the functionally defined subpopulation-specific change in afferent mechanical sensitivity after nerve injury. This failure is possibly due to the number of uninvolved cells, both irrelevant functional subpopulations and those spared by the injury, that are present in whole DRG manipulations. Whole DRG PCR has yielded valuable results, like identifying the regulation of *Gfrα3* after injury (D. L. H. Bennett et al. 2000), which ended up being responsible for regenerated afferents' heat phenotype (Jankowski et al. 2010), but it ignores the incredible heterogeneity of primary sensory neurons (Usoskin et al. 2014; Chiu et al. 2014; Goswami et al. 2014; Li et al. 2015) and the possibility of subpopulation-specific changes.

Here I will examine how nerve injury and regeneration may change transducer expression in myelinated and unmyelinated peptidergic and nonpeptidergic afferents using single cell PCR,

and then attempt to find a transducer necessary for the mechanical irregularities observed in nociceptors after injury.

3.2 MATERIALS AND METHODS

3.2.1 Animals

Adult male Swiss-Webster mice ordered from Hilltop Lab Animals were used for this study. Animals were group housed in a 12hr/12hr light-dark cycle. Mice used for the transcriptional profiling experiments were all obtained in the same Hilltop Lab Animals order. Survival surgeries were done using isoflurane anesthesia (2%) under a dissection microscope after verifying negative tail pinch reflex. Terminal surgeries used isoflurane anesthesia followed by intramuscular ketamine/xylazine. All animal use protocols were approved by the University of Pittsburgh Institutional Care And Use Committee (IACUC) and were in accordance with AAALAC-approved practices.

3.2.2 Nerve crush

A small incision was made in the skin above the saphenous nerve at mid-thigh. The saphenous nerve was isolated from the surrounding tissue and crushed two times in the same place for 10 seconds each using #3 forceps. After the nerve crush was visualized, the animal was sutured using 7-0 silk thread and returned to its home cage.

3.2.3 Nerve injections (Dye and siRNA)

Nerve injections used a small incision at the level of the knee to access the saphenous nerve. After isolating the saphenous nerve from the surrounding tissues with paraffin film, the nerve was injected with 0.1-0.2µL of solution using a picospritzer and borosilicate glass electrodes. Two types of nerve injections were done for backlabeling and siRNA knockdown. For the

purpose of backlabeling, twenty-four hours before cell pick-up the nerve was injected with Isolectin Binding protein 4 (IB4) or Wheat Germ Agglutinin (WGA) conjugated to Alexa 488. siRNA injections were done procedurally in the same way, but the nerve was injected with Penetratin-1 conjugated siRNA at weekly intervals over the four weeks between nerve crush and recording to maintain knockdown (Jankowski et al. 2006; Jankowski et al. 2012).

3.2.4 Cell dissociation and pickup

L2 and L3 Dorsal Root Ganglia ipsilateral to the backlabeling were removed and dissociated as previously published (Malin et al. 2007). Briefly, DRGs were removed from the animals, treated with papain and then collagenase/dispase, and plated onto laminin coated coverslips. Coverslips were then placed in culture conditions for 45 minutes to promote adhesion. Before pickup, cultures were flooded with cell collection buffer(140mM NaCl, 10mM Glucose, 10mM HEPES, 5mM KCl, 2mM $CaCl_2$, 1mM $MgCl_2$). Fluorescent cells were picked up with borosilicate glass pipettes (World Precision Instruments) held by a 3-axis micromanipulator. After confirming pickup using fluorescence, pipette tips were broken off into tubes containing 3uL of lysis buffer (Epicentre, MessageBOOSTER kit), and stored at -80^{o}C. Qualitative description of cell size was noted, and effort was taken to collect both large and small cells from WGA backlabeled animals.

3.2.5 Single cell amplification and qPCR

Transcripts from single cells were reverse transcribed and linearly preamplified using the MessageBOOSTER kit for cell lysate (Epicentre). After preamplification, the products were cleaned with RNA Cleaner & Concentrator-5 columns (Zymo Research) and transcript levels were quantified using qPCR with optimized primers and SsoAdvanced SYBR Green Master Mix. Cycle-time (Ct) values were determined using regression. Quantification threshold was determined to be interreplicate average of 35 Ct, the point where replicates have a 95% chance of reoccurring, and the GAPDH threshold for cell inclusion was set to 25 Ct to ensure we could detect transcripts a thousand-times less prevalent than GAPDH. If a cell met the criteria for inclusion, it would be corrected for primer efficiencies using the Pfaffl method (Pfaffl 2001).

3.2.6 *Ex vivo* preparation

As described previously, in this preparation the neurons composing the saphenous nerve and their innervation field are removed intact and recorded from using sharp electrodes in the L2 and L3 DRGs (Lawson et al. 2008; McIlwrath et al. 2007). Briefly, the animal is perfused with oxygenated ice cold ACSF, laminectomized, and the right leg and remaining T12 to S1 spinal column are removed and placed in a dissection dish of circulating, oxygenated ice cold ACSF. Once in the dish, the skin is removed from the leg and the saphenous nerve is isolated from the surrounding tissue, ultimately leading to a preparation with spinal column, saphenous nerve, and skin. After the dissection is complete, ACSF is warmed to create a bath temperature of 31°C and a suction electrode is attached to the saphenous nerve.

Sharp electrodes (impedance >200MOhms) are used to record from DRG cells. Recording electronics include a patch clamp amplifier (Axoclamp 200B) with high impedance headstage, an audio monitor and oscilloscope for online activity monitoring, and a data acquisition board paired with a computer for data storage. The program Spike2v6 is used for further online monitoring and offline analysis.

3.2.7 Expression analysis of injured afferents

Automated hierarchical clustering was performed on uninjured afferents, which resulted in a distribution of cells with multiple subtypes (Figure 2). Each injured afferent was determined to belong to the same group as the uninjured afferent that it was the shortest Euclidean distance from (summed squared difference of relative expression levels). Of those groups, the most prevalent were analyzed for expression level changes: the myelinated nonpeptidergic (NF1-3) and peptidergic (PEP2) afferents and the unmyelinated peptidergic (PEP1,NP3) and nonpeptidergic (NP1) unmyelinated afferents. Injured cells that were most similar to the other populations (TH, M8, NP2) were not quantitatively analyzed further due to the extremely small number of cells available impeding statistical comparisons.

3.3 RESULTS

3.3.1 Subpopulation agnostic single cell analysis reveals growth factor receptor upregulation

To facilitate comparison to previous studies, which typically used whole DRG homogenate, we first compared all of our collected afferents at each timepoint post injury to our uninjured sample (Figure 7). In order to do so, we first had to decide how to do single cell qPCR comparisons. qPCR can have two outcomes: 1) the sample passes the emittance threshold and generates a value; 2) the sample never passes threshold. Thus, comparisons of two groups must compare the probability of detecting expression as well as the average transcript level among cells expressing the transcript. Parallel changes are easy to interpret, but orthogonal changes are more difficult. For instance, after injury there is a substantial increase in the probability of detection of the artemin receptor, Gfrα3, in this lumped population of all afferents, but a nonsignificant decrease in Gfrα3 level ($p=0.08\sim0.45$). This could be due to *de novo* low level expression, which increases the probability of detection while pulling down the average level, or the novel expressing cells might be indistinguishable from the original expressers and the entire distribution may have shifted down. Of the transducers, Piezo2 expression is detected in significantly more cells one and four weeks after injury, again indicating potential *de novo* expression.

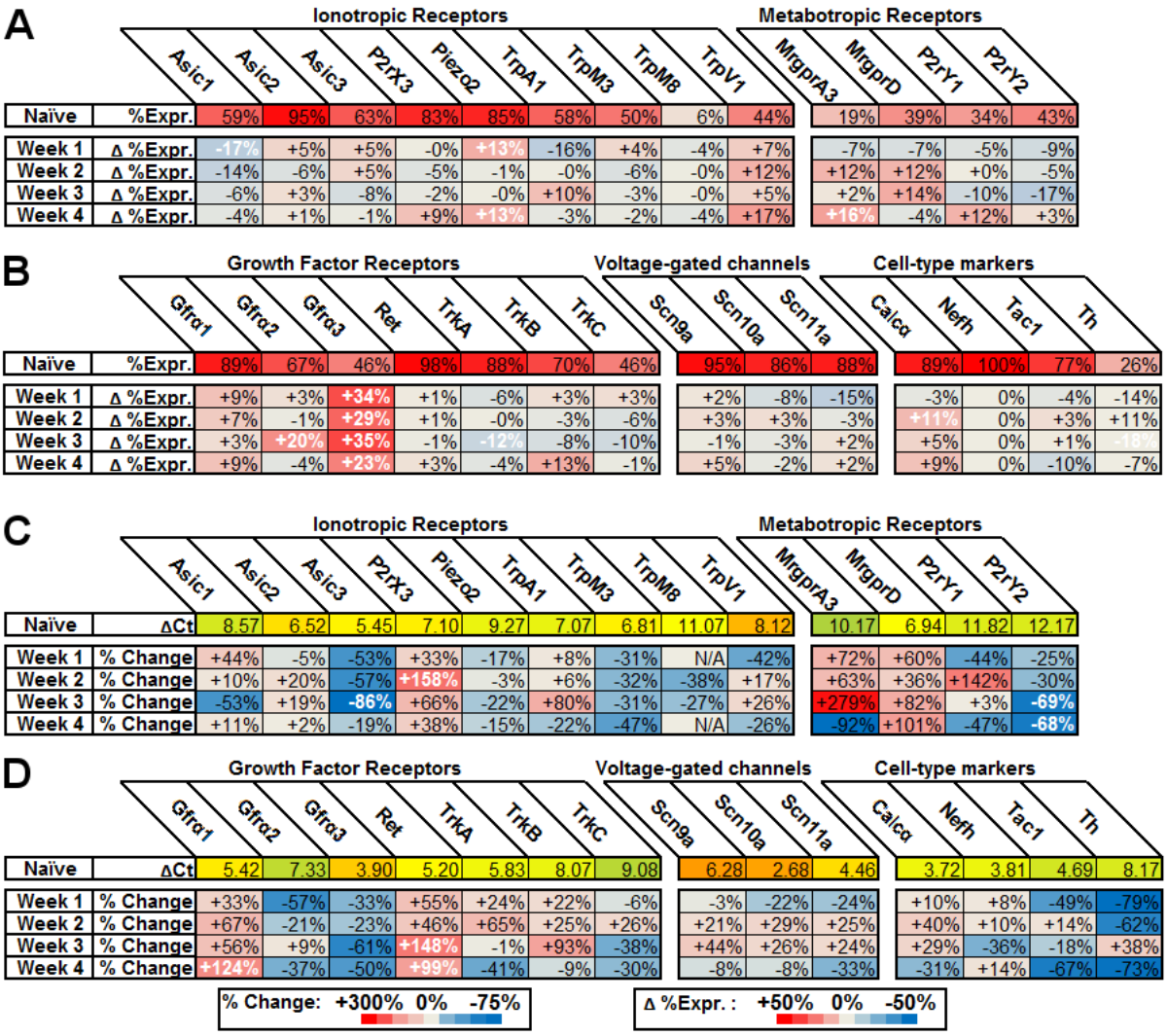

Figure 7. Injury-induced transcriptional changes in all backlabeled primary afferents (A-B) Probability of transcript detection in the naïve population and absolute changes in that probability after injury. Bold white text indicates significance in a binomial proportion test at the 0.05 level. (C-D) Naïve average expression level relative to *Gapdh* and relative changes in that level after injury. Bold white text indicates significance in a two-tailed t-test at the 0.05 level. Naïve N=120, Week 1 N=59, Week 2 N=55, Week 3 N=53, and Week 4 N=54.

3.3.2 Subpopulation-based analysis unmasks and localizes transcriptional changes

We hypothesized that the massive DRG cell heterogeneity could be masking changes in individual, transcriptionally-defined subpopulations. Naïve cells had already been assigned to a subpopulation (Figure 2), and injured cells were assigned to the same subpopulation as the cell they were closest to in the naive data set (Euclidean distance based on ΔCt). Comparisons were then made between the naïve subpopulation and the matching injured subpopulation. This approach minimizes differences observed between the naïve and injury conditions by only assigning post-injury cells to the subpopulation with the most similar naïve cell. Four subpopulations were analyzed: unmyelinated nonpeptidergic (MrgprD), unmyelinated peptidergic (Sst/Tac1), myelinated nonpeptidergic (Nefh high/Calcα low), and myelinated peptidergic (Nefh high/Calcα high) cells. Somatostatin and Tac1 populations were lumped due to minimal differences in their expression.

Cells most similar to the small, excluded groups (N=21) were not included in the following population analysis. Of these, 14 were MrgprA3, 4 were TrpM8, and 3 cells were Th. Combined injured MrgprA3 cells (3 from Week 1, 2 from Week 2, 6 from Week 3, 3 from Week 4) showed no significant changes ($p>0.1$). Comparing the first two weeks and the last two weeks to the uninjured cells found only one significant result, a downregulation of Gfrα3 in the first two weeks ($p<0.02$). When the injured TrpM8 cells (2 from Week 2, 2 from Week 3) were compared to the uninjured cells, significantly upregulated *Gfrα3* levels ($p<0.001$) after nerve crush despite the low comparison N. *TrpA1*, *Scn9a*, and *Ret* were approaching significant upregulation in the TrpM8 population ($0.05<p<0.1$).

Although there are not very many of them, the three Th cells recovered (1 from Week 1, Week 3, and Week 4) hint at some interesting possibilities. As expected, *Gfrα2* was so low in the single Week 1 cell that it would qualify as an outlier if included in the uninjured data set (Grubb's test, $p<0.05$) and *Gfrα3* levels were higher than any uninjured cell. The surprise came in Weeks 3 and 4, where cells were very different from uninjured Th cells. These Week 3 and 4 cells now expressed markers of the peptidergic subpopulation. They had *TrpV1*, *Tac1*, *Calcα*, and *Gfrα3* levels all comparable to the Tac1 population, but still expressed *Th*, *P2rY1*, and *Asic1*, markers of the Th subpopulation.

Unmyelinated nonpeptidergic cells show a significant shift in their growth factor receptors after nerve injury and demonstrate the expected two-phase transcriptional shifts (Figure 8B,D). One week after injury, this subpopulation shows dramatic growth factor receptor regulation. There is a decrease in *Gfrα2* levels and a concomitant increase in both Gfrα3 levels and the proportion of cells expressing *Gfrα3*. More minor changes are observed in Trk transcripts, with the proportion of cells expressing them increasing significantly one week after injury. Voltage-gated sodium channels also appear to be regulated in the first week after injury, with *Scn10a* (Nav1.8) and *Scn11a* (Nav1.9) transcripts levels dropping by 63% and 73%, respectively. As regeneration progresses, the proportion of cells with detectable *Gfrα3* and *TrkB* transcript remains elevated relative to uninjured afferents, but *Gfrα3* transcript levels do quickly return to normal. *Gfrα2* levels also do not appear to recover in this population within 4 weeks of injury. Notable upregulation occurs in *Gfrα1* levels around the time we expect reinnervation of the skin to occur and is still maintained four weeks after injury.

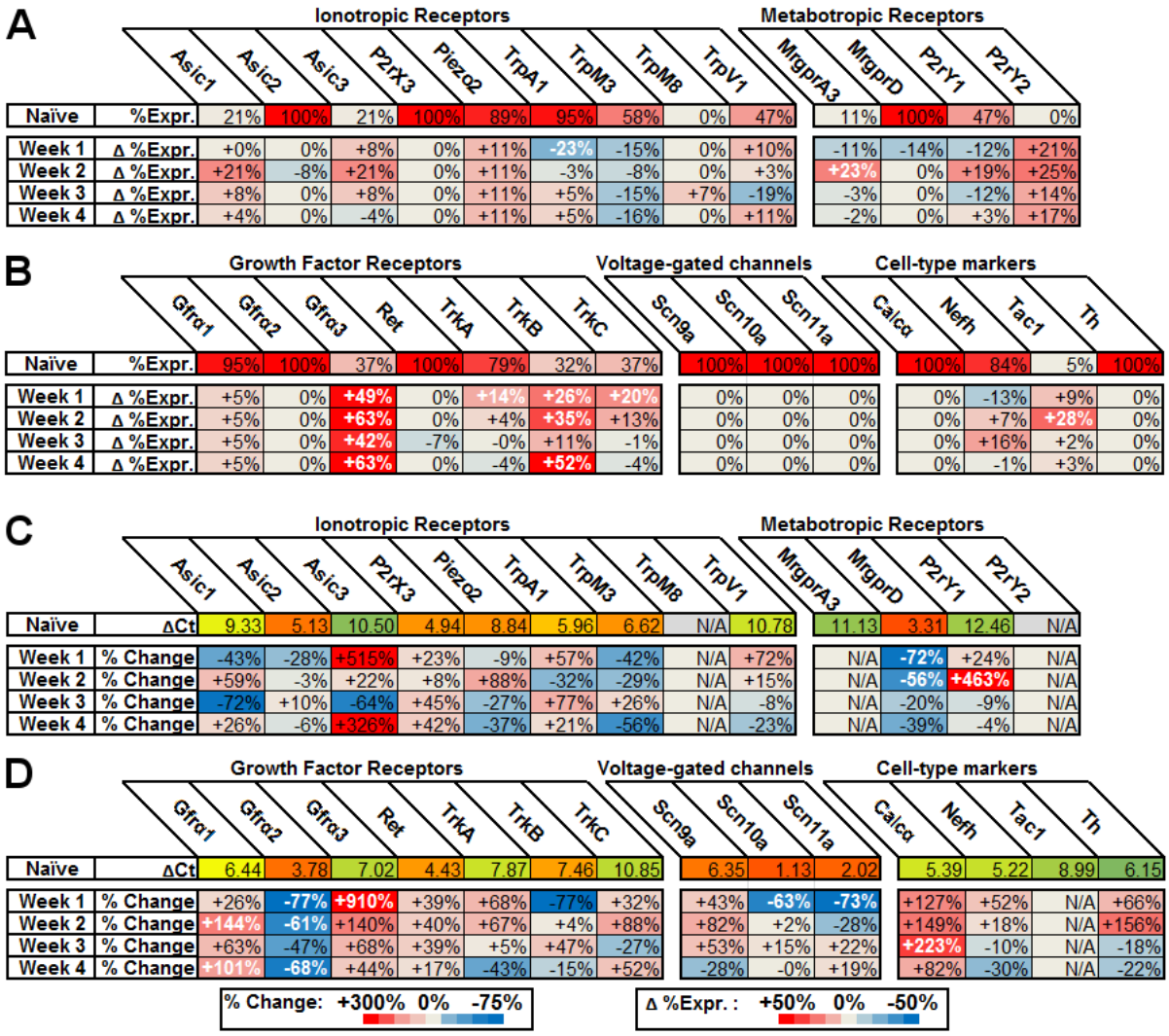

Figure 8. Unmyelinated nonpeptidergic subpopulation changes in backlabeled primary afferents (A-B) Probability of transcript detection in the naïve population and absolute changes in that probability after injury. Bold white text indicates significance in a binomial proportion test at the 0.05 level. (C-D) Naïve average expression level relative to *Gapdh* and relative changes in that level after injury. Bold white text indicates significance in a two-tailed t-test at the 0.05 level. Naïve N=19, Week 1 N=15, Week 2 N=13, Week 3 N=15, and Week 4 N=13.

The transcriptional profile of unmyelinated peptidergic cells also shows substantial injury-related changes (Figure 9). Unlike the unmyelinated nonpeptidergic population, this group immediately upregulates the expression of *Ret*, a co-receptor for the growth factor receptor family, possibly in a bid to increase the efficacy of its existing growth factor receptors. However, similar to the unmyelinated nonpeptidergic subpopulation, *Gfrα1* is also upregulated in this subpopulation starting at two weeks after injury, near the time of reinnervation. There is notable downregulation of *Scn11a* transcript across multiple time points, but *Scn10a* is unaffected. Most striking about this subpopulation is its regulation of ionotropic receptors. There seems to be *de novo* expression of *Asic3*, *P2rX3*, and *Piezo2* across multiple weeks, but *TrpA1* and *TrpM3* are actually detected less frequently after injury. Levels of *P2rX3* increase after injury, mimicking its *de novo* expression, but *Asic3* and *TrpA1* levels significantly fall. Markers of cell type are also affected after injury, with an increase in *Nefh* levels and a decrease in relative transcript levels of neuropeptides *Calcα* and *Tac1*. These *Nefh* increases potentially correspond to hypertrophied, regenerating axons (Malcangio et al. 2000), while the *Calcα* and *Tac1* changes have also been seen in previous immunohistochemical studies (Wang et al. 2014; Bennett et al. 2006).

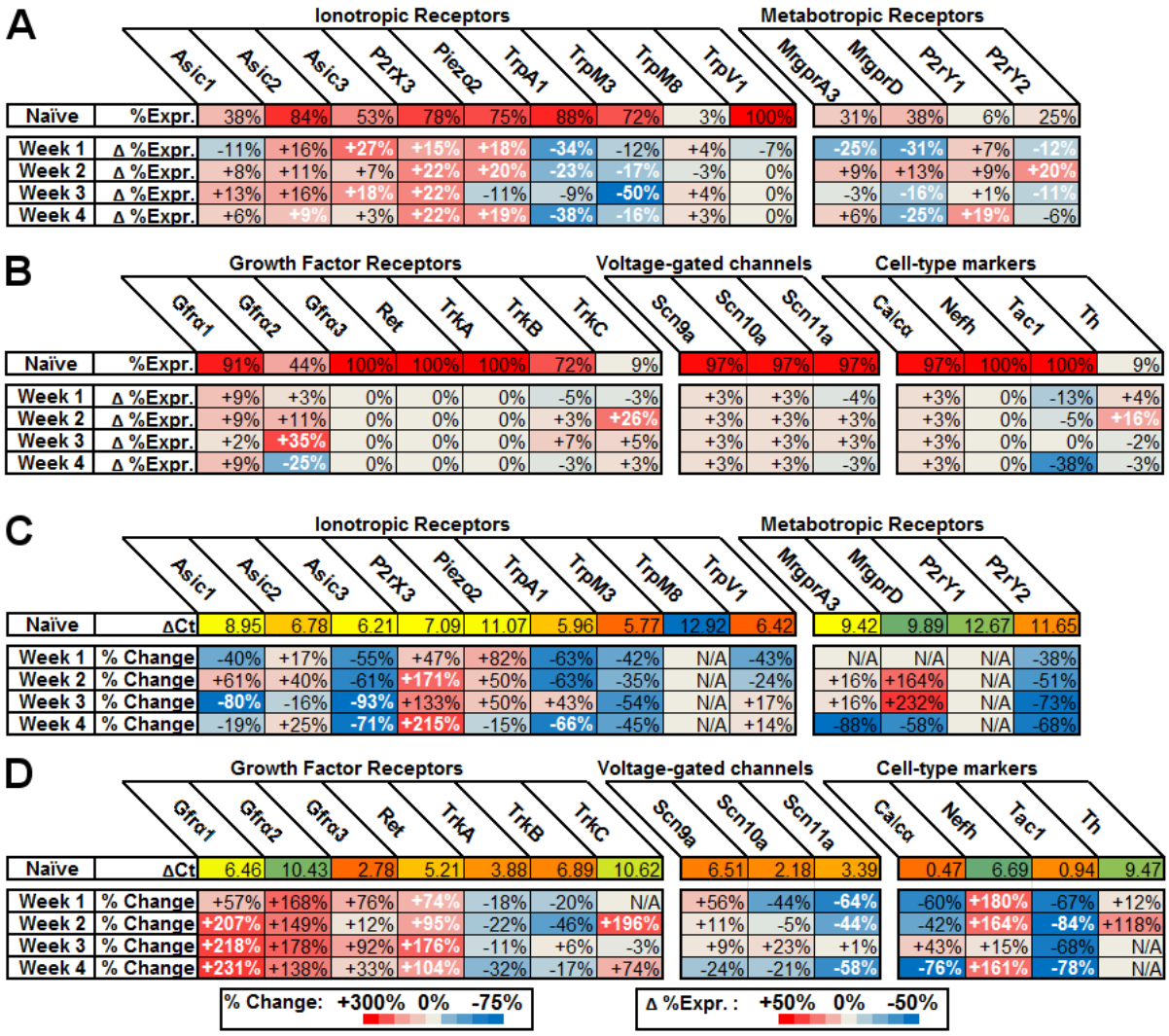

Figure 9. Unmyelinated peptidergic subpopulation changes in backlabeled primary afferents (A-B) Probability of transcript detection in the naïve population and absolute changes in that probability after injury. Bold white text indicates significance in a binomial proportion test at the 0.05 level. (C-D) Naïve average expression level relative to *Gapdh* and relative changes in that level after injury. Bold white text indicates significance in a two-tailed t-test at the 0.05 level. Naïve N=32, Week 1 N=15, Week 2 N=20, Week 3 N=14, and Week 4 N=16.

Putative myelinated nonpeptidergic cells only have a few coherent changes (Figure 10), but the changes they do have are almost exclusively changes in growth factor receptor transcript levels. One week after injury, *Gfrα3* is detectable in 67% of the collected cells, compared to 0% in uninjured afferents, which is consistent with the other cell populations. *TrkA* levels are transiently upregulated one week after injury in the cells that still express it, but it is detectable in significantly fewer cells after nerve injury. *Gfrα2* levels drop 80% and generally stay down for all four weeks, although the number of cells with detectable expression does not change. Levels of the *Gfrα1* transcript trend downwards for 3 weeks before increasing significantly four weeks after injury, which is surprising considering the consistent upregulation seen in other subpopulations over this period. Perhaps this population, which already expresses high levels of *Gfrα1* in the uninjured animal, did not need to produce more transcript for the regeneration process.

Other than growth factor receptors, *Piezo2* levels drop by 55% one week after injury, but recover subsequently. Similar to the unmyelinated nonpeptidergic population, this population shows a decrease in the proportion of cells expressing *Scn10a* and *Scn11a* at week 1, with the *Scn11a* change being more long-lived.

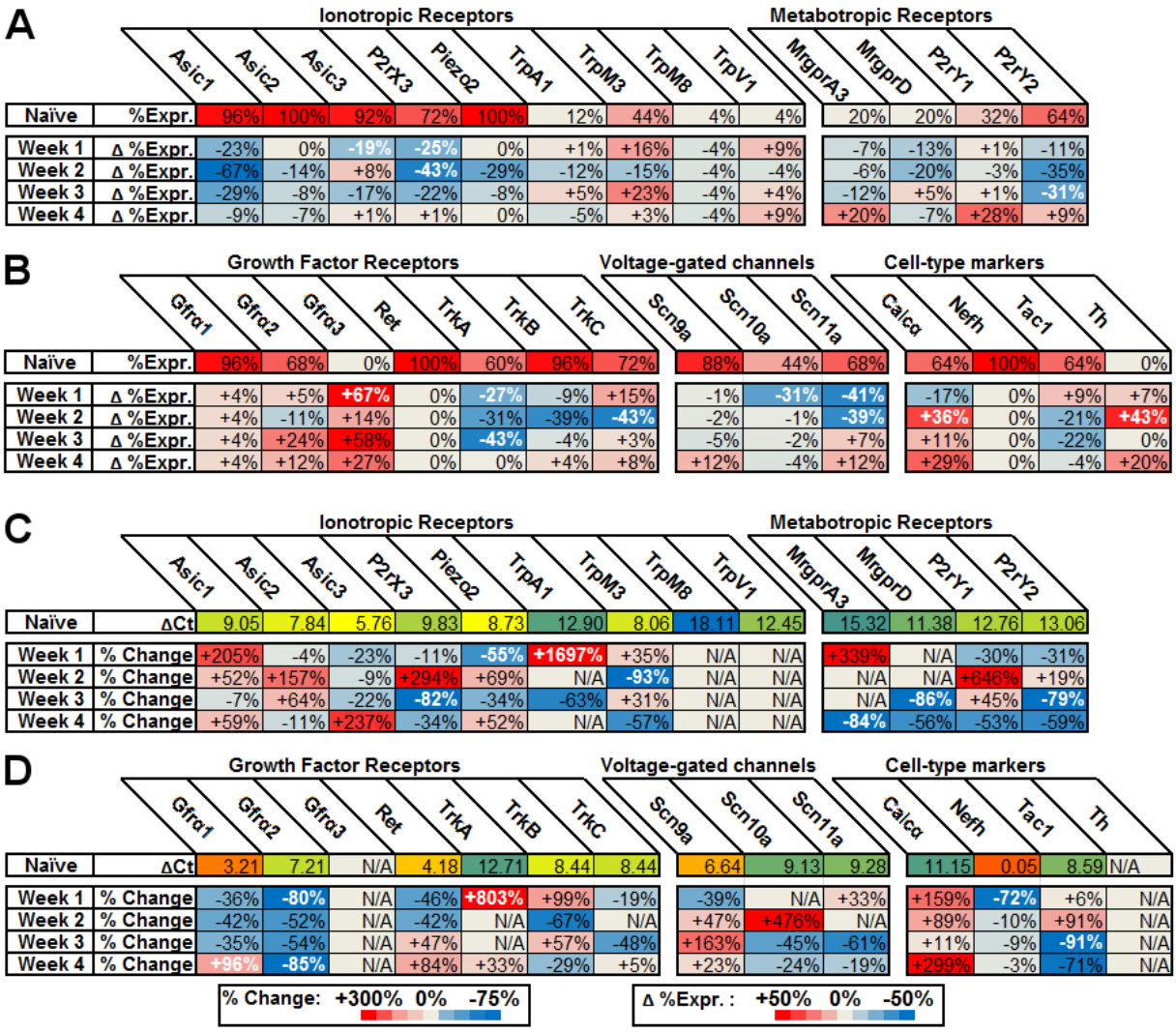

Figure 10. Myelinated nonpeptidergic subpopulation changes in backlabeled primary afferents (A-B) Probability of transcript detection in the naïve population and absolute changes in that probability after injury. Bold white text indicates significance in a binomial proportion test at the 0.05 level. (C-D) Naïve average expression level relative to *Gapdh* and relative changes in that level after injury. Bold white text indicates significance in a two-tailed t-test at the 0.05 level. Naïve N=25, Week 1 N=15, Week 2 N=7, Week 3 N=12, and Week 4 N=15.

Similar to the unmyelinated nonpeptidergic subpopulation, putative myelinated peptidergic cells show *de novo Gfrα3* expression at weeks one to three after nerve injury (Figure 11). There was no baseline expression, so a level comparison with uninjured large peptidergic afferents is not possible, but the expression level of *Gfrα3* in expressing cells from this population is not significantly different from that of the injured unmyelinated nonpeptidergic population (two tailed t-test, $p>0.05$). Transcript levels for the growth factor receptor co-receptor, Ret, are also upregulated after injury at weeks one and three.

The complement of mechanotransduction channels in large peptidergic fibers also change after injury, but in unexpected ways. The mechanical sensitivity of these afferents increases after nerve injury (Jankowski et al. 2009), but most of the mechanotransduction channels seem to decrease their expression after injury. The number of cells expressing *P2rX3*, thought to be potentially involved in indirect mechanical transduction via ATP release from mechanically sensitive keratinocytes (Baumbauer et al. 2015), decreases significantly two and three weeks after injury, with levels trending down at all four weeks. Levels of *Asic3*, thought to potentially be important for mechanosensation in this population (Price et al. 2001), also decrease shortly after injury and are sustained for four weeks. Two mechanoreceptor levels are increased four weeks after nerve injury, however. Levels of putative mechanoreceptor, *Asic1*, have increased 1660% relative to controls four weeks after injury, but only 3/7 cells express the transcript and previous publications indicate ASIC1 is not important for cutaneous mechanosensation (Page et al. 2004).

Piezo2 is not significantly affected in this population at any timepoint, but expression is consistently near-100% and the levels are comparable to the myelinated nonpeptidergic fibers where PIEZO2 is thought to play an essential role (Ranade et al. 2014). If expression of PIEZO2 is proportional to transcript, as for TRPV1 and P2X3, and levels in myelinated nonpeptidergic fibers are sufficient to drive expression, then it would also be expressed in this subpopulation at functional levels in this population and is an attractive candidate mechanotransducer.

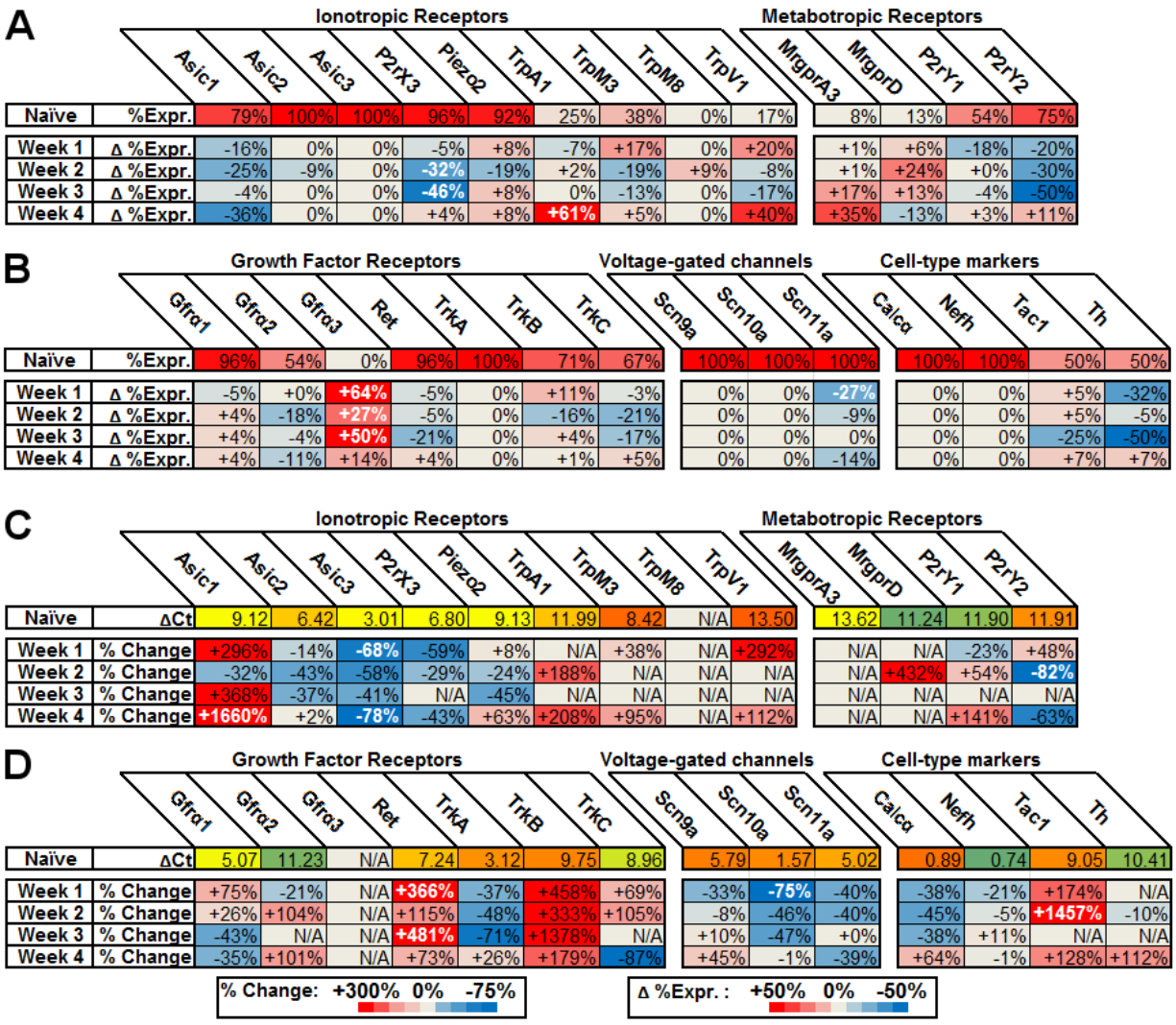

Figure 11. Myelinated peptidergic subpopulation changes in backlabeled primary afferents

(A-B) Probability of transcript detection in the naïve population and absolute changes in that probability after injury. Bold white text indicates significance in a binomial proportion test at the 0.05 level. (C-D) Naïve average expression level relative to *Gapdh* and relative changes in that level after injury. Bold white text indicates significance in a two-tailed t-test at the 0.05 level. Naïve N=24, Week 1 N=11, Week 2 N=11, Week 3 N=4, and Week 4 N=7.

3.3.3 Transcriptionally defined subpopulations converge shortly after nerve injury and diverge following reinnervation

Upon closely examining the changes one week after injury, it is apparent that each population changes in a way that makes it more similar to the other subpopulations. *Gfrα3* is upregulated in cells that formerly did not express it, but is unaffected in populations where it was already ubiquitous. *Gfrα2* is downregulated in the nonpeptidergic populations where it was high, but trend towards upregulation in the Tac1 population where it was previously low. Overall, despite being anchored to the naïve populations by the group assignment method, the detected populations converge at one week after injury. This convergence can be measured by tracking the difference between pairs of populations (Figure 12), defined here as the Euclidean distance between the average relative transcript expression levels for populations A and B:

$$\text{distance}_{t+1-t} = \sqrt{\sum_{\Delta Ct \in gene} (\Delta Ct_A - \Delta Ct_B)^2}$$

This convergence and subsequent divergence is exemplified by the comparison of unmyelinated nonpeptidergic and peptidergic groups (Figure 12A). Given that we have traced four subpopulations, it is possible to make six pairwise comparisons. The initial distance between naïve subpopulations varies widely (15.42 ΔCt for unmyelinated peptidergic vs. unmyelinated nonpeptidergic; 29.69 ΔCt for unmyelinated peptidergic vs. myelinated peptidergic), but they are consistent in their convergence at week 1 and divergence at weeks 2-4. The normalized distances between populations (Figure 12B) show a significant effect of time post-injury (two-factor ANOVA without replication, $p<0.001$). This can be further seen in Figure 12C, which shows significant differences between week one and weeks three and four.

If the populations are converging on one common state one week after injury, then it makes sense to look at which transcripts contribute to this convergence. As each gene represents a different term of the distance equation, convergence can be broken down on a week-by-week basis by looking at how these gene-dependent terms change. Genes that contribute less to the distance between populations one week after injury than they did in uninjured animals are responsible for convergence. Normalizing this to the change in distance between the pair of populations creates a percentage convergence metric and allows comparisons between pairs. Further averaging it between pairs shows the genes driving convergence across all populations.

When quantified in this way, the vast majority (22/27) of genes assayed contribute to convergence one week after injury. The most significant contributors are *Gfrα3* (20%), *Scn10a* (8%), *Asic3* (8%), and *TrkA* (7%), with the remaining 18 of transcripts below 5% contribution.

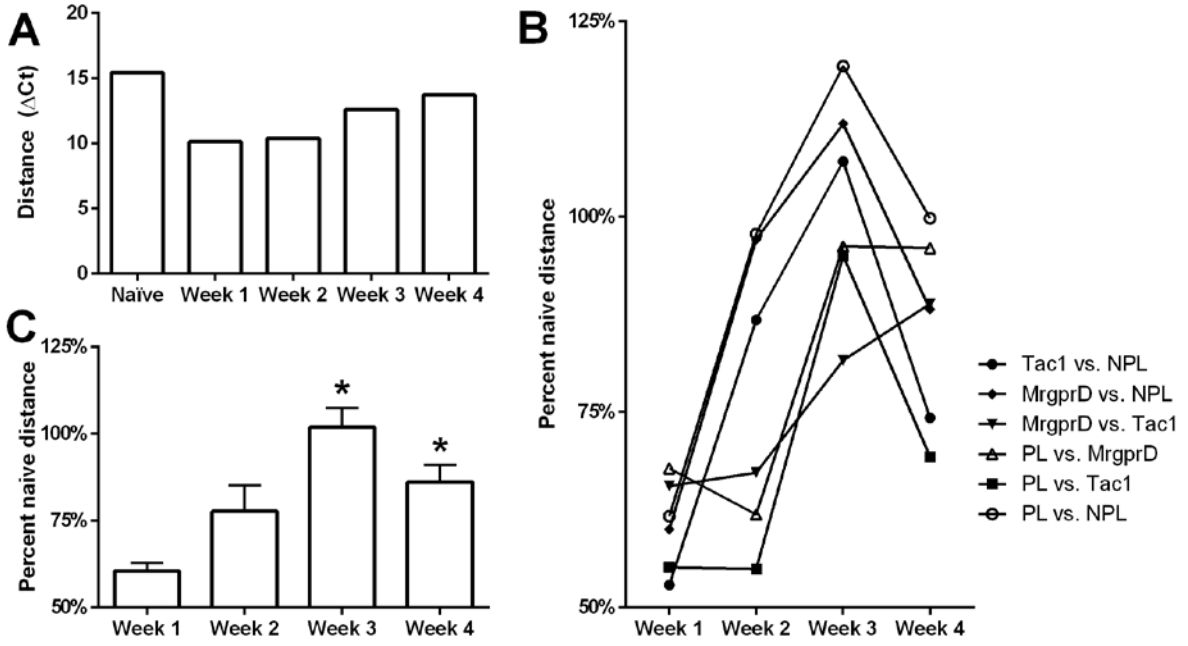

Figure 12. Pairwise distances between populations (A) Euclidean distance between the average expression levels of the unmyelinated nonpeptidergic and unmyelinated peptidergic subpopulations (B) the distance between all 6 pairwise permutations at each time point normalized to the respective naïve Euclidean distance (C) Average of B with error bars representing standard error. Asterisks indicate a significant difference from Week 1 (two-tailed t-test, $p<0.05$).

3.3.4 Persistent transcriptional changes after reinnervation may explain injury-induced alterations in mechanical transduction

The subsequent divergence of transcript levels restores the normal heterogeneity of expression levels, but the timing of this divergence appears to differ between the populations. Nonpeptidergic large cells diverging from the other populations at week two (Figure 12B), while the other populations resume their normal distance from each other by weeks three and four. Notably, there are still significant differences between these regenerated populations and the naïve cells even at 4 weeks after injury. These deviations are particularly notable in unmyelinated peptidergic cells, a subpopulation that is thought to be substantially altered after nerve injury. This population has clear disturbances in some transcripts, including *P2rX3* and *Piezo2*, which have been implicated in hyperalgesia and mechanical sensation, respectively (Coste et al. 2010; Ferrari et al. 2015; Bradbury et al. 1998; North 2004).

At four weeks after nerve crush, every cell in the unmyelinated peptidergic subpopulation expresses detectable *P2rX3* transcript and the level is significantly elevated (Figure 13A,B). Twenty-two percent of cells (7/32) in the naïve unmyelinated peptidergic subpopulation express levels of *P2rX3* that are predicted to be functional (Figure 4D) and the regeneration process increases this proportion significantly to 56% (9/16) of unmyelinated peptidergic cells in the week 4 sample (Fisher's exact test, $p<0.01$).

The proportion of cells expressing *Piezo2* is also significantly increased after nerve crush in this subpopulation (Fisher's exact test, $p=0.05$) (Figure 13C). *Piezo2* expression has recently been shown to be critical for some cutaneous and proprioceptive mechanoreceptors, but not all (Coste et al. 2010; Ranade et al. 2014; Woo et al. 2015; Florez-Paz et al. 2016). PIEZO2 expression alone can confer mechanical sensitivity in heterologous expression systems (Coste et al. 2010), so *de novo* expression of *Piezo2* could be responsible for the post-injury gain of mechanical sensitivity previously reported this subpopulation (Jankowski et al. 2009). Other factors may be required as well, as our data shows that *Piezo2* is expressed at high levels in unmyelinated afferents before injury (Figure 2, Figure 5), yet *Piezo2* knockout has no effect on unmyelinated afferent properties (Ranade et al. 2014). Recent studies indicate that mechanical membrane properties have a substantial impact on the ability of PIEZO2 to transduce mechanical

forces (Soattin et al. 2016; Jia et al. 2016), which may be relevant considering the increased Nefh expression in this population after injury.

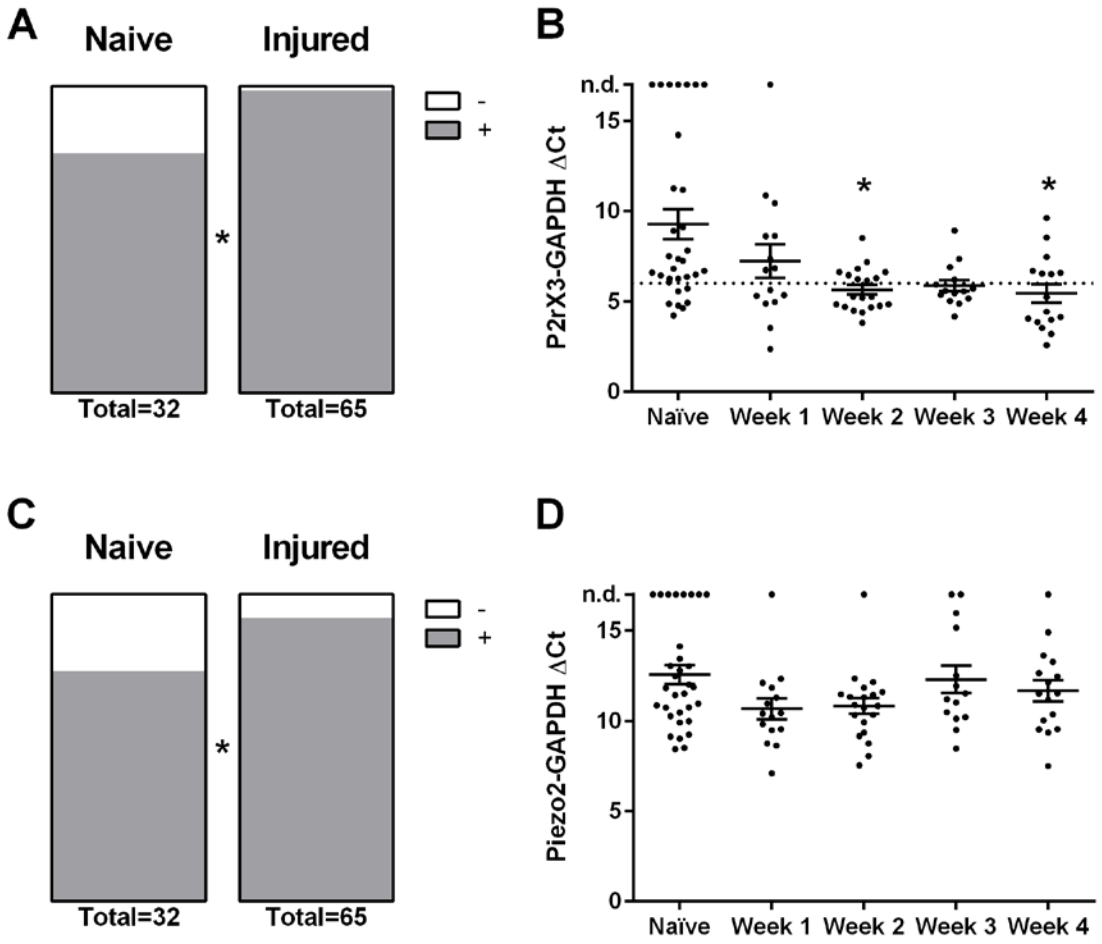

Figure 13. Putative mechanotransducer expression in the unmyelinated peptidergic subpopulation (A-B) *P2rX3* expression quantified as proportion of cells expressing detectable *P2rX3* (A) and *P2rX3* levels with mean ± SEM indicated (B). (C-D) Piezo2 expression quantified as proportion of cells expressing detectable Piezo2 (A) and Piezo2 levels with mean ± SEM indicated (B). Asterisks indicate significant differences from naïve ($p<0.05$) with a chi squared test or two-tailed t-test, respectively.

3.3.5 *Piezo2* knockdown reverses the injury-induced gain in mechanical sensitivity

Piezo2 is a known mechanotransducer that likely confers mechanical sensitivity to a population of A-fibers in uninjured animals (Ranade et al. 2014; Coste et al. 2010). Here, we have shown that it is regulated after nerve injury and may be responsible for de novo mechanical sensitivity in the unmyelinated peptidergic subpopulation of afferents after injury and regeneration. In order to assess this possibility, we injected Penetratin-1 conjugated *Piezo2* siRNA into the saphenous nerve after nerve crush to knock down *Piezo2* expression in regenerated primary afferents. Four weeks after injury, we recorded and characterized siRNA-exposed regenerated afferents as well as afferents that did not receive *Piezo2* siRNA.

Nerve crushed animals had myelinated nociceptors with significantly decreased mechanical thresholds relative to naïve (Figure 14B), in agreement with previous work (Jankowski et al. 2009). This change could be blocked by *Piezo2* siRNA treatment, which restored the mechanical thresholds to naïve levels. The same effect was not observed in C-mechanoheat and C-mechanoheatcold cells (Figure 14C), which had neither a significant decrease in mechanical threshold nor a significant increase in threshold following *Piezo2* siRNA exposure. This is also in accordance with previous work, which did not detect any effect of *Piezo2* knockout on C-fiber mechanical thresholds (Ranade et al. 2014).

Previous work indicates the emergence of a TRPV1+ C-mechanoheat population following nerve injury (Jankowski et al. 2009; Lawson et al. 2008; Jankowski et al. 2010; Jankowski et al. 2012). The most prominent expression of TRPV1 occurs in the unmyelinated peptidergic subpopulation (Figure 2), which shows *de novo Piezo2* expression following nerve injury (Figure 9). Thus, we tested whether this *Piezo2* upregulation was necessary for the gain in mechanical sensitivity in this subpopulation by comparing the phenotype distribution of siRNA treated afferents to crushed and uninjured afferents (Figure 14DEF). The proportion of C-heat fibers increased in regenerated afferents relative to uninjured afferents (chi-squared test, $p=0.014$), and was again significantly enriched by *Piezo2* siRNA treatment (chi-squared test, $p=0.020$).

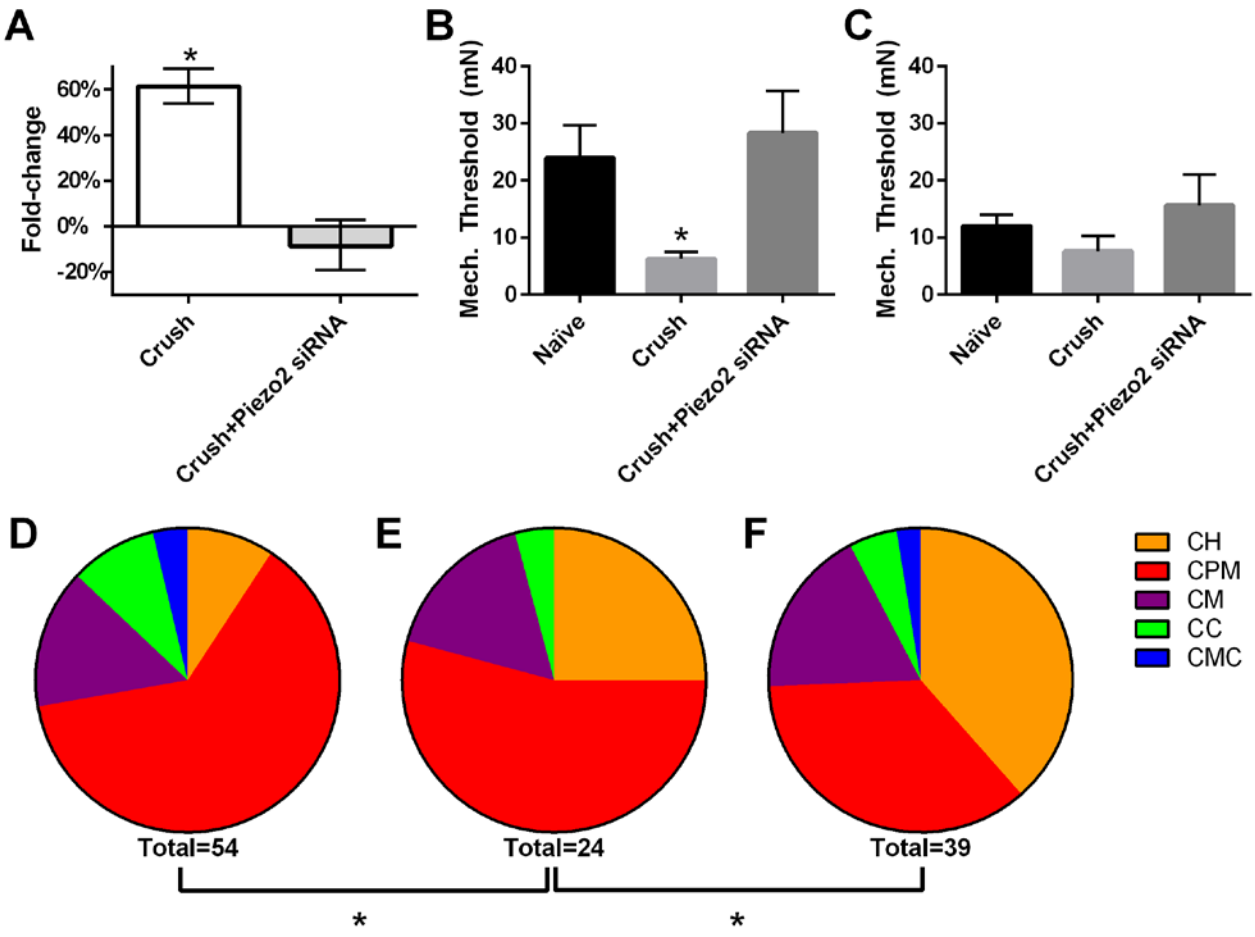

Figure 14. *Piezo2* knockdown affects post-injury physiology (A) *Piezo2* levels increase 1 week after whole nerve crush and are restored to baseline via simultaneous *Piezo2* siRNA injection as assessed by whole DRG PCR. (B) Mechanical thresholds in myelinated HTMRs. Asterisk indicates significant difference from the Naïve condition ($p<0.05$) (C) Mechanical thresholds of C-polymodal fibers. C-fiber phenotype distributions for: (D) Uninjured afferents. (E) Nerve crushed afferents. (F) Nerve crushed afferents that have been treated with *Piezo2* siRNA.

3.4 DISCUSSION

The data presented herein strongly support the idea that the expression of regenerating heterogeneous afferent populations transcriptionally converge while recovering from injury and growing back out to the periphery, only to diverge once more after reaching their target tissue.

The divergence does not completely restore the original transcriptional profile of afferents, but leaves some artefacts of the process that may be responsible for the observed alterations in the regenerated afferent properties.

The artemin and GDNF receptors, respectively *Gfrα3* and *Gfrα1*, were heavily implicated in this process and appear to be important in slightly different stages of the regeneration process. *Gfrα3* is upregulated across multiple populations in the first week post-injury. Drawing analogy to the regeneration timeline, it would appear that *Gfrα3* is upregulated during the initial growth cone formation and extension back out to the target organ. Studies have consistently found that artemin improves afferent survival, but does not cause the massive neurite branching seen with some other neurotrophic factors like NGF (L. E. Wong et al. 2015; Widenfalk et al. 2009; Wang et al. 2014; Bennett et al. 2006; A. W. Wong et al. 2015; R. Wang et al. 2008). These would be desirable properties in a neurotrophic factor used to encourage directed regrowth to a target tissue. In the first week, detectable levels of *Gfrα3* are found in more than 60% of every population, and average relative expression levels exceeded 7 ΔCt. The sub-100% detection of *Gfrα3* may reflect unappreciated divisions in subpopulations, but it is more likely that the very transient expression produces sufficient protein for the regeneration process, as has been previously hypothesized (Jankowski et al. 2010), and our one week transcriptional snapshot did not capture that burst in every afferent. On a protein level, this expansion has been previously characterized using histology in the first week after axotomy (Wang et al. 2011).

The increases in *Gfrα1* occur two to four weeks after injury, as axonal growth cones have started their journey out of the DRG but likely before they reach the target tissues. Indeed, by the second week nearly 100% of every subpopulation expresses detectable *Gfrα1* and the average relative expression levels are 5 ΔCt or higher, comparable to the highest expressing population in uninjured animals. Like artemin, GDNF promotes the regeneration and survival of afferents (Bennett et al. 1998), but is notorious for causing nerve coils (i.e. honeypot issues) when included in nerve regrowth substrates or allografts (Eggers et al. 2013; Tannemaat et al. 2008; Santosa et al. 2013; Shakhbazau et al. 2013). It is almost as if GDNF signaling is informing the afferents that they have traveled far enough and reached the target tissue, an idea supported by the observed upregulation of GDNF in the skin after denervation (Jankowski et al. 2009).

Furthermore, our data show that even after reaching the skin the transcriptional profiles of the peptidergic populations are still significantly different from naïve afferents. Some of these

changes may explain the two mechanical phenotypes observed in injured afferents: increased mechanical sensitivity in myelinated nociceptors (myelinated peptidergic population), and a gain of mechanical sensitivity in TRPV1+ afferents (unmyelinated peptidergic population).

Asic3, a putative mechanotransducer for myelinated nociceptors (Price et al. 2001; Page et al. 2005), is downregulated in the myelinated peptidergic subpopulation (Figure 5). Instead of an increase in mechanical threshold or mechanical insensitivity, however, this population becomes more mechanically sensitive (Figure 14A). This change depends on *Piezo2* expression, as it is reversed with *Piezo2* siRNA treatment. Thus, *Piezo2* levels appear to determine the mechanical sensitivity of this population of regenerated afferents after nerve injury, although it is not essential in uninjured animals (Coste et al. 2010; Ranade et al. 2014). It could also be that other properties of the cell (e.g. mechanical membrane properties) have changed during the regeneration process and now *Piezo2* is capable of driving activity in this afferent population (Soattin et al. 2016; Jia et al. 2016).

The unmyelinated peptidergic subpopulation's phenotypic shift also shows *Piezo2* dependence, with knockdown significantly increasing the number of mechanically insensitive C-fibers (Figure 14DEF), but causing no change in the mechanical thresholds of the remaining mechanically sensitive cells. The importance of *Piezo2* expression for any kind of cutaneous unmyelinated afferent is novel, as mechanical thresholds of C-fibers are not significantly affected in *Piezo2* knockout animals (Ranade et al. 2014). This emergence of a *Piezo2*-dependent mechanically sensitive subpopulation follows *de novo Piezo2* expression in the unmyelinated peptidergic subpopulation. The knockdown of *Piezo2* causes an increase in the unimodal heat-sensitive fibers, as you would expect if the heat sensitive unmyelinated peptidergic population lost mechanical sensitivity. A loss of mechanical sensitivity in any other subpopulation would lead to either an increase in unimodal cold-sensitive fibers or the creation of heat-cold sensitive afferents, neither of which were observed. Thus, it seems likely that *Piezo2* knockdown is removing mechanical sensitivity from unmyelinated peptidergic fibers.

In conclusion, although the peripheral nerve regeneration literature does not acknowledge the heterogeneity of regenerating afferents, it may still be quite accurate because the afferents appear to transcriptionally converge during the early regeneration process. Substantially more work needs to be done to investigate the control of subsequent transcriptional divergence following presumed tissue reinnervation, with *Gfrα1* and its ligand GDNF being attractive

starting points. Changes in individual regenerated subpopulations that persist after reinnervation may be responsible for the sensory abnormalities reported by patients (e.g. mechanical allodynia). In this case, subpopulation-specific regulation of Piezo2 appears to confer novel mechanical sensitivity to regenerated unmyelinated peptidergic afferents and is capable of affecting regenerated myelinated nociceptor mechanical thresholds after injury, despite being thought to play no role in either population without injury (Ranade et al. 2014).

4.0 GENERAL DISCUSSION

4.1 USING SINGLE CELL QPCR TO PREDICT FUNCTION

A large part of this thesis was spent developing the single cell qPCR technique, investigating how the technique could be used, and building a conceptual framework for single cell comparisons. Previous publications have correlated *absolute* single cell mRNA transcript level with channel function for voltage gated ion channels in extremely homogenous sets of *Cancer Borealis* (Jonah crab) neurons (Schulz et al. 2006; Ransdell et al. 2010). However, our work shows that it is possible to use *relative* single cell mRNA level in murine neurons to predict transducer function and subsequent neuron phenotype for some transcripts, which has substantial implications for the possibility of estimating function using molecular biology.

This technique has limitations. It requires excellent molecular biology acumen and machine-like pipetting precision. It can only be expected to work for proteins that are not translationally regulated and do not functionally depend on the expression of other proteins. The single cell qPCR results it generates represent a single snapshot of potentially dynamic transcript expression. Any functional hypotheses it generates still need to be verified using physiology.

It also has major advantages. Single cell qPCR is quicker than physiology. It can be used on afferents that have not yet returned to their target tissue. It allows the investigation of many transcripts at once, and thus detailed class assignments. The data in this document hopefully exemplify what the technique can do. This technique can be used, as it was in this case, to assay changes in the expression of many genes simultaneously and develop theories about how the regulation of those genes affects primary afferent properties. The survey led us to a candidate transcript that otherwise would not have been considered due to the report indicating it was unimportant for normal C-fiber mechanical transduction (Ranade et al. 2014). Knockdown of

said gene, *Piezo2*, resulted in the unmasking of a mechanically insensitive, heat sensitive group of C-heat cells after injury.

We have just scratched the surface of what is going to be possible with the combination of next generation sequencing and physiology, but the results are promising. More work remains to be done with regards to seeing how far this technique can be extended and optimized.

4.2 TRPM8 POPULATION

Work examining cold sensation in mammals has consistently distinguished two populations of cold sensitive fibers (Iggo 1959; Hensel et al. 1960; Campero et al. 2009). One population is activated at low temperatures (<14°C) and its firing rate quickly plateaus (Iggo 1959). The second population precisely encodes decreases in temperature, can become spontaneously active between 24 and 16°C, and cannot be further activated below that point (Hensel et al. 1960). These were, for a time, termed "static cold" and "dynamic cold" fibers respectively. Most studies report that all members of the static cold population are mechanically sensitive, but the dynamic cold subtype can be further split into mechanically insensitive and sensitive populations (Pierau F-K et al. 1975; Zimmermann et al. 2009).

A second classification criterion, menthol sensitivity, has also been used to split the cold fibers. Studies agree that the dynamic cold fibers are menthol sensitive, while the static cold responders are menthol insensitive (Campero et al. 2009). This indicated that the menthol receptor, eventually discovered and named TRPM8 (Peier et al. 2002; Reid et al. 2002), was only expressed in the dynamic population of afferents. The discovery of the TRP channels (TRPA1 and TRPM8, both putative cold sensors) provided a molecular marker for cold sensation, which prompted dissociated DRG culture electrophysiology work intended to discern the mechanism of cold sensitivity.

This led to a third classification criterion, tetrodotoxin (TTX) sensitivity, which divided cold responses once more. The two major TTX insensitive ion channels expressed in the DRG are Nav1.8 and Nav1.9 (Elliott & Elliott 1993). Nav1.8 is cold insensitive and is thought to be responsible for the majority of the voltage gated sodium current in action potentials of a mix of large and small diameter afferents (Zimmermann et al. 2007; Djouhri et al. 2003). Nav1.9

effectively constitutes a leak current and is partially responsible for determining the resting membrane potential and excitability of the predominantly-small DRG cells that express it (Ho & O'Leary 2011). As such, it was reasonable to expect that both populations of cold sensitive afferents would have TTX insensitive currents. However, results showed that action potentials could be entirely abolished in somal recordings from some menthol sensitive cold fibers with 100nM TTX application (Reid et al. 2002; Xing et al. 2006). This implied that at least a subpopulation of dynamic cold cells did not express sufficient Nav1.8 to drive action potential generation in the presence of TTX. Though it has not been previously demonstrated in specific, our findings show that while the sodium channel complement of TrpM8 cells makes them very unique among small diameter afferents, they are in line with what might have been expected from the literature.

An unexpected finding was the expression of *Tac1* in this subpopulation. Previous work with the TRPM8-GFP mouse had reported no colocalization with SP in the spinal cord, though it did note that TRPM8+ fibers projected to outer Lamina I of the dorsal horn very near the SP band (Dhaka et al. 2008). Substance P colocalization with TRPM8 had only previously been reported in human work looking at the cutaneous fibers (Axelsson et al. 2009). Regardless, likely proximity of projections from our most vigorous heat (Tac1 population) and cold (TrpM8 population) responders raises questions about whether these two fiber types could both be using substance P to modulate thermal sensation circuits. The release of SP is activity dependent and can cause prolonged activity in superficial spinal cord neurons (Henry et al. 1975), so the presence of SP in the TRPM8 subpopulation implies that vigorous and sustained activity in this population may cause pain that is comparable to activation of the Tac1 population.

This possibility is further supported by the thermal grill illusion, where alternating innocuous warm and cool bars give a burning pain sensation when applied to the skin (Craig & Bushnell 1994). The dorsal horn is topographically organized, with medial to lateral dorsal horn corresponding to proximal to distal projection areas for that dermatome (Brown et al. 1997). Simultaneous presentation of alternating warm and cool bars would activate neighboring sets of Tac1 and TrpM8 afferents. These populations could release SP into the superficial dorsal horn, which would sensitize the neurokinin 1 receptor (NK1) expressing projection neurons. This sensitization could potentiate the static warm and cool responses, making the resulting activity painful.

4.3 EXPRESSION CHANGES AFTER INJURY

Post-injury transcriptional changes could be separated into two regimes. The first regime was characterized by decreased interpopulation distance and upregulation of growth factor receptors thought to be important for cell survival after injury (Widenfalk et al. 2009; Bennett et al. 1998; D. L. Bennett et al. 2000). It is possible, however, that there are transcriptional changes that occur and abate before 7 days after injury. The increases in expression observed one week after injury could be a result of such very transient upregulation. Previous reports have found injury-induced transcriptional regulation of various transcripts that manifest and abate in less than one week post-injury, like the purinergic receptor *P2rY1* (Barragán-Iglesias et al. 2016), voltage gated sodium channels Nav1.3 and 1.6 (Kim et al. 2001; Dib-Hajj et al. 1996), growth factor receptors *TrkA* and *TrkB* (Webber et al. 2008; Funakoshi et al. 1993), transcription factor *Sox11* (Jankowski et al. 2006), and TRP channels *TrpC3, TrpC4,* and *TrpC5* (Staaf et al. 2009). If many transcripts are regulated only in the first 1-6 days after injury and expression subsequently stabilizes, this could be interpreted as a third transcriptional regime. In this case, the goals for the three regimes would be: 1) prevention of cell death and preparation for axon regrowth 2) guide and elongate the regenerating axonal 3) return the afferent to its original properties.

The first set of changes largely serves to maintain DRG cell health in a changing neurotrophic factor environment and provide the axon growth cone with the proteins it needs to regenerate. Although they are not necessarily sustained at the first week, *Gfrα3*, *TrkA*, and *TrkB* levels seem to briefly spike, as evidenced by the increased proportion of cells expressing detectable levels of those transcripts after injury. This finding makes sense given their roles in neurite formation, axon outgrowth, and regeneration (A. W. Wong et al. 2015; Lippoldt et al. 2013; L. E. Wong et al. 2015; Jankowski et al. 2010; Wang et al. 2014; Widenfalk et al. 2009; Bennett et al. 2006; S. Wang et al. 2008; R. Wang et al. 2008; Webber et al. 2008; Funakoshi et al. 1993). The expression levels are generally not maintained, however, which raises two possibilities. First, it could be that the brief burst of transcription had a commensurate burst of translation that made all the related protein the DRG cells will need for the regeneration process, as appears to be the case for *Gfrα3* (Jankowski et al. 2010). Second, it could be that the transcript is restricted to the growth cone. Axonal protein synthesis has been shown to play an important role in the regeneration process (Zheng et al. 2001; Gomes et al. 2014), and there is evidence for

proteins like TRKA being highly expressed in the growth cone while downregulated in the soma (Webber et al. 2008). The *Gfrα3* expression has been thoroughly investigated (Jankowski et al. 2010) and is essential for upregulation of TRPV1 (Jankowski et al. 2012) that causes the expansion of the heat sensitive, mechanically insensitive fiber class C-Heat normally seen after injury.

The second set of changes lasts for two weeks after nerve crush in the peptidergic and unmyelinated nonpeptidergic fibers, but only one week in the myelinated nonpeptidergic fibers. In this document I have assumed this transcription supports a period of stable axonal growth that ends when the cells reach the skin. There are several reasons for this assumption. Previous work with mid-thigh saphenous nerve crush and cut has shown that some reinnervation occurs before 12 days post injury and most occurs before 21 days (Jing et al. 2012; Jankowski et al. 2008). A fraction of regenerating fibers, our data argues the large nonpeptidergic subpopulation, reach the skin at or before two weeks after nerve injury. From two to three weeks after nerve injury the rest of the surviving fibers seem to reach the skin. This theory is supported by the fact that $NF200^{+}$/$CGRP^{-}$ fibers are the first to reach the skin again after nerve injury (Kambiz et al. 2015; Devor et al. 1979).

This elongation period involves the upregulation of *Gfrα1* and downregulation of *Gfrα2*, both of which have been previously observed in subpopulation agnostic studies (Kashiba et al. 1998; Bennett et al. 1998; D. L. Bennett et al. 2000; Jankowski et al. 2009). Signaling through the GDNF receptor, GFRα1, has been shown to be neuroprotective (D. L. Bennett et al. 2000). Sources of GDNF also cause axonal trapping, where the axon fails to move on from the GDNF source, when used in bioengineering applications for regenerating nerves (Shakhbazau et al. 2013; Tannemaat et al. 2008; Eggers et al. 2013). GDNF has also been shown to be upregulated in denervated skin (Jankowski et al. 2009). Combining these findings, it could be that GFRα1 signaling occurs primarily when the axon reaches the skin, causing it to stop its migration and attempt to return to its original properties.

Normal expression patterns are not restored at four weeks after nerve injury and it is not clear that the regenerated afferents ever return to the pre-injury expression. Alterations in transcript expression following saphenous axotomy has been documented up to 10 weeks (Jankowski et al. 2009). Previous work dealt with the entire dorsal root ganglion, which raised the possibility that alterations in expression were due to disproportionate cell loss from specific

transcriptional populations. However, our work unambiguously indicates that expression is persistently changed within these populations.

Relative to the uninjured populations, the growth factor expression of regenerated cells is still quite different at four weeks after nerve injury. *Gfrα1* is upregulated in nonpeptidergic and unmyelinated peptidergic fibers and *Gfrα2* is downregulated in nonpeptidergic fibers. Perhaps these populations are still in the process of reinnervating or, in the case of myelinated nonpeptidergic fibers, finding their target end organ in the skin. It is currently unclear how myelinated nonpeptidergic fibers re-associate with hair fibers and touch domes, and it is possible that the process takes considerably longer than the trip back to the skin.

There were also changes in transduction channels that persisted four weeks after nerve injury. *Asic3* was observed to be downregulated in the peptidergic subpopulations, which has been previously reported (Poirot et al. 2006) in a subpopulation agnostic manner. *P2rX3* was also shown to be upregulated in the unmyelinated peptidergic small cells. This has been reported at the whole DRG level following CCI (Reinhold et al. 2015) and axotomy (Jankowski et al. 2009), but not persisting four weeks after nerve injury. P2X3 is normally not expressed in the unmyelinated peptidergic population and its expression would likely confer purine sensitivity. Keratinocytes have recently been shown to communicate with unmyelinated fibers (Baumbauer et al. 2015) and ATP is an attractive candidate for mediating that communication. Thus, ATP signaling from mechanosensitive keratinocytes could be conferring indirect mechanical sensitivity to a subpopulation of afferents and it is possible that *P2rX3* knockdown would also affect mechanical sensitivity.

4.4 PIEZO2 IS RESPONSIBLE FOR MECHANICAL TRANSDUCTION IN INJURED AFFERENTS

Mechanically sensitive TRPV1+ cells have been observed exclusively following nerve injury (Jankowski et al. 2009; Jankowski et al. 2010; Jankowski et al. 2012), while TRPV1 immunoreactivity is restricted to mechanically insensitive C-heat fibers in uninjured animals (Lawson et al. 2008). In our data, C-heat fibers are exclusively seen in the Tac1 subpopulation, which expresses *TrpV1* and has *de novo Piezo2* expression after nerve injury. Thus, I

hypothesized that Piezo2 was conferring mechanical sensitivity to the Tac1 peptidergic subpopulation. I tested this hypothesis using *Piezo2* siRNA knockdown following nerve crush, which expanded the subpopulation of mechanically insensitive C-heat fibers. This result is consistent with blocking the gain of mechanical sensitivity in the Tac1 subpopulation.

The Tac1 subpopulation projects directly to Lamina I of the dorsal horn and carries noxious heat information. If the activation of this population causes the sensation of burning pain under normal conditions, one can imagine that mechanical activation after injury would also cause burning pain, a phenomenon known as mechanical allodynia. Mechanical allodynia could, therefore, potentially be blocked with topical PIEZO2 antagonists. Although antagonists specific for PIEZO2 do not presently exist, one lab recently developed a high throughput mechanical assay and is working on pharmacological tools for manipulating the PIEZO family.

In the event that cutaneous PIEZO2 is completely blocked, it is likely that RA and SA1 LTMR activity would also be affected (Ranade et al. 2014; Woo et al. 2014). It is unclear how the absence of many low threshold inputs would affect the perception of touch, but it seems likely to be preferable to and safer than a nerve block.

5.0 FUTURE DIRECTIONS

5.1 RELATIVE TRANSCRIPT LEVEL AND FUNCTION

5.1.1 Does relative transcript level determine function in neurons?

We have shown that steady state expression level of *TrpV1* and *P2rX3* mRNA above certain thresholds predicts protein function in cultured DRG neurons. However, we have not shown that TRPV1 and P2X3 protein function depends on the mRNA. In order to address this, we would need to attempt to knock down expression of *TrpV1* or *P2rX3* using validated siRNA and re-generate Figure 4. If protein expression did not change during the course of the experiment, we would expect that there would be a rightward shift in the threshold relative to noninterfering siRNA controls. If protein expression did change, we would expect the threshold to remain constant. If sufficient care was taken to control for cell selection bias, knockdown could be verified on a single cell level by comparing average relative channel mRNA expression between active siRNA treated and noninterfering siRNA control.

5.1.2 Is transducer transcript level a more accurate predictor of function than cell class?

One unanswered question arising from this work is whether transcript level of a transducer is a better predictor of function than cell class. We have shown that transcript level can be correlated strongly with function, but transcript level is also correlated strongly with transcriptional class. For instance, if we are only interested in heat sensitivity, should we be looking at *MrgprD* and *Tac1* expression, or *TrpV1* and *TrpV2*? Both the MrgprD and Tac1 populations are predominantly heat sensitive, but TRPV1 and TRPV2 may be directly conveying thermal sensitivity. In order to address this, we would likely need to collect more functionally

characterized cells and recruit a collaborator skilled at bioinformatics. My data analysis yielded many results that I am confident in, but the story would benefit from a collaborator capable of more nuanced analyses. This question is of particular important because it directs future "molecular signature of function" experiments.

5.1.3 What is the proper reference gene for these comparisons?

We chose to use *Gapdh* as our reference gene when calculating relative expression because it has previously been shown to be unaffected by nerve injury (D. L. Bennett et al. 2000; Staaf et al. 2009). References genes are relevant only if they do not change with your manipulation, which is typically difficult to verify without running a variety of other reference genes simultaneously. Furthermore, *Gapdh* expression is known to vary widely between different cell types (Barber et al. 2005) and this document has focused on the idea of extreme DRG heterogeneity and the possibility of subpopulation-specific regulation masking larger changes. If *Gapdh* is variably regulated in different populations, it could be contributing to population-specific ΔCt noise that could be driving certain widely expressed channels to appear uncorrelated with their functions. This particular option seems unlikely, as we do not observe systematic increases or decreases in populations following injury.

Another potential problem involves the cellular localization of our reference gene product. GAPDH is a protein that localizes to the soma, while the majority of our proteins of interest are thought to have their primary effect in the distal axons. This distinction has been shown to be important, particularly if making comparisons between cells with variable axon diameters, as the ratio of axonal volumes can be dramatically different from somal volumes (Ransdell et al. 2010). As such, it might make sense to use a more ubiquitously localized protein like *β-Actin* instead of *Gapdh* as the reference gene. It may yet be helpful, however, to use a somally-localized mRNA as the reference transcript, considering the axon volume of these cells changes dramatically during the injury and regeneration process.

The stability of several transcripts have been examined in a mouse spinal nerve injury model, but not axotomy (Staaf et al. 2009). In order to evaluate these possibilities, we would need to generate primers for and run other potential reference genes that are distributed throughout the cell (i.e. *18s*, *β-Actin*), compare their levels across our timepoints after injury, and

assess the correlations between potential standard genes and genes of interest (as described in Appendix A).

5.2 INJURY-INDUCED TRANSCRIPTIONAL CHANGES

5.2.1 Do the different cell populations reinnervate the skin at different times?

Our data shows that the divergence of the myelinated nonpeptidergic fibers at 2 weeks after injury has nearly returned to baseline, while the other fibers lag by a week. There have also been previous reports that $CGRP^-$ myelinated fibers return to the skin faster than unmyelinated fibers (Kambiz et al. 2015), which would be consistent with this subpopulation, but there has been a report of GFRα1 expressing cells being less motile than cells that do not express GFRα1 (Guo et al. 2014). This raises the possibility that the different transcriptionally defined populations of cells reinnervate the skin at different rates.

From the experiments presented in this thesis, we can conclude that the different populations appear to reflect unique channels of sensory information projecting to the spinal cord. Imbalances between them during the reinnervation process could create unusual states of spinal cord input that could manifest as paresthesia. Although this state might only last for a few weeks in rodents (Kambiz et al. 2015), it could potentially last for months in humans, where the distances traveled are much longer and thus different reinnervation rates cause a much greater disparity in reinnervation time (Lu Bai et al. 2015). Verification of the order in which these populations reinnervate the hairy skin would be the first step in defining the population of sensory neurons possibly responsible for paresthesia, which would enable molecular approaches to target the proper population for silencing.

These experiments would involve cutaneous injections of a retrograde label like DiI and subsequent cell pickup. Experimental groups would be an uninjured group and 1, 2, and 3 week groups after crush of the sural nerve, with a 1 day control to confirm the specificity of the tracer injections. Recovered cells would be assessed using single cell PCR, assigned to a cell class as described in section 3.2.7, and compared between groups as a proportional distribution. If no change is seen, then different populations of afferents reinnervate skin at undistinguishable rates.

If, as expected, the nonpeptidergic myelinated population reinnervates the skin first, this population could be a good target for pharmacological manipulation.

5.2.2 Does successful reinnervation depend on *Gfrα1* transcript levels?

The early (≤1 week post-injury) transcriptional shift is accessible and important for the initiation of the regeneration process, and thus it is more frequently studied (Wang et al. 2011; Jankowski et al. 2006). However, the second transcriptional shift at 2-4 weeks could also be important in determining whether misguided reinnervation of tissues is maintained, with the alternative being cell loss. GDNF, the ligand for GFRα1, has been shown to be upregulated in the skin following axotomy (Jankowski et al. 2009), and in this document we have shown that *Gfrα1* is upregulated in various sensory neuron populations in this time period.

An experiment to answer this question would be to inject siRNA or a high dose of GFRα1 antibody and knock down *Gfrα1* expression levels during weeks 2 and 3, then do histology and quantify the effect on reinnervation and cell death. There are three possible results from this. First, it could be that GFRα1 signaling is unimportant for regeneration and regenerated afferents are not detectably different following its knockdown. Second, it could be that the absence of GFRα1 signal causes neurons to attempt to continue migrating, resulting in more superficial fibers with atypical terminal morphology. Finally, it could be that GFRα1 signaling is essential for cell survival in this later regeneration time period, and reducing the signaling will lead to cell death.

5.2.3 Do afferents switch groups during reinnervation?

The experiments outlined in this document assess current expression, taking snapshots of a dynamic system. In quiescent cells (neurons) from healthy, adult animals, it is possible to argue that steady state assumptions should apply and results from the single cell qPCR technique should reliably predict protein level for some transcripts. After injury, however, the system has been perturbed and steady state assumptions no longer apply. Knowing the current mRNA expression does not necessarily tell us which proteins are expressed, as we see when examining the disconnect between our very transient *Gfrα3* mRNA expression and GFRα3 protein

expression during the reinnervation process (Bennett et al. 2006). Transcript level is likely proportional to protein synthesis rate, and our single snapshot of each cell does not enable us to integrate this rate and calculate protein abundance.

This is particularly concerning in the most extreme case, the potential switching of afferent groups. This thesis has interpreted all injury-induced changes relative to the closest neighboring population. Thus, changes in the current version of each cell populations were discussed, but these changes were not traced to the original population members. The easiest way to trace population members would be to use an inducible Cre-recombinase transgenic animal line to label one of the transcriptionally-defined subpopulations and watch those cells go through the regeneration process. CreER driver lines are available for *MrgprD*, *Tac1*, and *Th*. The experiment would use those CreER driver lines crossed with a floxed reporter (like tdTomato) and induced with tamoxifen as adults. Following systemic tamoxifen washout, the saphenous nerve would be crushed in 75% of the mice. Pickup of fluorescent cells from both injured and uninjured mice would occur at 1, 2, and 3 weeks following injury with the experimenter blinded to the manipulation. Comparison between injured and uninjured controls would allow us to trace cells and determine whether they are switched out of a given population.

Although this experiment is worth doing, it does seem fairly unlikely that afferents would change their transcriptional group even following nerve injury. Such a change would likely cause easily detectable alterations in spinal cord input bands that have not been reported. As a first pass, it might be worth doing some spinal cord histology quantifying the extent of the Substance P band in injured and uninjured animals.

5.3 PIEZO2 AND MECHANOTRANSDUCTION

5.3.1 Is *Piezo2* necessary for mechanotransduction?

In order to definitively conclude that *Piezo2* is necessary for C-fiber mechanical sensitivity after nerve crush, we would need to dissociate the observed effect from the manipulation using a non-interfering siRNA control and the same injection scheme as with *Piezo2* siRNA. We would expect this non-interfering siRNA would have no impact on regeneration or the physiological

phenotype observed, as has been reported in past publications using this technique (Jankowski et al. 2008; Jankowski et al. 2010; Jankowski et al. 2012).

Additionally, we would need to confirm that Piezo2 knockdown does not affect growth cone motility and prevent some axons from returning to the skin. Plans have been made to do this through quantification of PGP9.5 labeled free nerve ending density.

Finally, we have shown knockdown of *Piezo2* upregulation at the mRNA level, but protein is the functional unit. The plan was to show protein knockdown following siRNA treatment using a western blot, but there have been difficulties finding a working PIEZO2 antibody. Commercial PIEZO2 antibodies label bands at 60kDa, while the PIEZO2 protein is over 300kDa, and our attempt to use one such antibody for western blot and immunostaining has not yielded viable results. The non-commercial antibody responsible for the single successful Piezo2 western blot in the literature is currently unavailable (Woo et al. 2014).

5.3.2 Is *Piezo2* necessary for mechanotransduction in uninjured CMH/CMHC cells?

It could be that *Piezo2* is upregulated in the peptidergic population and we are knocking it down and unmasking a population of C-heat fibers that had gained mechanical sensitivity. Another possibility, however, is that uninjured C-mechanoheat cells rely on PIEZO2 for mechanotransduction and we are converting them to C-heat fibers with *Piezo2* knockdown. Data from knockout animals does not support this possibility (Ranade et al. 2014), but ideally we would demonstrate the same effect in our *Piezo2* knockdown animals. This experiment would require the addition of another experimental group, animals that did not receive axotomy and just received *Piezo2* siRNA nerve injections.

5.3.3 Is GFR*α*1-GDNF signaling responsible for the upregulation of *Piezo2* after injury?

Some preliminary data from our lab and previous publications hint that the GDNF receptor, *Gfrα1*, maybe responsible for the mechanical changes observed after injury and the expansion of the thermal population. *Gfrα1* is expressed across populations after nerve injury and is significantly upregulated as the afferents return to the skin (Figure 7). Signaling through this receptor in GDNF-overexpressing mice resulted in C-fibers that were exquisitely sensitive

mechanical stimuli and almost complete (97%) thermal sensitivity (Albers et al. 2006). These changes would parallel the expansion of the C-heat population observed after injury and the gain of mechanical sensitivity in these fibers. Preliminary data from our lab also indicates that *Gfrα1* knockdown effectively eliminates the C-heat subpopulation following injury, but more data is needed before conclusions can be drawn about its effects on mechanical sensitivity (Baumbauer et al., in preparation). This appears to be a promising target in the search for the mediator of *Piezo2* upregulation and it could be pursued using largely the same experimental framework as included in this document.

6.0 CONCLUSION

Every technique that assesses individual afferents shows that afferents are incredibly heterogeneous. Regardless whether the lines between groups are drawn by anatomists, histologists, or physiologists, everyone agrees that there are many lines to draw. Thus, it is confusing that attempts to quantify changes in afferents after injury typically ignore the heterogeneity. One reason for this is that the level of population markers (CGRP, SP, GFRα2) change after injury and populations can no longer be identified with confidence in the same ways that they were previously. This document shows that mRNA levels can be used to divide primary afferents into a finite number of populations that are still identifiable after injury. From expression changes within those populations, we identified a mechanoreceptor, *Piezo2*, necessary for the mechanical sensitivity of an unmyelinated subpopulation after nerve injury. These findings have potential implications for the treatment of mechanical allodynia following nerve injury and show the potential of RNA profiling techniques in the identification of potential injury-induced changes.

APPENDIX A. VALIDATION OF THE SINGLE CELL PCR TECHNIQUE

The work contained in this thesis is critically dependent on our single cell PCR technique. Low accuracy would render our results unrepeatable, while low precision would leave us unable to detect changes between injury conditions. Thus before undertaking these projects, I validated the single cell PCR technique to ensure we could make relative level comparisons with high precision.

After trying a variety of techniques, we decided to use a T7 linear preamplification kit (MessageBOOSTER for cell lysate, Epicentre) followed by RNA cleaning (RNA Cleaner & Concentrator-5 columns, Zymo Research) and qPCR using MMLV reverse transcriptase and a master mix approved for our real time PCR machine (SsoAdvanced SYBR Green Master Mix, BIO-RAD). Unless otherwise indicated, everything in this appendix will refer to that specific combination of techniques performed by Robert Friedman.

A.1 VALIDATION OF LINEAR PREAMPLIFICATION

To verify that our preamplification was independent of both the specific RNA sequence being amplified and the starting amount of the specific mRNA, we preamplified 8 replicates of two different amounts of mRNA (10pg and 160pg) from Swiss-Webster lumbar whole DRG lysate. After preamplification, we pooled the replicate samples and proceeded through RNA cleaning and qPCR, running our twenty primer sets. The variable abundances of different mRNA templates in whole DRG lysate resulted in a wide distribution of Ct values, which allows us to assess whether the amplification depends on transcript starting amount starting from a wide range of different transcript levels.

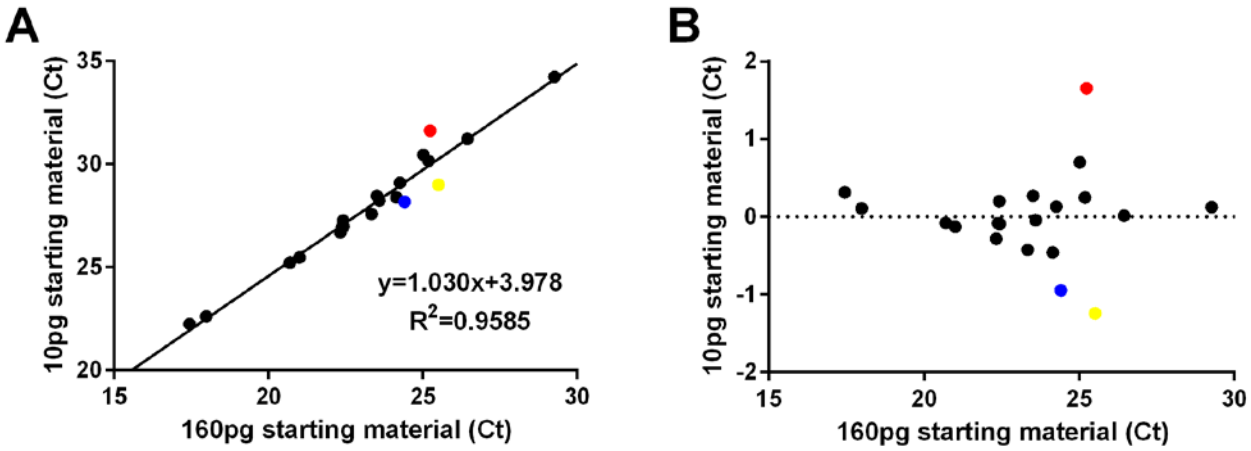

Figure 15. Preamplification linearity and sequence independence. A) Cycle thresholds obtained from qPCR of preamplified and pooled 10pg and 160pg starting material for different primer sets, corrected for primer efficiency. B) Residuals from the linear regression. The blue, red and yellow points are *Asic1*, *Piezo2*, and *P2rX3* respectively.

As can be seen in Figure 15A, the 16-fold difference between starting amounts of mRNA resulted in amplification not significantly different from linear (Runs test, p=0.59) with a slope of 1.030±0.0505 indicating that the cDNA yield of amplification depended linearly on the starting mRNA amount. The 16-fold change in starting material would be predicted to impart a 4 Ct offset (2^4=16), which was also supported by the observed 3.978±1.186 Ct offset. Thus, we concluded that the preamplification is linear to the extent of our ability to detect it.

Next, there exists the possibility that this linear amplification is preferential and perhaps even nonlinear for certain concentrations of certain transcripts, even though it is linear on the whole. Figure 15B contains both potential systematic variation that depends on the primer set and also primer-independent instrument error, so in order to proceed we needed to determine the instrument error of our qPCR process.

A.2 DETERMINATION OF REAL TIME QPCR INSTRUMENT ERROR

We always run our PCR in duplicate, so our single cell PCR results constitute a large, primer-

heterogeneous data set that can be used for the examination of within-sample instrument error. This analysis included 3,136 Ct readings constituting 1,530 pairs of replicates and 76 failed replications. Among the replicates, the first sample had a lower Ct (was measured to contain more template) 661 times, while the second sample had a lower Ct 869 times. This was significantly different from an even distribution (Chi-squared, $p<0.0001$), and can likely be attributed to systematic instrument or pipetting error.

The average absolute difference between replicates was 0.22 Ct, but the variation appeared to depend on Ct so that higher Ct samples had higher variance. To evaluate this, replicates were binned based on their average Ct. Within-sample deviations from the replicate mean were squared, summed within each bin, divided by the number of samples in the bin, giving a within-bin pooled variance (Figure 16A). As is readily apparent, there is substantial, sudden instrumental error above a between-well average of 33 Ct. The distribution of raw Ct measurements in Figure 16B shows the cause of this frequency spike, a near-inability to generate readings between 33.5 and 34.5 Ct. The absorbance growth curves reveal no obvious cause for such a deficit and in the dozen cases checked, the program was determining the Ct values properly. There may be a problem within the machine's design, and this data was submitted to BIO-RAD's engineering department for their consideration a year ago with no reply.

Regardless, this shows that our method has a pooled variance of less than 0.06 Ct (predicted replicate distribution standard deviation of 0.25) at or below an intrawell average of 33 Ct, which serves as the limit of quantification for this technique in my thesis that will not unduly sacrifice accuracy. The standard deviation for a ΔCt attributable to measurement error, therefore, would be 0.36, setting ± 0.70 Ct as the bounds of a 95% confidence interval. Thus, the 3 colored points in Figure 15B are outside the 95% confidence interval and may be due to preferential preamplification.

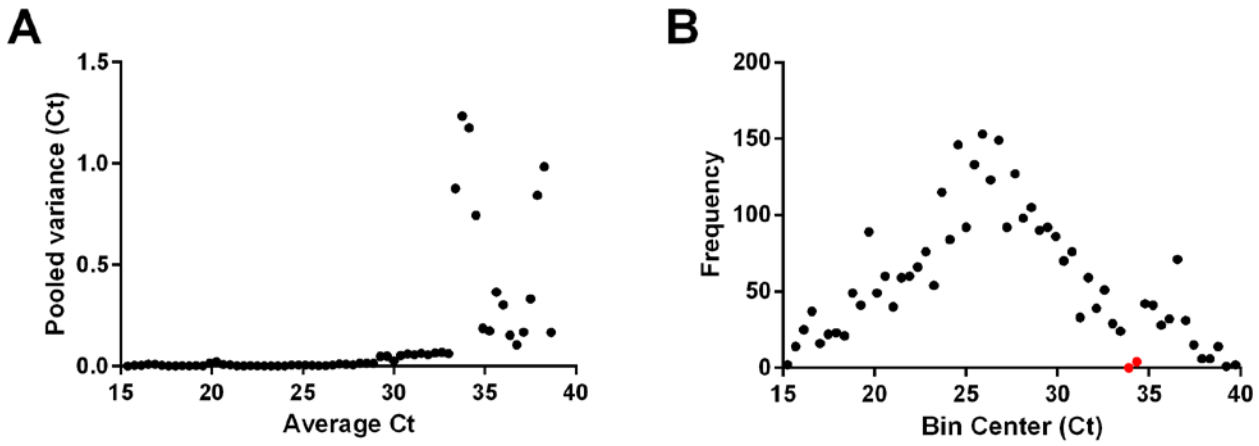

Figure 16. Instrumental variance in Ct measurements. A) Within sample pooled variance of Ct replicates. B) Distribution of raw Ct values measured in the data set. Red dots indicate that there were only 4 recorded Ct values between 33.5 and 34.5 Ct.

A.3 DETERMINATION OF REAL TIME QPCR LIMIT OF DETECTION

Wells in PCR represent a mix of numerical and categorical data. When they have a detectable level of template, they yield a numerical result that can be analyzed. However, they can also fail to have a detectable level of template and yield no result. This split between detectable and undetectable wells is categorical data. In Section A.2, I previously determined our limit of numerical quantification but did not touch upon the limit of categorical detection.

In order to define this limit, I used the same 3,162 samples investigated previously and find the point at which only 95% of wells with detectable sample have a replicate that also has detectable sample (Reiter et al. 2011). The lowest observed unpaired reading was 34.75Ct, and with 1Ct bins the 35 Ct bin is the first to have a sub-95% replication rate. Thus, 35 Ct was determined to be the categorical limit of detection for raw Ct values. This 35 Ct threshold can be corrected by efficiency and becomes the theoretical limit of detection for each gene.

A.4 PRIMER VALIDATION

Single cell PCR primers for use with our preamplification method must fall within 500 bases of the 3' end of the transcript. In this technique, first strand synthesis converts the lysate mRNA to cDNA, and then the linear preamplification incubates this cDNA library with a T7 reverse transcriptase. T7 reverse transcriptase (with the provided T7 primers) is high fidelity, only amplifies polyadenylated transcripts, starts every strand from the 3' end. Like every reverse transcriptase, T7 has a constant bias against certain transcripts and is prone to spontaneously aborting the reverse transcription process with a low rate. As the incubation goes on, more copies of each cDNA will be created, but some of those will be shorter than they should be. The linear preamplification step is capped at 4 hours to limit the buildup of these severely truncated transcripts, and the primers are required to be within 500 bases of the 3' end to further mitigate the effect of truncation.

This preamplification process gives a unique distribution of truncated transcripts. Thus, all primers must be validated with samples of DRG homogenate that have been preamplified using the same method. In order to span the range of possible single cell values, we used 10pg and 160pg of DRG starting material with four serial dilutions each to validate primers. This typically gave us a wide enough dynamic range to cover all the values seen in single cells and still fell within the range of the MessageBOOSTER for cell Lysate kit (Epicentre, 10-500pg range).

Finally, primer efficiencies were calculated by plotting the log of the dilution factor (x) against the Ct values (y) and doing a linear regression to find the slope of the line. We accepted a primer as validated if the calibration curve had an $R^2 \geq 0.97$. Although hypothetically it should not matter as it is corrected for, we also aimed to keep the slope between -3.08 and -3.44 (efficiencies between 95% and 110%.) Melt curves were examined for multiple modes and we ran the product out on a gel to confirm dimerization or nonspecificity and redesigned the primers as necessary.

A.5 SINGLE CELL STOCK SOLUTIONS

In the interest of running as many genes as possible, as well as keeping our results in the validated dynamic range of our technique, we created two dilutions of stock solution for each cell. The preamplification, cleaning, and second cDNA library creation process ends with a concentrated 11µL solution of sample, which is diluted 1:10 for 110µL of total volume. A 25µL aliquot of the 1:10 is taken and diluted again 1:2 for a final 50µL solution with a 1:20 dilution factor. High prevalence genes use 1µL of the 1:20 dilution per well (up to 25 high prevalence genes per cell), while our low prevalence genes use 1, 2, or 4 µL of the 1:10 dilution per well (10-40 low prevalence genes per cell), as indicated in Figure 17. At present, it is possible to run all 21 high prevalence genes and 12 low prevalence genes with 35µL of 1:10 and 8µL of the 1:20 single cell stock solutions left over for future experiments.

Gene	Forward	Reverse	Sample	Primer	R^2	E
Actb	AAGCCACCCCCACTCCTAAG	GCCTCAGACCTGGGCCATTC	1:20 1µL	250 nM	0.99	99%
Asic1	CAGGCCAGCTCTCCAATCTC	ACGTACACAGGTGATCTGCC	1:10 1µL	250 nM	1.00	102%
Asic2	GCACCTGTGGAGGAAGTACG	CCCGCCCCAAACAAAAATCAG	1:10 1µL	250 nM	1.00	102%
Asic3	GCAACACTCTGCTCCAGGAA	CGAGGTAACAGGTACGGTGG	1:10 1µL	250 nM	1.00	104%
Calcα	TGACAGCATGGTTCTGGCTT	GTCCCCAGAAGAGCAAGAGG	1:20 1µL	250 nM	1.00	100%
Gapdh	ATGAATACGGCTACAGCAACAGG	CTCTTGCTCAGTGTCCTTGCTG	1:20 1µL	250 nM	1.00	100%
Gfrα1	GACTCGGAATCCAGCCTACG	TGTGCACTTGTCCTCTCGTG	1:20 1µL	250 nM	1.00	97%
Gfrα2	CTTGGGGAGAAGGGCTGTTG	AGGAGAAGAGAGAAGGGGCA	1:20 1µL	250 nM	1.00	99%
Gfrα3	GCTGGTGTCTTGACTGCTCT	GACCCAAGGGACTAGGGGAA	1:20 1µL	250 nM	0.99	100%
Lys	GCCATATCGGCTCGCAAATC	AACGAATGCCGAAACCTCCTC	1:20 1µL	250 nM	0.99	102%
MrgprA3	ATAGCCCTCTTCTGGTCCTAACT	AGGCTCTTCATCACGGCTCT	1:10 2µL	250 nM	0.99	102%
MrgprD	CTGCTTCAGGCCAGCTCCTA	AGCATCTCTGTCACCTTGAGCA	1:20 1µL	250 nM	1.00	102%
Nefh	TTGCCCAGTACACGCTCCTG	GAGTACACCCTGGCGTGGTT	1:20 1µL	250 nM	1.00	111%
P2rX2	ATCCACGGACCCCAAAGGTTT	CCCAGTCACGTGGACATGGTTA	1:10 2µL	250 nM	0.97	99%
P2rX3	GGTGCCTAAGCCTCTTCTGG	AGGGATGGCGCTGAGTAAAC	1:20 1µL	250 nM	0.99	100%
P2rY1	GCCAGGACACTAACCCATCG	AACTGAAGGCCCACAAACCTC	1:10 4µL	250 nM	0.99	108%
P2rY2	AGGGAGGGGTCCCTGGAATG	ACCTTTGCCCATTCCTGCCTA	1:10 2µL	500 nM	1.00	104%
Piezo2	GACTGAGGCCACAGGGCT	GCAAGGAAAATGTCACACACTG	1:10 2µL	375 nM	1.00	99%
Pvalb	AACGCCCCGATATCTCCTGC	CACCCCCATCTCCTTGTGGG	1:20 1µL	250 nM	1.00	102%
Ret	CAACATGCCTACACGGTAAGTG	ATCTCAGGAACAGACAGACAATGG	1:20 1µL	250 nM	1.00	100%
Scn10a	GGCACTGTCGCATAGGGGT	ACCCTCAGGTATTGTCCGGC	1:20 1µL	250 nM	1.00	96%
Scn11a	CGGAAGGCCTGAAGGACAGTT	CCATACACCCAAATCCGCAGC	1:20 1µL	250 nM	1.00	99%
Scn9a	AGAACTGTGTTTGGAGCCATCA	GGCTACTTACTCATTTTCTGGGAG	1:20 1µL	250 nM	1.00	106%
Sst	GGTCTGCCAACTCGAACCCA	ATCGGGGGCCAGGAGTTAAG	1:10 1µL	375 nM	1.00	107%
Tac1	CTGTGCGTCTCTCTCACGCT	CACGAAACAGGAAACATGCTGCT	1:20 1µL	250 nM	1.00	95%
Th	CACCATCCGGCGCTCCTTAG	GTCCAGCCACACACATGGGA	1:20 1µL	250 nM	1.00	101%
TrkA	GAGCCAAGTTTTGGTGCCAG	GATGCTGGCCATGAAGCAAG	1:20 1µL	250 nM	1.00	101%
TrkB	AAGATGTGTCCCTGGGCTTC	AAGTGAGTCACGAGCTGCC	1:20 1µL	250 nM	1.00	101%
TrkC	CTGCTCCCCATGGTTGTAGG	GGGAGGCTGGAAATGAGGTC	1:20 1µL	250 nM	0.99	101%
TrpA1	TGAGCCACATGACAGAAGTCC	CTAAGCAGCAGCAACAACTGG	1:10 1µL	250 nM	1.00	99%
TrpM3	TCAGAGTTTTTCAAGGGCTGGT	TGGCCTACCTGCAACTGATG	1:10 4µL	500 nM	0.99	87%
TrpM8	TCAAGGGCATAGGTCAGGGA	TCAGCATCAGGACAAGGCTC	1:10 4µL	375 nM	0.95	102%
TrpV1	GGCGAGACTGTCAACAAGATTGC	TCATCCACCCTGAAGCACCAC	1:20 1µL	250 nM	0.99	109%

Figure 17. Primer information. A full list of the primers used in this thesis, complete with their sequences, the amount and dilution of sample used, the concentration of primer used, and the efficiency of each primer. Primers for *Asic1* and *Asic2* do not distinguish between a and b isoforms.

A.6 NON-MAMMALIAN SPIKE RNA FOR ABSOLUTE QUANTITATION

It is possible to estimate the absolute number of PCR copies in two ways. One option is to generate a calibration curve for each mRNA of interest. In this case, each peptide sequence is synthesized and used to generate a calibration curve (Schulz et al. 2006). The molecular weight

of each transcript is known, so it is possible to approximate the number of copies of transcript in a given weight of purified, synthesized RNA. Serial dilutions of this known RNA quantity would be put through the same amplification process as the experimentally acquired RNA, and the resulting copies versus Ct calibration curve would create a mapping that could be applied to later data.

The second option is to use a non-mammalian spike RNA (Nakamura et al. 2007). In this case, a known quantity of purified, non-mammalian cell RNA (such as *Lys*) is added to the original sample. Measurements are then corrected for primer efficiencies and interpreted relative to this non-mammalian transcript "spike" (i.e. a Gene Ct – Lys Ct of 2 means there is 4 times more *Lys* than the Gene. If there were 1000 copies of *Lys*, there are 250 copies of the gene). This is the approach that we attempted to use, as it does not require the expensive and cumbersome process of generating multiple calibration curves. Unfortunately, we found it was unsuitable for our purposes due to high variability in starting RNA quantity, which it does not control for.

In theory, a spike RNA added at the time of cell pickup controls for variability in the amplification process. This was true in a gross sense, in that failed amplifications led to low levels of Gapdh and low or undetectable levels of *Lys*. The amplification should not preferentially amplify one over the other (Figure 15A), so we expect any variance from amplification to affect both equally and create a linear correlation between their Ct values them with a slope of 1. Instead, we observed almost no correlation in the experimentally relevant *Gapdh* range, with a linear regression model explaining only 8% of the variability (Figure 18AB, slope significantly different from 0 with $p<0.0001$). Thus, we can conclude that amplification-related variance is a minor factor within the relevant *Gapdh* range and other factors, like LYS pipetting consistency and initial lysate RNA amount, dominate.

This point is driven home by a comparison between *Gapdh* and the near-ubiquitously detected gene, *Ret*. *Ret* is used as a population marker (Usoskin et al. 2014; Franck et al. 2011; Stantcheva et al. 2016) and our analyses agree that it is variably regulated in different populations, which should add variability to the comparison between it and *Gapdh*. A linear model explains 53% of the variability between *Ret* and *Gapdh,* with a slope of 1.12, allowing us to conclude that the factors that *Ret* and *Gapdh* have in common (amplification and initial lysate amount) explain the majority of their variance. This is true for other commonly detected transcripts as well, like *Scn9a* (slope=1.24, R^2=0.63) and *Nefh* (slope=1.93, R^2=0.59). The

relatively high slope of the *Nefh* comparison reflects the common correlation between it, *Gapdh*, and cell size.

In summary, *Lys* does appear to successfully control for amplification variance, but it introduces a new type of pipetting error and does not control for differences in initial lysate RNA amounts, which are substantial. *Gapdh* normalization controls for both amplification variance and initial lysate RNA amount, which make it a more suitable candidate for our experiments. The two risks with this normalization are that differences between our large and small cells will be washed out and that cell-size-dependent differences within genes that do not depend on cell size will be created. In this document, correlations discussed are typically within cell groups of the same size, so I do not think these factors are affecting the results.

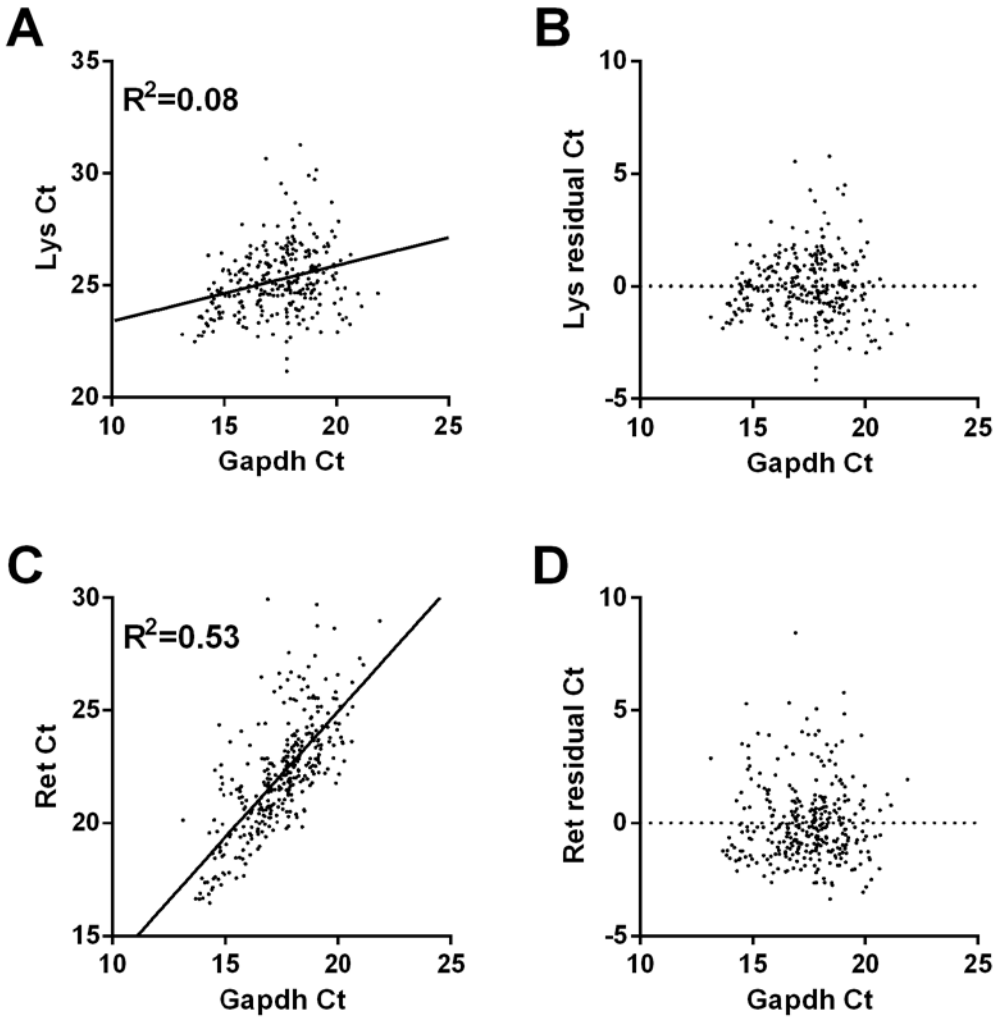

Figure 18. Comparison of potential standards. A) 1000 copies of *Lys* Ct vs. *Gapdh* Ct for all cells used in this document. B) Residual plot after removing the linear correlation between *Lys* and *Gapdh*. C) *Ret* Ct vs. *Gapdh* Ct for all cells used in this document. D) Residual plot after removing the correlation between *Ret* and *Gapdh*.

APPENDIX B. RESPONSE OF PRIMARY AFFERENTS TO CHANNELRHODOPSIN

Channelrhodopsin, a class of light sensitive cation channels, is a new tool that can be and has been used to incite activity within primary afferents. There is a tendency for authors to claim they are using it to recapitulate naturalistic stimulation. In this appendix, I will address that possibility and the extent to which it can be true for individual afferent types as well as examining a few interesting observations obtained from the stimulations of channelrhodpsin-containing afferents.

Three transgenic Cre mice were used to drive the activity of the Ai32 channelrhodpsin construct in this appendix. MrgprD-Cre drives expression in the MrgprD lineage population of somatosensory neurons. As assessed using single cell PCR pickup, this includes the MrgD (5/11 cells), MrgA3 (5/11 cells), and may include the Sst population (1/11 cells). Advillin-Cre drives near-ubiquitous expression across all peripheral somatosensory populations. It has also been reported to drive patchy recombination in the skin (potentially including Merkel cells) (Haeberle et al. 2004), but histology on the preparations used to obtain this data did not detect recombination in the skin. The final Cre line used was Keratin 14-Cre, which drives expression in K14 lineage keratinocytes, including Merkel cells. All Cre drivers cause expression of the Ai32 construct, which is placed in the ROSA26 locus after recombination, so channelrhodopsin expression should be relatively consistent across Cre lines.

All recordings were acquired from the right, distal hindpaw skin using a saphenous *ex vivo* preparation. Both extracellular (fiber teasing) and intracellular (sharp electrode) recording techniques were used, but will not be compared between.

B.1 A-FIBER CHANNELRHODOPSIN RESPONSES DEPEND ON THEIR MECHANICAL PHENOTYPE

As part of a collaboration with Professor Bin Feng to examine the biophysics of A-fiber responses, I recorded from the saphenous nerve of Advillin-Cre/Ai32 mice, isolating different

types of A-fibers and recording their responses to both mechanical and laser stimulation. Laser stimuli were 30 seconds long and were at 3 intensities (1.5, 3.5, and 5V command line). Of the 32 recorded myelinated fibers, 29 responded to laser and the single failure was an Aβ-RA.

RA fibers (n=8) were recognized by their 1-2 spike onset and 0-2 spike offset responses to mechanical stimulation. They did not encode laser intensity within the range used (1-21mW), and fired an average of 1.4 spikes to laser onset, comparable to mechanical onset. Aδ-RAs (n=4) were the only RAs that fired more than one action potential in response to laser onset, with Aβ-RAs always firing exactly one spike. As can be seen in (Figure 19), these fibers can fire reliably to reptitive stimulation, although the latency between laser onset and spike varies both as a function of time and frequency of stimulation. Electrical latency was 9ms in this case and the minimum time between laser onset and action potential was 11ms, showing that the minimum latency from laser to action potential generation is less than 2ms.

Nonadapting fibers (n=7), putative myelinated nociceptors, had tonic discharge rates that were proportional to pressure. These fibers typically fired only once in response to laser onset (average 1.1 spikes per onset) and no differences were observed between Aβ (n=5) and Aδ (n=2) cells. Similarly, smoothly adapting cells (n=9), putative WDR fibers, had low coefficients of variance and did not respond vigorously to laser stimulation. They sometimes had multi-spike responses to 3.5 and 5V laser intensities, but none higher than 0.6Hz and had an average of 2.9 spikes per per stimulus of 2.9. No differences were observed between Aβ (n=4) and Aδ (n=5) afferents.

SA1 fibers (n=5) were recognized by their Aβ conduction velocity and high ISI CoV during the static phase of the mechanical response. These fibers fired multiple action potentials in response to laser stimulation. This activity retained a high CoV (average CoV 0.99) at all intensities. The firing rates seem to be inhibited by the highest laser setting (Figure 19, not significant), and were typically lower than the static phase of mechanical stimulation (1.6-22Hz in response to laser).

SA1 fibers are known to associate with Merkel cell complexes, a cluster of electrically active, highly specialized skin cells that directly contribute to their responses via signaling with an unknown transmitter (Baumbauer et al. 2015; Woo et al. 2014). There has been one report of Advillin expression in Merkel cells (Haeberle et al. 2004), which could mean that the observed SA1 responses are mediated by Merkel cell activity rather than direct afferent activation.

Although post-experiment histology did not find any evidence this was the case, I already had collected the control data for Baumbauer et al. (2015). For this paper, I recorded from SA1 fibers using the ex vivo saphenous preparation while stimulating Merkel cells and surrounding Keratinocytes with channelrhodopsin using the K14-Cre/Ai32 mice. The firing rate in response to Merkel cell activation alone was significantly lower than stimulation with 1.5 or 3.5V laser (t-test, $p<0.01$), but was not significantly different from 5V laser ($p=0.09$). These two experiments were done at different times and thus the laser intensity is not identical between the two, but my expectation is actually that the K14-Cre animals were stimulated with a weaker laser than these Advillin-Cre animals. With that and the fact that we post-hoc histology found no recombined skin cells, I find it unlikely that the repetitive activity seen in these cells is due to Merkel cell activation.

Thus, even in the case of near-constant depolarization with channelrhodopsin, SA1 cells fire irregularly and the firing is comparable to that induced by K-14 lineage activation. Hopefully the modeling of Professor Feng will reveal how the irregular spiking seen in SA1 fibers can arise from intrinsic membrane properties. It may also be worth noting at this point that SA1 fibers appear to be transcriptionally different from the RA, WDR, and myelinated nociceptor fibers and fall into a parvalbumin group that is known to contain proprioceptors (Figure 3), and differences in expression may explain the differences in response properties in this case.

Although I typically assume mechanical pressure causes continuous inward current on mechanosensitive cells, the story appears to be more complicated. No single fiber had its properties perfectly emulated by continuous channelrhodopsin stimulation. RA fibers failed to respond to the offset of laser. WDR and HTMR fibers only fired once despite firing repetitively to mechanical stimulation. SA1 fibers did not show their normal initial burst of activity. It could be that these fibers are gated by more complicated mechanisms than simple pressure detection, or it could just be that tonic depolarization of their entire terminal field with laser is a poor emulation of mechanical stimulation at their end organs.

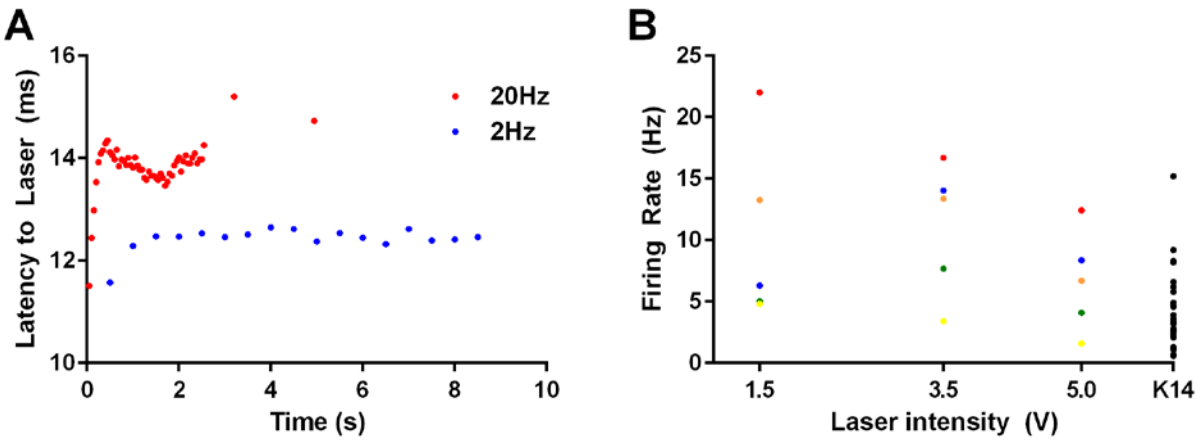

Figure 19. Dynamics of A-fibers to channelrhodopsin stimulation. A) Latency of an Aδ RA fiber to 5ms, 5V laser stimulation at two frequencies. B) Firing rate versus laser intensity for five SA1 cells in the Advillin-Cre/Ai32 mice and all recorded cells from the K14-Cre/Ai32 mice (K14).

B.2 MRGPRD CELLS RESPOND TO LASER WITH TONIC DISCHARGE COMPARABLE TO MECHANICAL STIMULI

Intracellular recordings were also obtained from twelve laser responsive cells from MrgprD-Cre/Ai32 animals, one of which can be seen in Figure 20. These cells responded to five second laser stimulation with discharge that was laser intensity dependent and was comparable to their responses to mechanical stimulation. These findings are consistent with our previous work recording from C-fibers in TrpV1-Cre/Ai32, Peripherin-Cre/Ai32, and Advillin-Cre/Ai32 mouse lines. Individual neuron may be variably sensitive to laser and it is not clear that this sensitivity has anything to do with their responsiveness to other modalities, but more data needs to be collected before conclusions can be drawn

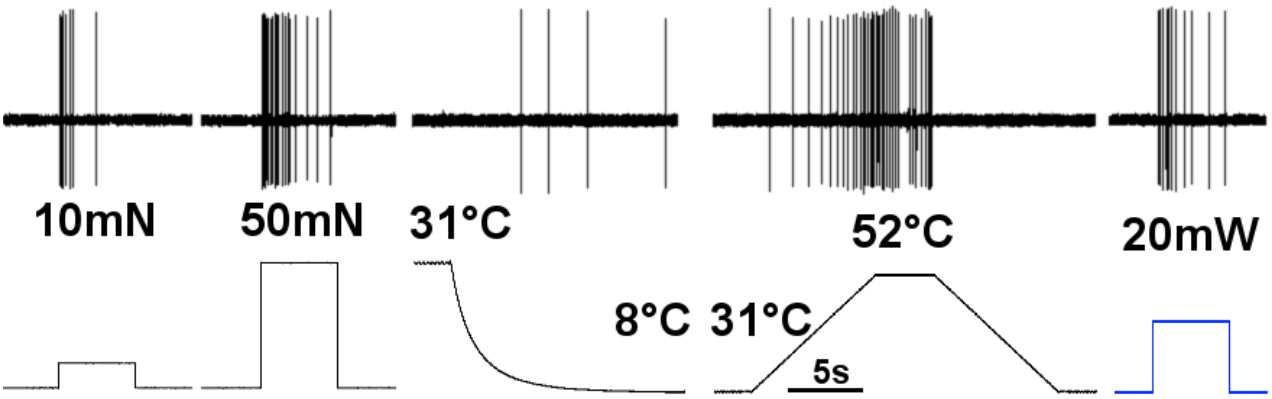

Figure 20. MrgprD-Cre/Ai32 example cell. Responses of one MrgprD-Cre/Ai32 cell to mechanical, thermal, and laser stimulation.

B.3 ON THE POSSIBILITY OF RECREATING NATURALISTIC STIMULATION USING CHANNELRHODOPSIN

In summary, it is possible to recapitulate naturalistic firing patterns in some classes of A-fiber primary afferents in isolation, but any stimulus reconstruction that involves a single subpopulation is inherently not naturalistic. For instance, it is possible to recapitulate a normal RA response using two pulses of light for the onset and offset of a stimulus, but doing so would cause incongruous response patterns in WDR, HTMR, and SA1 fibers. Similarly, it is possible to recapitulate the SA1 static phase of a very light mechanical stimulus using low intensity sustained laser, but probably not the onset. Attempts to reconstruct naturalistic stimuli in A-fibers may have a purpose for slice electrophysiology, where it is sometimes useful to view populations of afferents in isolation, but they should probably not be used for behavior.

Channelrhodopsin responses in C-fibers, which fire continuously in response to activation, are much closer to the response properties of neurons to mechanical and thermal stimulation. More work needs to be done before it is possible to conclude that we can recapitulate natural stimulation in C-fibers using channelrhodopsin, but the results so far are much more promising than in A-fibers.

BIBLIOGRAPHY

Abe, J. et al., 2005. TRPM8 protein localization in trigeminal ganglion and taste papillae. *Molecular Brain Research*, 136(1-2), pp.91–98.

Abraira, V.E. & Ginty, D.D., 2013. The sensory neurons of touch. *Neuron*, 79(4), pp.618–639.

Adriaensen, H. et al., 1983. Response properties of thin myelinated (A-delta) fibers in human skin nerves. *Journal of neurophysiology*, 49(1), pp.111–122.

Albers, K.M. et al., 2006. Glial cell-line-derived neurotrophic factor expression in skin alters the mechanical sensitivity of cutaneous nociceptors. *The Journal of neuroscience : the official journal of the Society for Neuroscience*, 26(11), pp.2981–90.

De Alvarenga Yoshida, R. et al., 2012. Fibular nerve injury after small saphenous vein surgery. *Annals of Vascular Surgery*, 26(5), pp.729.e11–729.e15.

Averbeck, B. et al., 2013. Thermal grill-evoked sensations of heat correlate with cold pain threshold and are enhanced by menthol and cinnamaldehyde. *European Journal of Pain (United Kingdom)*, 17(5), pp.724–734.

Axelsson, H.E. et al., 2009. Transient receptor potential vanilloid 1, vanilloid 2 and melastatin 8 immunoreactive nerve fibers in human skin from individuals with and without Norrbottnian congenital insensitivity to pain. *Neuroscience*, 162(4), pp.1322–1332.

Bagheri, S.C. et al., 2009. Microsurgical Repair of Peripheral Trigeminal Nerve Injuries From Maxillofacial Trauma. *Journal of Oral and Maxillofacial Surgery*, 67(9), pp.1791–1799.

Bagheri, S.C. et al., 2010. Retrospective Review of Microsurgical Repair of 222 Lingual Nerve Injuries. *Journal of Oral and Maxillofacial Surgery*, 68(4), pp.715–723.

Bai, L. et al., 2015. Genetic Identification of an Expansive Mechanoreceptor Sensitive to Skin Stroking. *Cell*, 163(7), pp.1783–1795.

Bai, L. et al., 2015. Natural history of sensory nerve recovery after cutaneous nerve injury following foot and ankle surgery. *Neural regeneration research*, 10(1), pp.99–103.

Baker, M. & Bostock, H., 1997. Low-threshold, persistent sodium current in rat large dorsal root ganglion neurons in culture. *Journal of neurophysiology*, pp.1503–1513.

Barber, R.D. et al., 2005. GAPDH as a housekeeping gene: analysis of GAPDH mRNA expression in a panel of 72 human tissues. *Physiological genomics*, 21(3), pp.389–395.

Barber, R.P. et al., 1979. The origin, distribution and synaptic relationships of substance P axons in rat spinal cord. *The Journal of comparative neurology*, 184(2), pp.331–51.

Barclay, J. et al., 2002. Functional downregulation of P2X3 receptor subunit in rat sensory neurons reveals a significant role in chronic neuropathic and inflammatory pain. *The Journal of neuroscience : the official journal of the Society for Neuroscience*, 22(18), pp.8139–8147.

Barragán-Iglesias, P. et al., 2016. Predominant role of spinal P2Y1 receptors in the development of neuropathic pain in rats. *Brain Research*, 1636, pp.43–51.

Baumbauer, K.M. et al., 2015. Keratinocytes can modulate and directly initiate nociceptive responses. *eLife*, 4(September 2015), pp.1–14.

Bennett, D.L. et al., 1998. A distinct subgroup of small DRG cells express GDNF receptor components and GDNF is protective for these neurons after nerve injury. *The Journal of neuroscience : the official journal of the Society for Neuroscience*, 18(8), pp.3059–3072.

Bennett, D.L. et al., 2000. The glial cell line-derived neurotrophic factor family receptor components are differentially regulated within sensory neurons after nerve injury. *The Journal of neuroscience : the official journal of the Society for Neuroscience*, 20(1), pp.427–437.

Bennett, D.L.H. et al., 2006. Artemin has potent neurotrophic actions on injured C-fibres. *Journal of the Peripheral Nervous System*, 11(4), pp.330–345.

Bennett, D.L.H. et al., 2000. The Glial Cell Line-Derived Neurotrophic Factor Family Receptor Components Are Differentially Regulated within Sensory Neurons after Nerve Injury. *J. Neurosci.*, 20(1), pp.427–437.

Berdan, R.C., Easaw, J.C. & Wang, R., 1993. Alterations in membrane potential after axotomy at different distances from the soma of an identified neuron and the effect of depolarization on neurite outgrowth and calcium channel expression. *Journal of neurophysiology*, 69(1), pp.151–164.

Bradbury, E.J., Burnstock, G. & McMahon, S.B., 1998. The expression of P2X3 purinoreceptors in sensory neurons: effects of axotomy and glial-derived neurotrophic factor. *Molecular and cellular neurosciences*, 12(4-5), pp.256–268.

Brignell, J.L., Chapman, V. & Kendall, D.A., 2008. Comparison of icilin- and cold-evoked responses of spinal neurones, and their modulation of mechanical activity, in a model of neuropathic pain. *Brain research*, 1215, pp.87–96.

Brown, A.G. & Iggo, A., 1967. A quantitative study of cutaneous receptors and afferent fibres in the cat and rabbit. *The Journal of physiology*, 193(3), pp.707–33.

Brown, A.G.I.A., 1963. The structure and function of cutaneous “touch corpuscles” after nerve crush. *J. Physiol.*, (September), pp.19–24.

Brown, P.B., Koerber, H.R. & Millecchia, R., 1997. Assembly of the dorsal horn somatotopic map. *Somatosensory & motor research*, 14(2), pp.93–106.

Brumovsky, P., Villar, M.J. & Hökfelt, T., 2006. Tyrosine hydroxylase is expressed in a subpopulation of small dorsal root ganglion neurons in the adult mouse. *Experimental neurology*, 200(1), pp.153–165.

Brushart, T.M., 1988. Preferential reinnervation of motor nerves by regenerating motor axons. *The Journal of neuroscience : the official journal of the Society for Neuroscience*, 8(3), pp.1026–31.

Bulut, T., 2015. Prognostic factors in sensory recovery after digital nerve repair. *ACTA ORTHOPAEDICA et TRAUMATOLOGICA TURCICA*, 50(2), pp.157–161.

Burgess, P.R. et al., 1974. Patterning in the regeneration of type I cutaneous receptors. *J Physiol*, 236(1), pp.57–82.

Burgess, P.R. & Horch, K.W., 1973. Specific regeneration of cutaneous fibers in the cat. *Journal of neurophysiology*, 36(1), pp.101–14.

Burgess, P.R. & Perl, E.R., 1967. Myelinated afferent fibres responding specifically to noxious stimulation of the skin. *The Journal of physiology*, 190(3), pp.541–62.

Burgess, P.R., Petit, D. & Warren, R.M., 1968. Receptor Types in Cat Hairy Supplied Skin by Myelinated. *Journal of Neurophysiology*, 31(6), pp.833–848.

Campero, M. et al., 2009. Human cutaneous C fibres activated by cooling, heating and menthol. *The Journal of physiology*, 587(Pt 23), pp.5633–5652.

Caterina, M.J., 2000. Impaired Nociception and Pain Sensation in Mice Lacking the Capsaicin Receptor. *Science*, 288(5464), p.306.

Chambers, M. & Iggo, A., 1967. Slowly-adapting cutaneous mechanoreceptors. *Journal of Physiology*, 192(1961), p.26P–27P.

Chambers, M.R. et al., 1972. The structure and function of the slowly adapting type II mechanoreceptor in hairy skin. *Quarterly journal of experimental physiology and cognate medical sciences*, 57(4), pp.417–45.

Chen, C.C. et al., 1995. A P2X purinoceptor expressed by a subset of sensory neurons. *Nature*, 377(6548), pp.428–31.

Chiu, I.M. et al., 2014. Transcriptional profiling at whole population and single cell levels reveals somatosensory neuron molecular diversity. *eLife*, 3.

Christianson, J.A. et al., 2006. Transient receptor potential vanilloid 1-immunopositive neurons in the mouse are more prevalent within colon afferents compared to skin and muscle afferents. *Neuroscience*, 140(1), pp.247–257.

Coimbra, A., Sodré-Borges, B.P. & Magalhães, M.M., 1974. The substantia gelatinosa Rolandi of the rat. Fine structure, cytochemistry (acid phosphatase) and changes after dorsal root section. *Journal of neurocytology*, 3(2), pp.199–217.

Colburn, R.W. et al., 2007. Attenuated cold sensitivity in TRPM8 null mice. *Neuron*, 54(3), pp.379–86.

Coste, B. et al., 2010. Piezo1 and Piezo2 are essential components of distinct mechanically activated cation channels. *Science (New York, N.Y.)*, 330(6000), pp.55–60.

Craig, A.D. & Bushnell, M.C., 1994. The thermal grill illusion: unmasking the burn of cold pain. *Science (New York, N.Y.)*, 265(5169), pp.252–5.

Cruikshank, W., 1795. Experiments on the Nerves, particularly on their Reproduction; and on the Spinal Marrow of living Animals. *Philosophical Transactions of the Royal Society of London*, 85, pp.177–189.

Deng, A. et al., 2016. Active skin perfusion and thermoregulatory response in the hand following nerve injury and repair in human upper extremities. *Brain Research*, 1630, pp.38–49.

Devor, M. et al., 1979. Two modes of cutaneous reinnervation following peripheral nerve injury. *The Journal of Comparative Neurology*, 185(1), pp.211–220.

Dhaka, A. et al., 2008. Visualizing cold spots: TRPM8-expressing sensory neurons and their projections. *The Journal of neuroscience : the official journal of the Society for Neuroscience*, 28(3), pp.566–575.

Dib-Hajj, S. et al., 1996. Down-regulation of transcripts for Na channel alpha-SNS in spinal sensory neurons following axotomy. *Proceedings of the National Academy of Sciences of the United States of America*, 93(25), pp.14950–4.

Dib-Hajj, S.D., Tyrrell, L., et al., 1998. NaN, a novel voltage-gated Na channel, is expressed preferentially in peripheral sensory neurons and down-regulated after axotomy. *Proceedings of the National Academy of Sciences of the United States of America*, 95(15), pp.8963–8968.

Dib-Hajj, S.D., Black, J.A., et al., 1998. Rescue of alpha-SNS sodium channel expression in small dorsal root ganglion neurons after axotomy by nerve growth factor in vivo. *Journal of neurophysiology*, 79(5), pp.2668–76.

Djouhri, L. et al., 2003. The TTX-resistant sodium channel Nav1.8 (SNS/PN3): expression and correlation with membrane properties in rat nociceptive primary afferent neurons. *The Journal of physiology*, 550(Pt 3), pp.739–52.

Dong, X. et al., 2001. A diverse family of GPCRs expressed in specific subsets of nociceptive sensory neurons. *Cell*, 106(5), pp.619–632.

Doughty, S.E., Atkinson, M.E. & Shehab, S.A.S., 1991. A quantitative study of neuropeptide immunoreactive cell bodies of primary afferent sensory neurons following rat sciatic nerve peripheral axotomy. *Regulatory Peptides*, 35(1), pp.59–72.

Dowd, E. et al., 1998. P2X receptor-mediated excitation of nociceptive afferents in the normal and arthritic rat knee joint. *British journal of pharmacology*, 125(2), pp.341–6.

Eggers, R. et al., 2013. Lentiviral Vector-Mediated Gradients of GDNF in the Injured Peripheral Nerve: Effects on Nerve Coil Formation, Schwann Cell Maturation and Myelination. *PLoS ONE*, 8(8).

Elliott, A.A. & Elliott, J.R., 1993. Characterization of TTX-sensitive and TTX-resistant sodium currents in small cells from adult rat dorsal root ganglia. *The Journal of physiology*, 463, pp.39–56.

English, A.W., 2005. Enhancing axon regeneration in peripheral nerves also increases functionally inappropriate reinnervation of targets. *Journal of Comparative Neurology*, 490(4), pp.427–441.

Ernfors, P. et al., 1994. Lack of neurotrophin-3 leads to deficiencies in the peripheral nervous system and loss of limb proprioceptive afferents. *Cell*, 77(4), pp.503–512.

Ferrari, L.F. et al., 2015. Contribution of Piezo2 to endothelium-dependent pain. *Molecular pain*, 11(1), p.65.

Florez-Paz, D. et al., 2016. A critical role for Piezo2 channels in the mechanotransduction of mouse proprioceptive neurons. *Scientific Reports*, 6, p.25923.

Franck, M.C.M. et al., 2011. Essential role of Ret for defining non-peptidergic nociceptor phenotypes and functions in the adult mouse. *European Journal of Neuroscience*, 33(8), pp.1385–1400.

Fujiwara, S. et al., 2014. SOX10 Transactivates S100B to suppress schwann cell proliferation and to promote myelination. *PLoS ONE*, 9(12), pp.1–17.

Fukuoka, T., Miyoshi, K. & Noguchi, K., 2015. De novo expression of Nav1.7 in injured putative proprioceptive afferents: Multiple tetrodotoxin-sensitive sodium channels are retained in the rat dorsal root after spinal nerve ligation. *Neuroscience*, 284, pp.693–706.

Funakoshi, H. et al., 1993. Differential Expression of mRNAs for Neurotrophins and Their Receptors after Axotomy of the Sciatic Nerve. *The Journal of cell biology*, 123(2), pp.455–465.

Garc a-Caballero, T. et al., 1989. Calcitonin gene-related peptide (CGRP) immunoreactivity in the neuroendocrine Merkel cells and nerve fibres of pig and human skin. , 92, pp.127–132.

Gibbins, I.L., Furness, J.B. & Costa, M., 1987. Pathway-specific patterns of the co-existence of substance P, calcitonin gene-related peptide, cholecystokinin and dynorphin in neurons of the dorsal root ganglia of the guinea-pig. *Cell and Tissue Research*, 248(2), pp.417–437.

Gibson, S.J. et al., 1984. Calcitonin gene-related peptide immunoreactivity in the spinal cord of man and of eight other species. *J. Neurosci.*, 4(12), pp.3101–3111.

Gibson, S.J. et al., 1981. The distribution of nine peptides in rat spinal cord with special emphasis on the substantia gelatinosa and on the area around the central canal (lamina X). *The Journal of comparative neurology*, 201(1), pp.65–79.

Godinho, M.J. et al., 2013. Immunohistochemical, Ultrastructural and Functional Analysis of Axonal Regeneration through Peripheral Nerve Grafts Containing Schwann Cells Expressing BDNF, CNTF or NT3. *PLoS ONE*, 8(8).

de Godoy, L.M.F. et al., 2008. Comprehensive mass-spectrometry-based proteome quantification of haploid versus diploid yeast. *Nature*, 455(7217), pp.1251–4.

Gomes, C. et al., 2014. Molecular determinants of the axonal mRNA transcriptome. *Developmental Neurobiology*, 74(3), pp.218–232.

Goswami, S.C. et al., 2014. Molecular signatures of mouse TRPV1-lineage neurons revealed by RNA-seq transcriptome analysis. *Journal of Pain*, 15(12), pp.1338–1359.

Greenbaum, D. et al., 2003. Comparing protein abundance and mRNA expression levels on a genomic scale. *Genome biology*, 4(9), p.117.

Guo, A. et al., 1999. Immunocytochemical localization of the vanilloid receptor 1 (VR1): relationship to neuropeptides, the P2X3 purinoceptor and IB4 binding sites. *The European journal of neuroscience*, 11(3), pp.946–58.

Guo, G., Singh, V. & Zochodne, D.W., 2014. Growth and turning properties of adult glial cell-derived neurotrophic factor coreceptor α1 nonpeptidergic sensory neurons. *Journal of neuropathology and experimental neurology*, 73(9), pp.820–36.

H.-S., X. et al., 2002. Identification of gene expression profile of dorsal root ganglion in the rat peripheral axotomy model of neuropathic pain. *Proceedings of the National Academy of Sciences of the United States of America*, 99(12), pp.8360–8365.

Haeberle, H. et al., 2004. Molecular profiling reveals synaptic release machinery in Merkel cells. , 101, pp.14503–14508.

Hamilton, S.G., McMahon, S.B. & Lewin, G.R., 2001. Selective activation of nociceptors by P2X receptor agonists in normal and inflamed rat skin. *Journal of Physiology*, 534(2), pp.437–445.

Han, L. et al., 2013. A subpopulation of nociceptors specifically linked to itch. *Nature neuroscience*, 16(2), pp.174–82.

Haroutounian, S. et al., 2014. Primary afferent input critical for maintaining spontaneous pain in peripheral neuropathy. *Pain*, 155(7), pp.1272–1279.

Harper, A.A. & Lawson, S.N., 1985. Conduction velocity is related to morphological cell type in rat dorsal root ganglion neurones. *The Journal of physiology*, 359, pp.31–46.

Van Hecke, O. et al., 2014. Neuropathic pain in the general population: A systematic review of epidemiological studies. *Pain*, 155(4), pp.654–662.

Henry, J.L., Krnjevíc, K. & Morris, M.E., 1975. Substance P and spinal neurones. *Canadian journal of physiology and pharmacology*, 53(3), pp.423–32.

Hensel, H., Iggo, a & Witt, I., 1960. A quantitative study of sensitive cutaneous thermoreceptors with C afferent fibres. *The Journal of physiology*, 153, pp.113–126.

Hippenmeyer, S. et al., 2005. A developmental switch in the response of DRG neurons to ETS transcription factor signaling. *PLoS Biology*, 3(5), pp.0878–0890.

Ho, C. & O'Leary, M.E., 2011. Single-cell analysis of sodium channel expression in dorsal root ganglion neurons. *Molecular and cellular neurosciences*, 46(1), pp.159–166.

Hokfelt, T. et al., 1975. Substance p: localization in the central nervous system and in some primary sensory neurons. *Science*, 190(4217), pp.889–890.

Hökfelt, T. et al., 1976. Immunohistochemical evidence for separate populations of somatostatin-containing and substance P-containing primary afferent neurons in the rat. *Neuroscience*, 1(2), pp.131–IN24.

Holzer, P., 1991. Capsaicin : Cellular Selectivity Targets , for Thin Mechanisms of Action , Sensory Neurons. *Pharmacological Review*, 43(2), pp.143–201.

Horch, K.W., Tuckett, R.P. & Burgess, P.R., 1977. A key to the classification of cutaneous mechanoreceptors. *The Journal of investigative dermatology*, 69(1), pp.75–82.

Horch, K.W., Whitehorn, D. & Burgess, P.R., 1974. Impulse generation in type I cutaneous mechanoreceptors. *Journal of neurophysiology*, 37(2), pp.267–281.

Hunt, S.P. & Rossi, J., 1985. Peptide- and Non-Peptide-Containing Unmyelinated Primary Afferents: The Parallel Processing of Nociceptive Information. *Philosophical Transactions of the Royal Society B: Biological Sciences*, 308(1136), pp.283–289.

Iggo, A., 1959. Cutaneous heat and cold receptors with slowly conducting (C) afferent fibres. *Quarterly journal of experimental physiology and cognate medical sciences*, 44(June), p.362.

Iggo, A., 1969. Cutaneous thermoceptors in primates and sub-primates. *The Journal of Physiology*, 200(2), pp.403–430.

Ikeda-Miyagawa, Y. et al., 2015. Peripherally increased artemin is a key regulator of TRPA1/V1 expression in primary afferent neurons. *Molecular pain*, 11(1), p.8.

Ishikawa, K. et al., 1999. Changes in expression of voltage-gated potassium channels in dorsal root ganglion neurons following axotomy. *Muscle & nerve*, 22(April), pp.502–507.

Islam, S. et al., 2012. Highly multiplexed and strand-specific single-cell RNA 5’ end sequencing. *Nature protocols*, 7(5), pp.813–828.

Jankowski, M.P. et al., 2012. Dynamic changes in heat transducing channel TRPV1 expression regulate mechanically insensitive, heat sensitive C-fiber recruitment after axotomy and regeneration. *The Journal of neuroscience : the official journal of the Society for Neuroscience*, 32(49), pp.17869–17873.

Jankowski, M.P. et al., 2010. Enhanced Artemin/GFR 3 Levels Regulate Mechanically Insensitive, Heat-Sensitive C-Fiber Recruitment after Axotomy and Regeneration. *Journal of Neuroscience*, 30(48), p.16272.

Jankowski, M.P. et al., 2009. Sensitization of cutaneous nociceptors after nerve transection and regeneration: possible role of target-derived neurotrophic factor signaling. *The Journal of neuroscience : the official journal of the Society for Neuroscience*, 29(6), pp.1636–47.

Jankowski, M.P. et al., 2008. Sox11 transcription factor modulates peripheral nerve regeneration in adult mice. *Brain research*, 1256, pp.43–54.

Jankowski, M.P. et al., 2006. SRY-box containing gene 11 (Sox11) transcription factor is required for neuron survival and neurite growth. *Neuroscience*, 143(2), pp.501–514.

Jaworucka-Kaczorowska, a. et al., 2015. Saphenous vein stripping surgical technique and frequency of saphenous nerve injury. *Phlebology: The Journal of Venous Disease*, 30(135), pp.210–216.

Jensen, T.S. & Finnerup, N.B., 2014. Allodynia and hyperalgesia in neuropathic pain: clinical manifestations and mechanisms. *The Lancet. Neurology*, 13(9), pp.924–935.

Jessell, T. et al., 1979. Substance P: Depletion in the dorsal horn of rat spinal cord after section of the peripheral processes of primary sensory neurons. *Brain Research*, 168(2), pp.247–259.

Jia, Z. et al., 2016. Regulation of Piezo2 mechanotransduction by static plasma membrane tension in primary afferent neurons. *Journal of Biological Chemistry*, 291(17), p.jbc.M115.692384.

Jing, X. et al., 2012. The transcription factor Sox11 promotes nerve regeneration through activation of the regeneration-associated gene Sprr1a. *Experimental Neurology*, 233(1), pp.221–232.

Johnson, R.D. et al., 1995. Rescue of Motoneuron and Muscle Afferent Function in Cats By Regeneration Into Skin . I . Properties of Mferents. , 73(2).

Kambiz, S. et al., 2015. Long-term follow-up of peptidergic and nonpeptidergic reinnervation of the epidermis following sciatic nerve reconstruction in rats. *Journal of neurosurgery*, 123(1), pp.254–69.

Kashiba, H., Hyon, B. & Senba, E., 1998. Glial cell line-derived neurotrophic factor and nerve growth factor receptor mRNAs are expressed in distinct subgroups of dorsal root ganglion neurons and are differentially regulated by peripheral axotomy in the rat. *Neurosci Lett*, 252(2), pp.107–110.

Kelamangalath, L. et al., 2015. Neurotrophin Selectivity in Organizing Topographic Regeneration of Nociceptive Afferents. *Experimental neurology*, 271, pp.262–278.

Kestell, G.R. et al., 2015. Primary afferent neurons containing calcitonin gene-related peptide but not substance P in forepaw skin, dorsal root ganglia, and spinal cord of mice. *Journal of Comparative Neurology*, 523(17), pp.2555–2569.

Kim, C.H. et al., 2002. Changes in three subtypes of tetrodotoxin sensitive sodium channel expression in the axotomized dorsal root ganglion in the rat. *Neuroscience Letters*, 323(2), pp.125–128.

Kim, C.H. et al., 2001. The changes in expression of three subtypes of TTX sensitive sodium channels in sensory neurons after spinal nerve ligation. *Molecular Brain Research*, 95(1-2), pp.153–161.

Kobayashi, K. et al., 2005. Distinct expression of TRPM8, TRPA1, and TRPV1 mRNAs in rat primary afferent neurons with Aδ/C-fibers and colocalization with Trk receptors. *Journal of Comparative Neurology*, 493(4), pp.596–606.

Koerber, H.R. et al., 2010. Cutaneous C-polymodal fibers lacking TRPV1 are sensitized to heat following inflammation, but fail to drive heat hyperalgesia in the absence of TPV1 containing C-heat fibers. *Molecular pain*, 6(1), p.58.

Koerber, H.R., Mirnics, K. & Mendell, L.M., 1995. Properties of regenerated primary afferents and their functional connections. *Journal of neurophysiology*, 73(2), pp.693–702.

Koerber, H.R., Seymour, A.W. & Mendell, L.M., 1989. Mismatches between peripheral receptor type and central projections after peripheral nerve regeneration. *Neuroscience letters*, 99(1-2), pp.67–72.

Koerber, H.R. & Woodbury, C.J., 2002. Comprehensive phenotyping of sensory neurons using an ex vivo somatosensory system. *Physiology and Behavior*, 77(4-5), pp.589–594.

Koerber, R.H., Seymour, A.W. & Mendell, L.M., 1991. Tuning of Spinal Networks in Individual Afferents to Frequency Components of Spike Trains. *Journal of Neuroscience*, 11(10), pp.3178–3187.

Koltzenburg, M., Stucky, C.L. & Lewin, G.R., 1997. Receptive properties of mouse sensory neurons innervating hairy skin. *Journal of Neurophysiology*, 78(4), pp.1841–1850.

Krekoski, C.A., Parhad, I.M. & Clark, A.W., 1996. Attenuation and recovery of nerve growth factor receptor mRNA in dorsal root ganglion neurons following axotomy. *Journal of Neuroscience Research*, 43(1), pp.1–11.

Kress, M. et al., 1992. Responsiveness and functional attributes of electrically localized terminals of cutaneous C-fibers in vivo and in vitro. *Journal of neurophysiology*, 68(2), pp.581–595.

Kupari, J. & Airaksinen, M.S., 2014. Different requirements for GFRα2-signaling in three populations of cutaneous sensory neurons. *PloS one*, 9(8), p.e104764.

Langley, J.N. & Hashimoto, M., 1917. On the suture of separate nerve bundles in a nerve trunk and on internal nerve plexuses. *The Journal of physiology*, 51(4-5), pp.318–46.

Lawson, J.J. et al., 2008. TRPV1 unlike TRPV2 is restricted to a subset of mechanically insensitive cutaneous nociceptors responding to heat. *The journal of pain : official journal of the American Pain Society*, 9(4), pp.298–308.

Lawson, S., Caddy, K. & Biscoe, T., 1974. Development of rat dorsal root ganglion neurones. *Cell and tissue research*, 413, pp.399–413.

Lawson, S.N., Crepps, B. a & Perl, E.R., 1997. Relationship of substance P to afferent characteristics of dorsal root ganglion neurones in guinea-pig. *The Journal of physiology*, 505 (Pt 1, pp.177–91.

Lawson, S.N., Crepps, B. & Perl, E.R., 2002. Calcitonin gene-related peptide immunoreactivity and afferent receptive properties of dorsal root ganglion neurones in guinea-pigs. *The Journal of physiology*, 540(Pt 3), pp.989–1002.

Leah, J.D., Herdegen, T. & Bravo, R., 1991. Selective expression of Jun proteins following axotomy and axonal transport block in peripheral nerves in the rat: evidence for a role in the regeneration process. *Brain research*, 566(1-2), pp.198–207.

Lee, Y. et al., 1985. Coexistence of calcitonin gene-related peptide and substance P-like peptide in single cells of the trigeminal ganglion of the rat: immunohistochemical analysis. *Brain Research*, 330(1), pp.194–196.

Leung, A.Y. et al., 2005. Qualitative and quantitative characterization of the thermal grill. *Pain*, 116(1-2), pp.26–32.

Li, C.-L. et al., 2015. Somatosensory neuron types identified by high-coverage single-cell RNA-sequencing and functional heterogeneity. *Cell Research*, pp.1–20.

Li, L. et al., 2011. The functional organization of cutaneous low-threshold mechanosensory neurons. *Cell*, 147(7), pp.1615–1627.

Li, L. & Ginty, D.D., 2014. The structure and organization of lanceolate mechanosensory complexes at mouse hair follicles. *eLife*, 3, p.e01901.

Lippoldt, E.K. et al., 2013. Artemin, a glial cell line-derived neurotrophic factor family member, induces TRPM8-dependent cold pain. *The Journal of neuroscience : the official journal of the Society for Neuroscience*, 33(30), pp.12543–52.

Liu, Q. et al., 2009. Sensory neuron-specific GPCR Mrgprs are itch receptors mediating chloroquine-induced pruritus. *Cell*, 139(7), pp.1353–65.

Luo, W. et al., 2009. Molecular Identification of Rapidly Adapting Mechanoreceptors and Their Developmental Dependence on Ret Signaling. *Neuron*, 64(6), pp.841–856.

Makwana, M. & Raivich, G., 2005. Molecular mechanisms in successful peripheral regeneration. *FEBS Journal*, 272(11), pp.2628–2638.

Malcangio, M. et al., 2000. SHORT COMMUNICATION Abnormal substance P release from the spinal cord following injury to primary sensory neurons. , 12(November 1999), pp.1999–2001.

Malin, S. a, Davis, B.M. & Molliver, D.C., 2007. Production of dissociated sensory neuron cultures and considerations for their use in studying neuronal function and plasticity. *Nature protocols*, 2(1), pp.152–60.

Maricich, S.M. et al., 2009. Merkel cells are essential for light-touch responses. , 324, pp.1580–1582.

McIlwrath, S.L. et al., 2007. Overexpression of neurotrophin-3 enhances the mechanical response properties of slowly adapting type 1 afferents and myelinated nociceptors. *The European journal of neuroscience*, 26(7), pp.1801–1812.

McKay Hart, A. et al., 2002. Primary sensory neurons and satellite cells after peripheral axotomy in the adult rat: Timecourse of cell death and elimination. *Experimental Brain Research*, 142(3), pp.308–318.

McKemy, D.D., Neuhausser, W.M. & Julius, D., 2002. Identification of a cold receptor reveals a general role for TRP channels in thermosensation. *Nature*, 416(6876), pp.52–58.

Medici, T. & Shortland, P.J., 2015. Effects of peripheral nerve injury on parvalbumin expression in adult rat dorsal root ganglion neurons. *BMC Neuroscience*, pp.1–10.

Michael, G.J. & Priestley, J. V, 1999. Differential expression of the mRNA for the vanilloid receptor subtype 1 in cells of the adult rat dorsal root and nodose ganglia and its downregulation by axotomy. *The Journal of neuroscience*, 19(5), p.19.

Mishra, S.K. & Hoon, M.A., 2013. The cells and circuitry for itch responses in mice. *Science (New York, N.Y.)*, 340(6135), pp.968–971.

Molliver, D.C. et al., 1995. Presence or absence of TrkA protein distinguishes subsets of small sensory neurons with unique cytochemical characteristics and dorsal horn projections. *The Journal of comparative neurology*, 361(3), pp.404–16.

Munns, C., AlQatari, M. & Koltzenburg, M., 2007. Many cold sensitive peripheral neurons of the mouse do not express TRPM8 or TRPA1. *Cell calcium*, 41(4), pp.331–42.

Nakamura, F. & Strittmatter, S.M., 1996. P2Y1 purinergic receptors in sensory neurons: contribution to touch-induced impulse generation. *Proceedings of the National Academy of Sciences of the United States of America*, 93(19), pp.10465–10470.

Nakamura, N. et al., 2007. Laser capture microdissection for analysis of single cells. *Methods in molecular medicine*, 132, pp.11–8.

Nielsch, U., Bisby, M.A. & Keen, P., Effect of cutting or crushing the rat sciatic nerve on synthesis of substance P by isolated L5 dorsal root ganglia. *Neuropeptides*, 10(2), pp.137–45.

Noguchi, K. et al., 1990. Co-expression of α-CGRP and β-CGRP mRNAs in the rat dorsal root ganglion cells. *Neuroscience Letters*, 108(1-2), pp.1–5.

North, R.A., 2004. P2X3 receptors and peripheral pain mechanisms. *The Journal of physiology*, 554(Pt 2), pp.301–308.

Nurse, C.A., Macintyre, L. & Diamond, J., 1984a. A quantitative study of the time course of the reduction in Merkel cell number within denervated rat touch domes. , 11, pp.521–533.

Nurse, C.A., Macintyre, L. & Diamond, J., 1984b. Reinnervation of the rat touch dome restores the Merkel cell population reduced after denervation. *Neuroscience*, 13(2), pp.563–71.

Ochs, S., 1977. The early history of nerve regeneration beginning with Cruikshank's observations in 1776. *Medical history*, 21(3), pp.261–274.

Omura, T. et al., 2005. Different expressions of BDNF, NT3, and NT4 in muscle and nerve after various types of peripheral nerve injuries. *Journal of the Peripheral Nervous System*, 10(3), pp.293–300.

Page, a J. et al., 2005. Different contributions of ASIC channels 1a, 2, and 3 in gastrointestinal mechanosensory function. *Gut*, 54(10), pp.1408–1415.

Page, A.J. et al., 2004. The ion channel ASIC1 contributes to visceral but not cutaneous mechanoreceptor function. *Gastroenterology*, 127(6), pp.1739–47.

Peier, A.M. et al., 2002. A TRP channel that senses cold stimuli and menthol. *Cell*, 108(5), pp.705–715.

Petruska, J.C. et al., 2000. Distribution of P2X1, P2X2, and P2X3 receptor subunits in rat primary afferents: Relation to population markers and specific cell types. *Journal of Chemical Neuroanatomy*, 20(2), pp.141–162.

Pfaffl, M.W., 2001. A new mathematical model for relative quantification in real-time RT-PCR. *Nucleic acids research*, 29(9), p.e45.

Pierau F-K, Torrey, P. & Carpenter, D.O., 1975. Afferent new fiber activity responding to temperature changes of scrotal skin of the rat. *Journal of neurophysiology*, 38(3), pp.601–12.

Poirot, O. et al., 2006. Distinct ASIC currents are expressed in rat putative nociceptors and are modulated by nerve injury. *The Journal of physiology*, 576(Pt 1), pp.215–34.

Price, J., 1985. An lmmunohistochemical and Quantitative Examination of Dorsal Root Ganglion Neuronal Subpopulations. *Journal of Neuroscience*, 5(8), pp.2051–2059.

Price, J. & Mudge, A.W., 1983. A subpopulation of rat dorsal root ganglion neurones is catecholaminergic. *Nature*, 301(5897), pp.241–243.

Price, M.P. et al., 2001. The DRASIC cation channel contributes to the detection of cutaneous touch and acid stimuli in mice. *Neuron*, 32(6), pp.1071–1083.

Ramón y Cajal, S., 1928. *Degeneration & regeneration of the nervous system*, London: Oxford University Press Humphrey Milford.

Ranade, S.S. et al., 2014. Piezo2 is the major transducer of mechanical forces for touch sensation in mice. *Nature*, 516(7529), pp.121–125.

Ransdell, J.L., Faust, T.B. & Schulz, D.J., 2010. Correlated Levels of mRNA and Soma Size in Single Identified Neurons: Evidence for Compartment-specific Regulation of Gene Expression. *Frontiers in molecular neuroscience*, 3, p.116.

Rau, K.K. et al., 2009. Mrgprd enhances excitability in specific populations of cutaneous murine polymodal nociceptors. *The Journal of neuroscience : the official journal of the Society for Neuroscience*, 29(26), pp.8612–8619.

Razaq, S. et al., 2015. The pattern of peripheral nerve injuries among Pakistani soldiers in the war against terror. *Journal of the College of Physicians and Surgeons--Pakistan : JCPSP*, 25(5), pp.363–6.

Reid, G., Babes, A. & Pluteanu, F., 2002. A cold- and menthol-activated current in rat dorsal root ganglion neurones: properties and role in cold transduction. *The Journal of physiology*, 545(Pt 2), pp.595–614.

Reinhold, A.K. et al., 2015. Differential transcriptional profiling of damaged and intact adjacent dorsal root ganglia neurons in neuropathic pain. *PLoS One*, 10(4), p.e0123342.

Reiter, M. et al., 2011. Quantification noise in single cell experiments. *Nucleic acids research*, 39(18), p.e124.

Rogers, M. et al., 2006. The role of sodium channels in neuropathic pain. *Seminars in cell & developmental biology*, 17, pp.571–581.

Rydh-Rinder, M. et al., 1996. Effects of peripheral axotomy on neuropeptides and nitric oxide synthase in dorsal root ganglia and spinal cord of the guinea pig: An immunohistochemical study. *Brain Research*, 707(2), pp.180–188.

Santosa, K.B. et al., 2013. Nerve allografts supplemented with schwann cells overexpressing glial-cell-line-derived neurotrophic factor. *Muscle & nerve*, 47(2), pp.213–23.

Sarria, I., Ling, J. & Gu, J.G., 2012. Thermal sensitivity of voltage-gated Na+ channels and A-type K+ channels contributes to somatosensory neuron excitability at cooling temperatures. *Journal of Neurochemistry*, 122(6), pp.1145–1154.

Schulz, D.J., Goaillard, J.-M. & Marder, E., 2006. Variable channel expression in identified single and electrically coupled neurons in different animals. *Nature neuroscience*, 9(3), pp.356–362.

Seddon, H.J., 1943. Three types of nerve injury. *Brain*, 66(4), pp.237–288.

Shakhbazau, A. et al., 2013. Doxycycline-regulated GDNF expression promotes axonal regeneration and functional recovery in transected peripheral nerve. *Journal of Controlled Release*, 172(3), pp.841–851.

Skofitsch, G. et al., 1985. Corticotropin releasing factor-like immunoreactivity in sensory ganglia and capsaicin sensitive neurons of the rat central nervous system: Colocalization with other neuropeptides. *Peptides*, 6(2), pp.307–318.

Skofitsch, G. & Jacobowitz, D.M., 1985. Calcitonin gene-related peptide coexists with substance P in capsaicin sensitive neurons and sensory ganglia of the rat. *Peptides*, 6(4), pp.747–754.

Skofitsch, G. & Jacobowitz, D.M., 1985. Galanin-like immunoreactivity in capsaicin sensitive sensory neurons and ganglia. *Brain research bulletin*, 15(2), pp.191–5.

Soattin, L. et al., 2016. The biophysics of piezo1 and piezo2 mechanosensitive channels. *Biophysical Chemistry*, 208, pp.26–33.

Staaf, S. et al., 2009. Differential regulation of TRP channels in a rat model of neuropathic pain. *Pain*, 144(1-2), pp.187–199.

Stantcheva, K.K. et al., 2016. A subpopulation of itch-sensing neurons marked by Ret and somatostatin expression. *EMBO reports*, pp.1–16.

Story, G.M. et al., 2003. ANKTM1, a TRP-like channel expressed in nociceptive neurons, is activated by cold temperatures. *Cell*, 112(6), pp.819–829.

Stucky, C.L. & Lewin, G.R., 1999. Isolectin B(4)-positive and -negative nociceptors are functionally distinct. *The Journal of neuroscience*, 19(15), p.505.

Susarla, S.M. et al., 2007. Functional Sensory Recovery After Trigeminal Nerve Repair. *Journal of Oral and Maxillofacial Surgery*, 65(1), pp.60–65.

Takashima, Y., Ma, L. & McKemy, D.D., 2010. The development of peripheral cold neural circuits based on TRPM8 expression. *Neuroscience*, 169(2), pp.828–42.

Tannemaat, M.R. et al., 2008. Differential effects of lentiviral vector-mediated overexpression of nerve growth factor and glial cell line-derived neurotrophic factor on regenerating sensory and motor axons in the transected peripheral nerve. *European Journal of Neuroscience*, 28(8), pp.1467–1479.

Taylor-Blake, B. & Zylka, M.J., 2010. Prostatic acid phosphatase is expressed in peptidergic and nonpeptidergic nociceptive neurons of mice and rats. *PLoS ONE*, 5(1).

Terzis, J.K. & Dykes, R.W., 1980. Reinnervation of glabrous skin in baboons: properties of cutaneous mechanoreceptors subsequent to nerve transection. *Journal of neurophysiology*, 44(6), pp.1214–25.

Thakur, M. et al., 2014. Defining the nociceptor transcriptome. *Frontiers in molecular neuroscience*, 7, p.87.

Tominaga, M. et al., 1998. The cloned capsaicin receptor integrates multiple pain-producing stimuli. *Neuron*, 21(3), pp.531–543.

Trojanowski, J.Q., Walkenstein, N. & Lee, V.M., 1986. Expression of neurofilament subunits in neurons of the central and peripheral nervous system: an immunohistochemical study with monoclonal antibodies. *The Journal of neuroscience : the official journal of the Society for Neuroscience*, 6(3), pp.650–660.

Truini, A. et al., 2013. Peripheral nociceptor sensitization mediates allodynia in patients with distal symmetric polyneuropathy. *Journal of Neurology*, 260(3), pp.761–766.

Usoskin, D. et al., 2014. Unbiased classification of sensory neuron types by large-scale single-cell RNA sequencing. *Nature neuroscience*, 18(1), pp.145–153.

Wang, R. et al., 2014. Artemin induced functional recovery and reinnervation after partial nerve injury. *Pain*, 155(3), pp.476–84.

Wang, R. et al., 2008. Persistent restoration of sensory function by immediate or delayed systemic artemin after dorsal root injury. *Nature neuroscience*, 11(4), pp.488–496.

Wang, S. et al., 2008. Effects of the neurotrophic factor artemin on sensory afferent development and sensitivity. *Sheng li xue bao : [Acta physiologica Sinica]*, 60(5), pp.565–570.

Wang, T. et al., 2013. Neurturin overexpression in skin enhances expression of TRPM8 in cutaneous sensory neurons and leads to behavioral sensitivity to cool and menthol. *The Journal of neuroscience : the official journal of the Society for Neuroscience*, 33(5), pp.2060–2070.

Wang, T. et al., 2011. Phenotypic switching of nonpeptidergic cutaneous sensory neurons following peripheral nerve injury. *PloS one*, 6(12), p.e28908.

Wasner, G. et al., 2004. Topical menthol - A human model for cold pain by activation and sensitization of C nociceptors. *Brain*, 127(5), pp.1159–1171.

Webber, C. a et al., 2008. Guiding adult Mammalian sensory axons during regeneration. *Journal of neuropathology and experimental neurology*, 67(3), pp.212–22.

Wellnitz, S.A. et al., 2010. The regularity of sustained firing reveals two populations of slowly adapting touch receptors in mouse hairy skin. *Journal of neurophysiology*, 103(6), pp.3378–3388.

Widenfalk, J. et al., 2009. Treatment of transected peripheral nerves with artemin improved motor neuron regeneration, but did not reduce nerve injury-induced pain behaviour. *Scandinavian journal of plastic and reconstructive surgery and hand surgery /*, 43(5), pp.245–250.

Witschi, R. et al., 2010. Hoxb8-Cre mice: A tool for brain-sparing conditional gene deletion. *Genesis*, 48(10), pp.596–602.

Wong, A.W. et al., 2015. Neurite outgrowth in normal and injured primary sensory neurons reveals different regulation by nerve growth factor (NGF) and artemin. *Molecular and Cellular Neuroscience*, 65, pp.125–134.

Wong, L.E. et al., 2015. Artemin promotes functional long-distance axonal regeneration to the brainstem after dorsal root crush. *Proceedings of the National Academy of Sciences of the United States of America*, 112(19), pp.6170–5.

Woo, S. et al., 2015. Piezo2 is the principal mechanotransduction channel for proprioception. *Nature neuroscience*, 18(12), pp.1756–62.

Woo, S.-H. et al., 2014. Piezo2 is required for Merkel-cell mechanotransduction. *Nature*, 509(7502), pp.622–626.

Woodbury, C.J. et al., 2004. Nociceptors lacking TRPV1 and TRPV2 have normal heat responses. *The Journal of neuroscience : the official journal of the Society for Neuroscience*, 24(28), pp.6410–6415.

Woodbury, C.J. & Koerber, H.R., 2003. Widespread projections from myelinated nociceptors throughout the substantia gelatinosa provide novel insights into neonatal hypersensitivity. *The Journal of neuroscience : the official journal of the Society for Neuroscience*, 23(2), pp.601–10.

Xing, H. et al., 2006. Chemical and cold sensitivity of two distinct populations of TRPM8-expressing somatosensory neurons. *Journal of neurophysiology*, 95(2), pp.1221–1230.

Ye, Y. & Woodbury, C.J., 2010. Early postnatal loss of heat sensitivity among cutaneous myelinated nociceptors in Swiss-Webster mice. *J Neurophysiol*, 103(3), pp.1385–1396.

Zhang, F.-X. et al., 2010. Inhibition of Inflammatory Pain by Activating B-Type Natriuretic Peptide Signal Pathway in Nociceptive Sensory Neurons. *Journal of Neuroscience*, 30(32), pp.10927–10938.

Zhang, X. et al., 1995. Complementary distribution of receptors for neurotensin and NPY in small neurons in rat lumbar DRGs and regulation of the receptors and peptides after peripheral axotomy. *The Journal of neuroscience : the official journal of the Society for Neuroscience*, 15(4), pp.2733–2747.

Zhang, X. et al., 1996. Peripheral axotomy induces increased expression of neurotensin in large neurons in rat lumbar dorsal root ganglia. *Neuroscience Research*, 25(4), pp.359–369.

Zheng, J.Q. et al., 2001. A functional role for intra-axonal protein synthesis during axonal regeneration from adult sensory neurons. *The Journal of neuroscience : the official journal of the Society for Neuroscience*, 21(23), pp.9291–9303.

Zimmermann, K. et al., 2009. Phenotyping sensory nerve endings in vitro in the mouse. *Nature protocols*, 4(2), pp.174–196.

Zimmermann, K. et al., 2007. Sensory neuron sodium channel Nav1.8 is essential for pain at low temperatures. *Neuroforum*, 13(3), pp.100–101.

Zylka, M.J., Rice, F.L. & Anderson, D.J., 2005. Topographically distinct epidermal nociceptive circuits revealed by axonal tracers targeted to Mrgprd. *Neuron*, 45(1), pp.17–25.